Leonhard Petzel, BSc

Coexistence of QI wireless charging and NFC

MASTER'S THESIS
to achieve the university degree of

Diplom-Ingenieur

Master's degree programme: Information and Computer Engineering

submitted to

Graz University of Technology

Supervisor

Univ.-Prof. Dipl.-Ing. Dr.techn. Bernd Deutschmann

Institute for electronics

Graz, February, 2020

AFFIDAVIT

I declare that I have authored this thesis independently, that I have not used other than the declared sources/resources, and that I have explicitly indicated all material which has been quoted either literally or by content from the sources used. The text document uploaded to TUGRAZonline is identical to the present master‘s thesis dissertation.

Date	*Signature*

Kurzfassung

In der Automobilbranche wird vermehrt an kontaktlosen Ladestationen mit integrierter NFC Funktionalität gearbeitet. Ein großes Problem des kontaktlosen Ladens mittels dem Qi Standard besteht darin, dass NFC Karten durch das starke magnetische Feld der Ladestation beschädigt werden können. Zudem beeinträchtigt das Ladesystem die NFC Kommunikation erheblich. Diese Thematik wurde in der Arbeit behandelt und Lösungsansätze wurden in Kooperation mit NXP Semiconductors entwickelt.

Nach einer Einführung in die Thematik und den Stand der Technik werden Grundlagen der NFC Technologie und des kontaktlosen Ladens mittels Qi Standards erklärt, um dem Leser auf die folgenden Kapitel vorzubereiten.

Danach werden die Einflüsse der Subsysteme auf einander systematisch analysiert. Dafür werden Experimente zur Bestimmung der dominanten Effekte und Fehlerquellen beschrieben. Störungen durch das magnetische Ladefeld werden analysiert. Weiters werden die Effekte von Antennengeometrien und Ferritfolien diskutiert. Um die Ursachen der Beschädigung von NFC Karten und Sticker zu verstehen wurden Simulationen zur Verteilung des Ladefeldes durchgeführt und Modelle zur maximalen Belastung von NFC Transpondern entwickelt.

Verschiedene Lösungsansätze und Verbesserungen eines Prototypens wurden vorgeschlagen, simuliert, getestet und bewertet. Zuletzt wird ein Demonstrationsaufbau vorgestellt und die Ergebnisse zusammengefasst.

Abstract

NFC and QI wireless charging are technologies, which recently get combined into single devices. A major threat of QI wireless charging is to damage NFC cards placed in the operating volume. Furthermore, the performance of the NFC system is impacted by the charging system. This thesis addresses these problems and presents solution, which were developed in cooperation with NXP Semiconductors.

After an introduction and the state of the art, the operation of NFC and of QI is introduced to the reader to convey required prior knowledge.

Then, different aspects of combined wireless charging and NFC sub systems are investigated to systematically gain an overview of the influences between the two systems and to detect sources of failures. By experiments the dominant effects and fault origins are examined. Furthermore, the effects of antenna shapes and ferrites are discussed and strategies to decouple the systems are introduced. In order to understand the damaging of NFC cards and tags, the distribution of the magnetic field of the wireless charging system was simulated. Moreover, different NFC ICs were measured to understand the effects on the chips. Finally, models for the stress on several NFC cards were developed based on measurement and simulation results.

Various improvements and solutions to discovered issues are proposed, simulated, tested and assessed. Finally, a working demonstration setup is presented and the findings are summarized.

Acknowledgements

I would like to thank all the people, who supported me and my work directly or indirectly.

I want to thank Professor Bernd Deutschmann and Dr. Dariusz Adam Mastela for their guidance and help.

Special thanks go to Harald Krepelka and Dragomir Strbac for their support with NFC and RFID. Their expertise was invaluable.

Furthermore, I want to thank Harald Robert for his support with building test setups. His practical experience is worth gold.

Further, I want to thank Jan Horak and his colleges for their help with qi wireless charging. Without their inputs, I maybe would not have managed to develop a working solution.

To understand the effects in an RFID card when exposed to wireless charging fields, I had several discussions with Björn Rasmußen. I want to thank him for his inputs.

During writing this theses, I realized how much software is required to get high quality results. Many of those programs are open source. I want to thank the communities for developing such great tools.

Contents

Glossary

AFI The “Application Family Identifier” can be used to set the application of a NFC card. Some protocols allow to selectively poll for only one application.. 15, 16

ALM “Active Load Modulation” is a technique used by active devices (devices with external power supply) to modulate the field. By generating a signal, the response can be much stronger, than it would be possible with passive load modulation.. 8

ASK “Amplitude Shift Keying” is amplitude modulation with discrete baseband signals. In the simplest form, the carrier is either on or off, depending on the bit value (This mode is also called OOK). However, some protocols specify a residual carrier to ensure uninterrupted power supply of passive transponders.. 7, 13, 14

CE “Card Emulation” is the procedure, where an active device with power supply, like a phone, communicates as NFC transponder and imitates the behaviour of a passive PICC. It is defined by the NFC Forum.. 5, 8, 83, 90, 109

FSK “Frequency shift keying” is a frequency modulation scheme on a discrete base band signal. Depending on the value to encode, one of several frequencies is selected for the carrier.. 13, 14, 22

ISO-DEP The “ISO Data Exchange Protocol” is a communication interface and compliant with ISO7816. It is supported by cards compliant to ISO14443-4. Devices supporting this technology are called named “Type 4” cards by the NFC Forum.. 17, 20

NCI The “NFC Controller Interface” is a protocol specification for communicating with NFC reader controllers. Ideally, when integrating an NCI based NFC chip in a design, the manufacturer of the chip should be interchangeable from software point of view. Also, the NCI protocol already abstracts low level protocol activities. The NFC chip is configured via NCI to detect certain tag types defined by the NFC Forum. Knowledge about the details of ISO14443, Felica or ISO15693 is not required.. 5

NFC Forum The NFC Forum is an industry association, which drives standardized interfaces and interoperable devices. They investigates many topics related to NFC.. 4, 13, 14, 17

NFC-DEP The "NFC Data Exchange Protocol" is a communication interface similar to ISO-DEP, but used by card emulating devices. It is defined in ISO 18092 / ECMA 340. ISO 14443-3 compatible devices and Felica compatible devices may implement NFC-DEP. However, an implementation is not mandated by the NFC Forum. NFC-DEP provides better security mechanisms and is required for some NFC applications. However, NFC-DEP is only implemented on active devices with external power supply.. 20

OOK "On-Off Keying" is a special case of ASK. Depending on the bit value to transmit, the carrier is either switched on or off. It is commonly used, because of the simple implementation. However, some protocols specify a residual carrier to ensure uninterrupted power supply of passive transponders.. 7, 13

PCD PCD stands for "Proximity Coupling Device". It is a term used in ISO-14443 for the NFC transmitter. Another synonym is NFC reader.. 5, 7, 13, 20

PICC PICC stands for "Proximity inductive coupling card". This term is defined in ISO14443 (proximity cards). PICCs are passive NFC transponders in the sense, that they do not have a power supply. In this thesis, the terms PICC and NFC card are used synonymously.. 4, 5, 7, 13, 18–20, 32, 34, 37, 43, 47, 54, 55, 60, 62, 63, 77, 86, 95

PSK "Phase Shift Keying" is a digital modulation scheme, where the binary baseband signal is translated into phase jumps of the carrier.. 14

PWM "Pulse Width Modulation" is a modulation scheme, where a supply voltage is switched on and off with a fixed frequency, but variable duty cycle (pulse length).. 82, 85–87, 110

UID A "Unique Identifier" is a number, which is used by the NFC card to identify itself. Depending on the protocol, the UID is either fixed or random.. 15, 16

WPC The "Wireless Power Consortium" is a standards development group. It develops the QI standard and investigates topics related to that topic. The most important companies, which either develop wireless power transmitters or receivers, are members of the Wireless Power Consortium.. 2, 88, 89

List of Figures

Chapter 1

Introduction

1.1 Motivation

Wireless charging and NFC simplify our life by removing small everyday actions. Both technologies are implemented in automobiles to increase the drivers comfort.

We as car drivers are annoyed by any extra actions, we have to take before leaving. Although, we want to use features of our phone like navigation or music streaming in the car, we do not want to manually set anything up. NFC can be used to automatically enable these kind of services in a secure way.

With the rising importance of smart phones also the topic of charging is becoming more important. Nowadays, wireless charging stations can be found for instance in public places, shopping centers, restaurants and also cars. Wireless charging is not only more comfortable than wired charging, but also reduces interoperability issues and removes the mechanical connectors, which are prone wear.

Combined wireless charging and NFC devices allow you to put our phone into the middle console and enable all kind or services while charging the device. Unfortunately, there are also challenges when combining these technologies. Charging systems negatively influence the NFC system and may even prevent successful communication. Moreover, NFC cards are damaged by the strong charging field, if they slip between charger and phone.

The industry is putting much effort into solving these issues. In cooperation with NXP Semiconductors, the problem is analyzed and solutions are developed.

1.2 State of the art

The topic of combining NFC and wireless charging is investigated by the industry already for several years. As a consequence, there are already patents on the market targeting different kinds of wireless charging and targeting different goals. However, many results are confidential property and only shared in work groups like the Wireless Power Consortium.

1.2.1 Patents

Continental owns a patent named “Methods and apparatus for loading, in particular WPT by NFC in a motor vehicle” for a combined NFC and wireless power transmission device.

In the patent the interactions between the two systems are described in detail. The major claim is, that NFC is used for finding a device. The patent number is DE102015211026A1.

A method for preventing NFC card destruction is presented in EP3447875: "Device and method for preventing NFC Card Destruction by Wireless Charging System". In the patented methodology, the magnetic field generated by the charger is measured. Furthermore, if an NFC card is found to be in the field, the maximal magnetic field strength of the wireless charger is limited in order to protect the card.

Patent number US20180183267 named "Wireless power transmitter and wireless charging method" describes NFC protection together with Rezence charging. In this application, the same antenna is used for wireless charging and detecting NFC cards. By sending a control signal at 13.56MHz, it can be assessed, if an NFC card is in the field. However, Rezence charging is very different from Qi charging, because the frequency of the magnet field is much higher (6.78 MHz).

1.2.2 Wireless Power Consortium

The threat of card damaging by Qi wireless charging is a well-known issue and was analyzed by the wireless power consortium (WPC). Different companies contributed measurement results for analysis purposes and developed strategies to overcome this issue.

Firstly, it was analyzed under which conditions NFC cards are damaged by wireless chargers by experiments with commercially available Qi wireless chargers. It was discovered, that 13.56MHz NFC cards are not detected by the foreign object detection strategies of QI and that they may be damaged during wireless charging.

Moreover, different scenarios were investigated and assessed. For example the threat of damaging cards was assessed in the different phases of the Qi protocol. In order to be reproducible, measurement setups and procedures were defined.

Among other contributions, NXP Semiconductors presented an algorithm to distinguish between NFC cards and NFC enabled phones and contributed ideas for integrating NFC antennas into one-coil charging solutions[14].

The outcomes resulted in a recommendation in the "QI wireless power transfer system power class 0 specification" in version 1.2.4 [17]. In the Annex E[1] of the document, three different physical setups for integrating NFC antennas into charging solutions are described. Furthermore, a section describes a process for detecting NFC cards in parallel to the QI charging. There, an algorithm to distinguish NFC enabled phones and cards is shown and recommended for the selection phase of the Qi protocol and whenever no wireless charging is active. Therefore only the static cases are covered, where an NFC card is already in the operating area, when the wireless charging would start.

During the actual power transfer, a simple polling strategy for a set of common NFC and RFID technologies is recommended. This procedure covers dynamic scenarios, where an NFC card moves into the magnetic field of the charger, while a device is being charged wirelessly.

When an NFC/RFID card is detected, the standard once recommends to not allow a *strong* charging signal, but does not elaborate, what a strong charging signal is. However, in another paragraph, it is recommended to abort wireless charging completely until the card is removed.

[1] NFC/RFID card protection by the PTx

A variant to the card and device distinguishing algorithm was implemented in the practical part of this work and is described in section sec:card-phone-distinguishing.

1.2.3 Combined NFC and Qi antennas

NFC antennas can be integrated in the Qi antennas as stated for example in [3]. According to the paper, both NFC and Qi antenna performed well. Because of the coupling, the quality factor of the NFC coil is decreased and the inductance of the NFC coil increased. However, these effects can be considered in the matching circuit of the NFC system.

The use case for such combined antennas is the integration into mobile phones. There are also patents (KR101922530) for this idea.

The effect of the positioning of the NFC antenna with respect to the Qi antenna is discussed in [8]. The goal of this work was to minimize the degradation of the Qi efficiency caused by the NFC system. The conclusion is, that the optimum is reached, when the magnetic coupling between the Qi and the NFC coil is minimized (where the H_z field is most cancelled).

In order to protect the mobile phone and to increase the efficiency, it is necessary to shield the mobile phone from the magnet field of the charger, which is achieved by a ferrite foil beneath the Qi coil. In a study the effects of shaping an amorphous ferrite foil on combined Qi and NFC coils was investigated [13]. It was found, that cutouts in the foil can increase the NFC communication distance.

1.2.4 Investigations on NFC transponders

Some investigations on NFC tags antennas were performed in [6]. A special antenna shape with two outer and six inner windings with opposite rotation shall minimize the power injected in the tag by a Qi charger. Basically, the NFC antenna and the Qi coil are decoupled by this design. This "magnetic isolation effect" is effective when the card is centered at the charging coil. Moreover, the paper claims that the tag can be even misaligned by 10mm and still shows a good attenuation of the Qi signal.

1.2.5 Standards

NFC / RFID related standards

There are several standards related to RFID and NFC. The most relevant protocols are described in section 2.3 in more detail. Firstly, the ISO 14443 norm handles lower layers of communication of so-called type A and type B proximity cards [7]. Moreover, there is a Japanese standard for so-called FeliCa cards. Another RF interface is described by the ISO15693 norm, which regulates so-called vicinity cards[2]. These standards will be described in more detail in section 2.3.

Other standards include ISO 10373 for test methods on 13.56MHz cards, ISO10536 for closed-coupled contactless integrated circuit cards in general (for both, inductive and capacitive transfer). Some mechanical aspects are covered in ISO 15457 and ISO 7810. RFID with all its frequencies is described in ISO 18000. Furthermore, as many RFID and

[2]They are designed for a greater operating distance.

NFC cards are used for identification, they might comply to ISO 7816. Especially the content of 7816-4 was used in the practical part of this work.

The previous listed standards define properties of proximity and vicinity cards, smart cards, identification cards, RFID and closed-coupled cards. Strictly speaking, these standards are not about NFC. But NFC has to be read in context of those standards. Finally there are several NFC specific standards. Most importantly, there is ISO18092 (NFCIP-1),which defines a faster communication mode for active NFC devices. On top of this standard, an advanced security protocol (NFC Sec) is defined. Finally, ISO21481 (NFCIP-2) links all those technologies.

The NFC Forum drives standardization and development of NFC. Moreover, the NFC Forum publishes specifications, which also summarize the essential information of many of the related standards. Therefore, the NFC Forum documents are an important source of information. Furthermore, NFC Forum certified products can be assumed to be interoperable.

The Qi standard

The QI protocol is defined by the wireless power consortium[17]. In addition to the protocol and physical specifications, the standard also provides many reference implementations. Therefore, it takes over concrete design consideration such as antenna layout, ferrite foil layout and matching circuit. In section 2.6 the Qi standard will be explained in more detail.

Unfortunately, the current NFC standards are insufficient for regulating simultaneous operation with Qi wireless charging. For example the maximum permitted field strength for certain card geometries is defined to be $7.5 A/m$. Obviously, this value is only valid at the NFC frequency. A magnetic charging field with frequencies between 100kHz and 200kHz exceeds this limit by far. Fortunately, the effect of the field on the card is smaller at lower frequencies (see section 3.3). However, when testing as described in ISO 10373, the effect of wireless charging on cards is underestimated.

Only recently, some attempts were made to define measurement setups for the limits of QI wireless charging field strengths to avoid damaging of cards. In the Annex E of the Qi specification [17], a special reference PICC is introduced for assessing, if a charging field would damage cards. The design is based on experiments with different smart cards.

1.3 Outline of the thesis

QI charging and NFC are getting combined in single systems for several reasons. However, there are challenges with parallel operation.

In this thesis, different aspects of combined QI charging and NFC systems are investigated. Challenges are identified and countermeasures developed and implemented. Finally, a functional solution was developed in cooperation with NXP Semiconductor Devices based on a demonstration board .

First, NFC is introduced. This section (2.1) includes matching circuits on the reader and on the transponder side as well as an introduction into the most important protocols. In this section also the used terminology is introduced.

The section is followed by an introduction into QI charging (section 2.6). For readers without previous knowledge, the principle of operation is explained. Moreover, the circuitry on the Power Transmitter is explained. Finally, certain aspects of the protocol like the power negotiation and Foreign Object Detection are discussed.

Then, an analysis of systems combining Qi charging and NFC can be found in section 3. First, influences between NFC and charging sub system are discussed and derived analytically. Then possible failure origins are investigated and discussed. Experiments were performed and are described to prove or refute theories. Therefore, also circuit and field simulations are discussed. Ideas how to solve challenges are collected and investigated in the next chapter.

The forth section is about solutions to challenges and problems. Based on the previous analysis, improvements are proposed, analyzed and evaluated. Both, hardware and software proposals are systematically evaluated. The tested ideas are measures against different error sources. Some of them are intended for card protection, others for NFC communication during wireless charging.

Finally, the results are discussed and future work is identified.

1.3.1 Description of challenges

The threat of card destruction

The strong magnetic field for wireless charging can damage NFC cards. This is a major threat inside the car. A wallet with NFC enabled cards could move into the charging field in the scenario of hard braking. Therefore, it shall be possible, to detect NFC cards during charging. Because NFC cards could otherwise be destroyed, the charging has to be stopped in case of card detection.

At the same time phones might have NFC enabled and might answer NFC requests, which are meant for card detection. In this case the goal is to distinguish cards from phones.

Parallel operation

Several services like Bluetooth pairing might be performed with NFC. In this case, it is desirable to enable NFC communication with a phone during wireless charging being active. Phones can either run as reader (PCD), as PICC using card emulation (CE) or using the peer to peer (P2P) communication mode.

Simultaneous communication is not a hard requirement for cards. If a card is detected, charging has to be stopped, anyway.

1.3.2 Description of the setup

The wireless charging system contains 3 coils, only one of which is selected with transmission gates at a time. This setup is standardized as MP-A9[17].

Directly on top of the 3 charging coils is an NFC antenna. For driving the NFC field, an NFC front end is used. It is addressed via the standardized NCI interface.

The NFC and the QI system with their matching circuits are integrated on a single PCB.

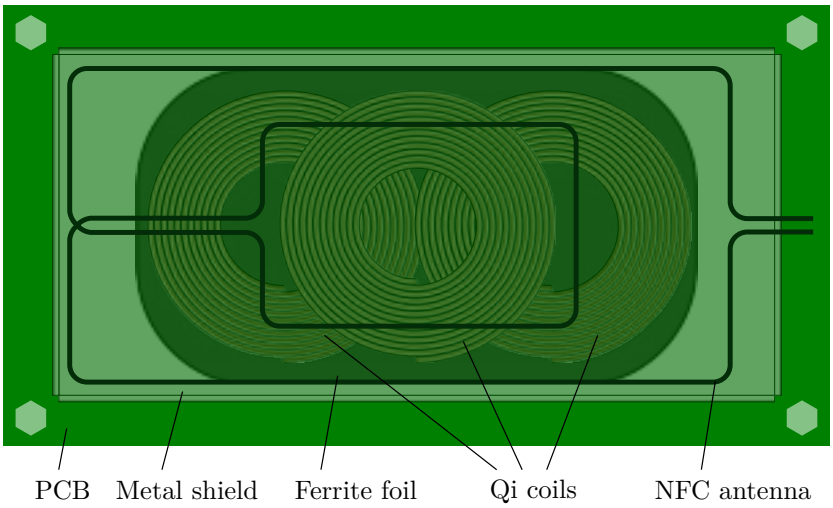

Figure 1.1: Sketch of the combined wireless charging and NFC setup

To get full control over the NFC front end (e.g., for analysis and development) a separate board was used.

This separation already excludes many error sources and allows to operate the charging and the NFC system independent of each other.

In order to give the reader a basic understanding of the technologies used, an introduction into NFC and QI is given in the next section.

Chapter 2

Fundamentals of NFC and Qi charging

In this section, the relevant topics about the technologies are summarized. Finally, possible disturbances on the NFC sub system are discussed. This then leads to the analysis of combined Qi charging and NFC systems in section 3.

2.1 Introduction into NFC

NFC stands for near field communication. NFC is used for wireless communication and for charging of low energy devices. As the name suggests, the maximum communication distance is short[1].

A major advantage of NFC is, that the receiver can harvest enough energy from the field to operate, why many receivers do not contain a battery. Energy and information is transmitted inductively. NFC utilizes the frequency band at 13.56MHz (±7kHz tolerance). Due to relatively simple modulation schemes like ASK and OOK of reader to card communication, a wide bandwidth is required.

The transmitter is called reader or PCD. The reader provides the 13.56MHz carrier field. When transmitting information, this carrier is modulated. The actual modulation scheme depends on the protocol used. Usually, it is amplitude modulation (ASK). Moreover, the reader is the master of the communication. Every information transfer is initiated by the reader ("Reader talks first").

The transponder is called PICC. PICCs are NFC cards without external power supply. These cards must be protected from the charging field. In the cards, a NFC coil is integrated. Often, the NFC coils are called antennas. However, the information and energy transfer is purely inductive. The coil on the card is used to harvest energy, to receive the reader's communication and to respond to the reader's requests.

All NFC cards respond with load modulation. By changing the impedance, the receiver modulates the current. This change is then detected by the NFC reader. This concept is called passive load modulation (PLM).

[1] Often 20cm are mentioned as maximum distance, which can be achieved by NFC. However, this is not a hard limit. Usually much lower read ranges of about 5cm to 10cm are achived by NFC readers.

On the other hand, the transponder can be a device with power source. A common case are smart phones. For this kind of devices, separate communication schemes and protocols are defined. However, they can also communicate with the older protocols. This functionality is called "card emulation" (CE). When they act as a card, they actively use energy when modulating the field. This scheme is called active load modulation (ALM).

2.2 Typical matching circuit of an NFC reader

The reader IC drives the modulated field with its TX pins. Figure 2.1 shows a typical balanced network for connecting TX and RX terminals to the antenna[12]. On the right, there is the NFC antenna. The matching network between TX and antenna enables the chip to optimally drive the antenna. Optimal means, that the antenna transmits the desired amount of energy with the minimum current at the TX pins. Furthermore, the maximum current rating must be obeyed.

A passive and linear two port circuit which connects a load to a source causes a so-called impedance transformation. Usually the source is called "matched" to the load, if the power transfer between source and load is maximized by the matching network in between. For linear systems that means, that the source must see the complex conjugate of the sources' impedance, the load must see the complex conjugate of the load's impedance and the matching network should not consume any power and therefore consists of reactive components only.

When speaking of matching networks with NFC readers, this definition cannot be applied. The reason is, that the source impedance of the TX pins of an NFC reader is very low. When a load was matched to this small impedance, the power consumption would by far exceed the absolute maximum ratings of all NFC reader chips. Instead, an output power P_T is targeted. A target impedance can be calculated from that power.

$$Z_T = \frac{V^2}{P_T}$$

Now the matching circuit is designed as if the source had this impedance. Finally, the goal is, that the source sees this optimal target impedance.

Usually, matching circuits consist of capacitors and coils only. Ideally, these components do not consume power. Therefore, all the power, which is drawn from the source, is dissipated in the load. By increasing the power by tuning the network, the load will therefore see higher voltages and currents.

A useful tool for the design is a smith chart of the impedance. Adding capacitors or coils in series or in parallel moves the impedance on circles there. It can be easily seen, that with only two reactive components, every impedance transformation can be achieved with the correct topology.

The matching circuit works only at the frequency, it is designed for. The resulting network can be seen as a resonance circuit. In a narrow frequency range, the target impedance is reached and the transmitted power is the designed value. Below and above this frequency, the impedance is too high or too low and the imaginary parts do not cancel anymore.

Unfortunately, the resonance frequency strongly depends on the load and the component values of the matching network. To reduce the impact of tolerances, the bandwidth

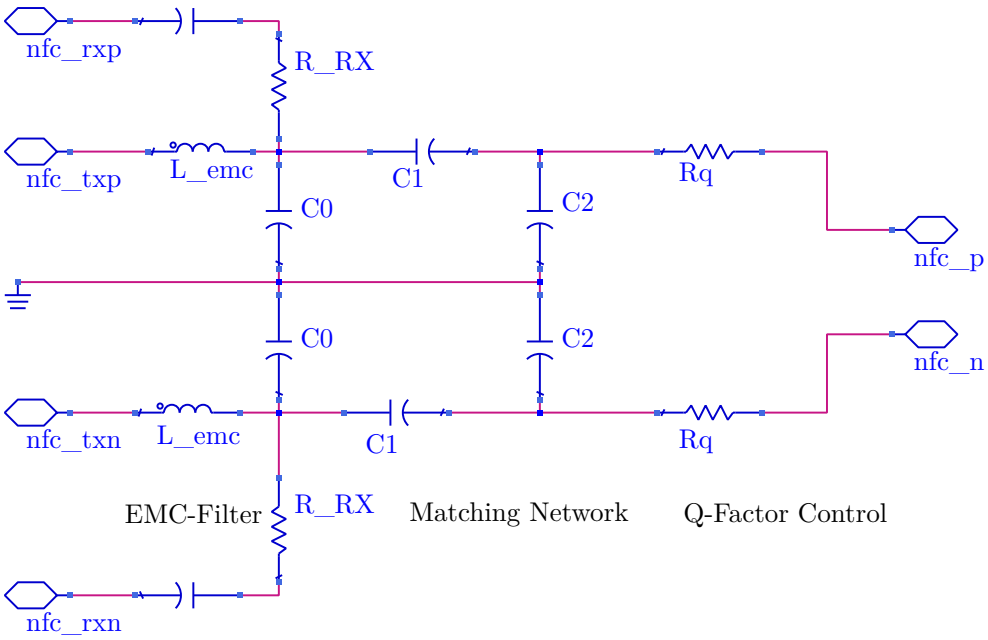

Figure 2.1: Typical matching circuit of the NFC reader

should not be chosen too narrow. A typical measure is the quality factor Q, which is for simple RLC circuits (see also [12]):

$$Q = \frac{X_{res}}{R_{res}} \tag{2.1}$$

For resonance circuits with more elements than one resistor, one capacitor and one coil, one has to be careful, which definition of Q (there are others[10]) and with definition of the bandwidth are used. Another common definition is:

$$Q = \frac{f_{\text{resonance}}}{\text{bandwith}} \tag{2.2}$$

Yet another definition suitable for more components is:

$$Q = 2\pi \frac{\text{oscillating (imaginary) energy}}{\text{dissipated (real) energy per period}}$$

The maximum output voltage and the maximum current, the chip can drive, are given in the data sheet. From them, the lower limit of the impedance for power adjustment can be calculated:

$$Z_{min} = \frac{U_{TX}}{I_{TX,max}} \approx 20\Omega \text{ for the IC used} \tag{2.3}$$

The impedance of the antenna does not match this impedance and is mainly inductive. If it was directly connected to the TX pins, the field would be weak and the current might still exceed the maximum absolute ratings of the chip.

There are different solutions for creating a matching network for NFC. A common one can be seen in figure 2.1. The figure shows a balanced circuit. That means, that the two signal lines txn and txp see the same impedances. Therefore, all components in the upper and the lower path are equal.

Mathematically put, this matching circuit is an under determined equation system. The unknowns are the values of L_{emc}, R_q and C0 to C2. The impedance seen by the NFC reader shall be a certain impedance close to the one in (2.3) to achieve a strong magnetic field. This is described by two equations, one for the real and one for the imaginary part. Three additional constraints have to be defined to get a unique solution.

Often, the resistor on the right of the figure 2.1 is chosen to obtain a certain quality factor of the NFC coil at 13.56MHz, according to (2.1). Small resistances result in a high quality factor and a narrow bandwidth. This is optimal for transmitting energy and filtering out distortions. But if the quality factor is high, detuning effects and tolerances have a bigger influence.

The first low pass (L_{emc}, C0) is called electromagnetic compatibility (EMC) filter. As the name suggests, it is used for EMC. But it is used for matching as well. Usual values for the inductance of the coils are between 300 and 500µH.

One more constraint is still required to get a unique solution. Often, the resonance frequency of the EMC filter $f_{EMC} = 1/2\pi\sqrt{L_{EMC}c_0}$ is chosen. This parameter determines, how the impedance seen by the IC changes with respect to the frequency. For typical reader applications, a possible design value could be 20MHz. Such a matching is easily detuned, which is often desired when maximizing the communication distance. [19] contains an analysis of the detuning caused by multiple transponders.

On the other hand, for so-called symmetrical matchings the last equation becomes $d\Re Z/df = 0$ at 13.56MHz instead. The impedance curve for symmetrical matchings is hermitian around 13.56MHz in first approximation ($Z(13.56\text{MHz} + \Delta) \approx Z^*(13.56\text{MHz} - \Delta)$), which is a desired property, if the NFC reader is also used in the card emulation mode. Moreover, these matchings are more robust against detuning effects, which is a welcome property for a combined wireless charging and NFC system.

Figure 2.2 shows the impedance over frequency curve of three different matchings. All three curves reach the target impedance of 25Ω at 13.56MHz (at this frequency all three curves intersect in one point). However, they are designed with different EMC cutoff frequencies. The blue curve shows a symmetrical matching with a low EMC cutoff frequency of 14.5MHz. Therefore the curve is almost symmetrical around the NFC carrier frequency. The red curve has an EMC cutoff frequency of 20MHz. It can be already guessed from this graph, that detuning effects will show greater influence on the network with the higher cutoff frequency.

From the initially five degrees of freedom, two are already fixed by setting the value of the EMC coil or by the condition of a symmetrical matching. Another degree is fixed by aiming for a certain quality factor. The two remaining degrees are fixed by the conditions, that the real and the imaginary part of the target impedance match the impedance of the network. Therefore, the network has a unique solution.

The design with the 5 reactive components (L_{emc}, C0-C2 and the NFC coil) creates a resonance circuit with two complex poles. For symmetrical matchings, this leads to a wider bandwidth (according to the definition in (2.2)) and better immunity to the coupling effects of PICCs, foreign objects in the field and tolerances.

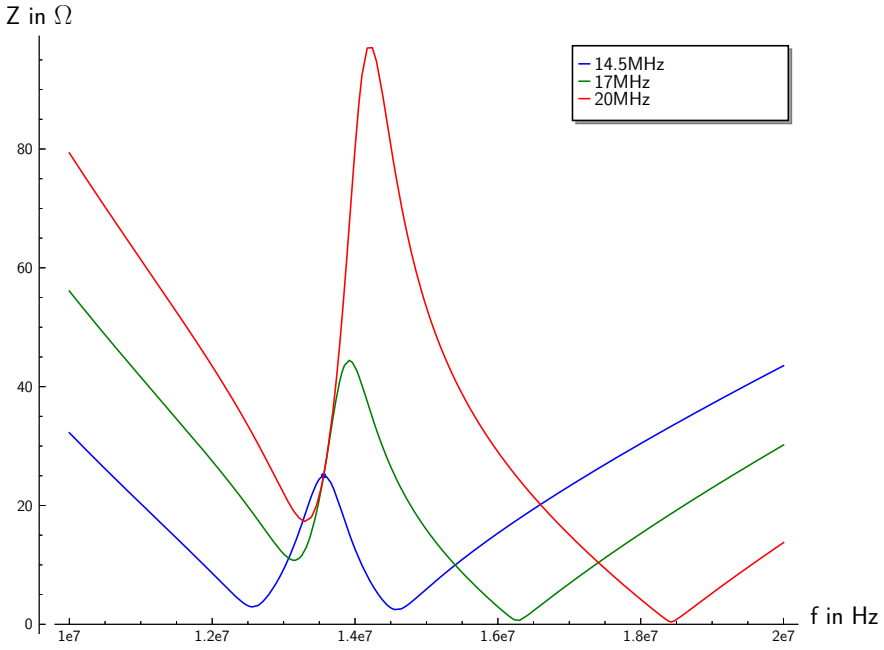

Figure 2.2: Impedance plot of the network over the frequency at different EMC cutoff frequencies

If a card is placed on the antenna, the circuitry on the card side will be coupled into the circuit of the reader. The antenna impedance changes and the matching circuit is not in the optimal region anymore. To avoid a significant loss of available power, when the card is in the field and needs energy, the Rq resistor is used to reduce the quality factor.

The RX pins in figure 2.2 are used for receiving the answer of an NFC card. The inductance of the EMC filter acts as a shunt impedance. A series capacitor decouples the DC point, which is set by the chip. The series resistor R_RX is responsible for limiting the peak input voltage of the IC to its specified maximum absolute rating of 1.2V.

2.2.1 NFC reader matching in combined Qi and NFC systems

When matching an NFC reader, it is important to design and test in a realistic environment. Ferrite foils and metallic shields are often used to firstly increase the efficiency of Qi wireless charging and secondly to protect electrical circuitry from electromagnetic interference. However, these components also affect NFC fields and therefore also the inductance L_a.

These influences are static and do not change during operation. However, a mobile phone laying directly on top of the NFC reader antenna also detunes the matching circuit very strongly. Because of metallic components in the phone, eddy currents can flow, which reduce the magnetic field of the NFC reader antenna. Therefore the effective inductance is reduced significantly in this scenario. In order to compensate for this effect, the matching network should be designed to be only moderately detuned with and without phone.

Figure 2.3 shows the real and the imaginary part of the impedance of a matching

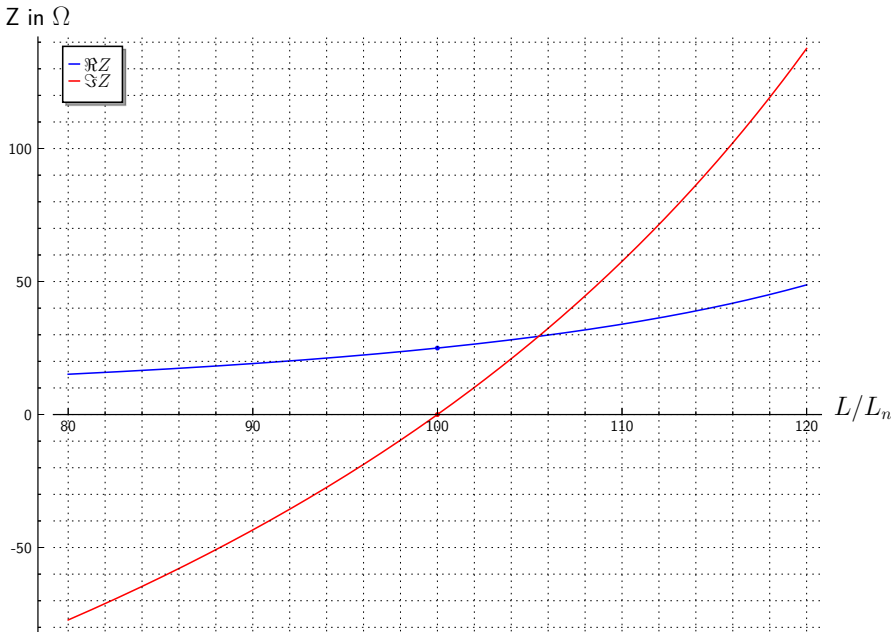

Figure 2.3: Real and imaginary part of the impedance of a matching network over the inductance of the NFC antenna

network as a function of the inductance. More accurately, on the ordinate the inductance of the NFC antenna is noted relatively to the nominal inductance, for which the network was calculated for. At 100% the target impedance of 25Ω is reached. Because of the detuning of phones, the inductance will vary in a certain range, which can be easily measured with a vector network analyzer. In order to get a good performance for both scenarios, with and without phone, the matching networks in this thesis were designed to have the following properties:

- $\Re Z > |\Im Z|$ for the range of possible inductance values.

  If the imaginary part exceeds the real part, than the reactive loading dominates the current consumption. For figure 2.3 the region, which fulfills this requirement, is from about 95% to 105% of the nominal inductance.

- $|Z| > Z_{min}$ for the range of possible inductance values.

  In figure 2.3 it can be seen, that the minimum of the impedance curve is not located at the nominal point. However, for every possible inductance the impedance must stay bigger than Z_{min} in order to obey the absolute maximum ratings of the IC.

2.3 NFC/RFID communication protocols

RFID consist of various protocols, which have historically grown and serve different purposes (see also section 1.2.5). The standards are developed by different institutions and

use different terminologies. For consistency the terminology of ISO14443 is used when applicable[2] in this thesis.

Only the most relevant protocols for understanding this thesis are described in this section. These technologies are often associated with NFC, but they are also used in various smart cards and therefore could be also assigned to the RFID ecosystem.

2.3.1 Radio frequency power and signal interface

Most protocols support different bit rates. Usually, the communication starts at the lowest bit rate. Higher rates can then be negotiated by PICC and PCD. In this chapter, only the slowest bit rates are taken into account.

The NFC field is usually created with a push-pull output driver. The reader directly modulates the carrier usually with amplitude shift keying (ASK). In comparison card to reader communications is more complex. Creating a separate magnetic field requires too much energy for a passive NFC card. Instead the impedance of the cards IC is modified in order to encode the data. Then the reader can detect this change.

Most protocols make the communication more robust by introducing a sub carrier. As a result the card to reader communication uses a two layered modulation scheme. The digital base band signal is modulated on the sub carrier and the sub carrier is modulated on the field using the load modulation (LDM) discussed before. The advantage of this more complicated scheme is, that for the NFC reader it is easier to detect if a sub carrier exists (amplitude is alternating), than if the base band signal was directly modulated on the magnet field.

Note also, that all modulation schemes work directly on digital signals. The reader to card communication works by on-off-keying (OOK) between two voltage levels. Also the sub carrier in card to reader modulation is a digital signal, which is modulated with OOK too. Moreover, the sub carrier is modulated again by a digital modulation scheme like OOK, binary phase shift keying (BPSK) or Frequency shift keying (FSK).

There are four protocols which describe the low level signal interface with passive cards, which are officially supported by the NFC Forum.

- Type A

  Type A or NFCA complies with ISO 14443-A, which is a widely used standard for proximity cards. The standard was developed by the company Micron, which was later bought by Phillips and became part of NXP Semiconductors.

  Type A cards use 100% amplitude modulation (ASK) for the reader to card communication. The bits are coded in a modified miller scheme, which makes sure, that there are no pauses longer than half of a bit period. The default bit rate is $\frac{f_c}{128} \approx 106 kbit/s$.

  For card to reader communication, a sub carrier is generated by the card. This sub carrier is modulated with 100% amplitude modulation. (The sub carrier is modulated or not modulated on the field, depending on the bit value)

  The card has a fixed frame delay time, after which it has to answer a request of the reader [7].

[2] The NFC forum uses a different terminology.

- Type B

  The early ISO14443 standard was only suited for memory cards. This led to the development of a "B variant". The ISO14443-B protocol is also called NFCB in the NFC Forum. Today both standards cover the same applications and offer similar functionality.

  The type B protocol uses 10% amplitude modulation (ASK) for reader to card communication. Thus one advantage is, that the card can always pull energy from the field and does not need to store energy for the low phases of the reader to card modulation. The bit rate is the same, as with type A.

  For card to reader communication, again a sub carrier is created. But instead of switching the sub carrier on and off (100% amplitude modulation), the sub carrier is phase modulated (PSK). Depending on, if the first or if the second half is load modulated, a one or a zero is modulated.

  Type B cards have more flexibility, when to answer. They may first generate an unmodulated sub carrier and start to modulate the answer some time later.

- FeliCa (Type F)

  With FeliCa a third technology fights for market share. The protocol is developed by Sony and is especially popular in Asia. FeliCa or NFCF complies to the Japanese standard JIS X6319-4 (High speed proximity cards).

  In the FeliCa protocol again 10% ASK is used for reader to card communication. However, in this protocol a Manchester coding scheme is used.

  The biggest difference in the physical layer is, that type F cards do not create a sub carrier. The load modulation is applied directly on the field (again Manchester encoded). As a consequence, the bit rates are usually higher, than with the other types. Common bit rates are 212kBit/s and 424kBit/s, where the lower one is usually supported by all cards.

  Also notable about this protocol is, that every packet starts with 8 bytes of fixed header information, where the first 6 bytes are only zeros[3].

- Vicinity cards

  Vicinity cards as defined in ISO15693 are designed to achieve bigger communication distances than the proximity cards defined by ISO14443. ISO15693 reader to card communication uses again ASK. The reader may use 10% or 100% modulation degree. In contrast to the previous methods, the coding scheme (1 out of 4 or even 1 out of 256) ensures, that the field has full amplitude most of the time at the price of a lower data throughput.

  Card to reader communication again works with a sub carrier. However, the sub carrier can be either amplitude or frequency modulated[4] (FSK).

[3] Because of the Manchester coding, the first 6 bytes look like a sub carrier.

[4] The frequency modulation is called "Dual Subcarrier" in the standard.

2.3.2 Initialization and anti collision

If multiple cards are placed on an NFC reader, it is still able to communicate with every card separately, as long as all cards can be powered.

The different protocols handle multiple cards in a similar way. After the "initialization and anti collision phase"[5], the NFC reader knows, which cards are in the field. Afterwards it can choose one card to activate and communicate with. Meanwhile one card is activated, the other cards are in the halt mode. They wait for a wake up packet, after which they can be activated by the reader.

Every card has an unique identification number (UID). This number is either hard coded or random.

- Type A

  The reader will start with a Request A (REQA). This is a 7 bit long command. Initially, all cards in the field will answer with an answer to request A (ATQA), which is 2 bytes long. The REQA/ATQA communication is used for detecting compatible devices. It is recommended not to relay on the information sent in the ATQA[1].

  With the ANTICOLLISION command, the reader asks for the UID of the cards in the field. The ANTICOLLISION command may already contain part of the UID. Then only cards, which start with that fraction of the UID may answer. The first ANTICOLLISION command contains no part of the UID. If a collision at the kth bit was found, the reader can choose to send a new ANTICOLLISION with that bit being 0 or being 1.

  The last ANTICOLLISION command contains the whole UID of one of the cards. This command is then called SELECT. The UID of a card can be of single, double or triple length. In case of double or triple length, the anti collision procedure is performed in stages. The UID is fixed at production for most type A cards.

  Devices, which emulate cards, are supposed to have a randomized UID. On every field reset, the UID shall be fresh. Such random identifiers can be identified by the value of the first byte of the UID. However, several phones could be found, which constantly present the same UID.

- Type B

  The minimal communication for activating type B cards contains following packets:

  REQB, ATQB, ATTRIB, Answer to ATTRIB.

  Every type B card may have an application identifier (AFI). The reader may poll for only cards used for a specific application. This can already avoid collisions.

  In contrast to type A cards, anti collision works with slots. Therefore, in the request B (REQB), the NFC reader defines a number of slots. Each card (with matching AFI) will choose one slot at random. The Slot-MARKER command is sent by the reader to poll for all cards in a specific slot. By separating the responses in slots, the probability of collisions is reduced. However, if there are still multiple cards in

[5]This term is used in 14443.

one slot, the already identified cards can be put into a halt state and the process can be repeated by sending again an ATQB.

The type B commands in the anticollision phase are longer, than the type A commands. A REQB contains already 5 Bytes. The ATQB is even 14 bytes long.

The ATTRIB command and response are used to select a card and to already exchange many attributes (like frame sizes and bit rates).

- FeliCa

  The anti collision phase of the FeliCa protocol is similar to this phase of the type B protocol. Like NFC-B it uses a slot based principle as well. However, the NFC reader does not poll for each slot separately, but the slots are separated by a constant time.

  The minimal command sequence for anticollision and initialisation is REQ (request), ATQ (request response), ATTR (attributes) and ATTR response.

- Vicinity cards

  With ISO15693 the terminology changes, but the operation principles stay similar to the type B and F mechanisms. First the reader sends an inventory request, which is the pedant to the request (REQ) command. As with ISO14443-B each card with matching AFI answers in one slot. However, the assignment of slot numbers is not randomized, but based on the UID. In case of a collision, a similar procedure to the type A anticollision can be performed. A mask for UIDs can be defined in the inventory command to restrict the command to only vicinity cards of one slot.

  Also it is interesting to note, that a selection command exists, which activates one card, but the reader can also include the UID in every command instead[6].

2.3.3 Higher protocol levels

On top of these basic commands to establish a connection, there are further commands defined, which are used to operate a card. For understanding this thesis, only lower level protocol properties of the last two sub sections are required. To provide some insight on how NFC works, this section contains a brief introduction on a higher level view.

Unfortunately there are different extensions and command sets for the protocols mentioned above, which can be used to build the NFC stack. For example a type A card may or may not support 14443-4 and ISO7816. However, this drastically changes, how to operate the card. Generally, all protocols share some important commands:

- Read command

  Usually there are one or multiple commands to read the cards memory.

- Write command

  Usually there are one or more commands to write data to the cards memory.

[6]The select command is not even mandated to be implemented by every card.

- Lock command

  Often, cards shall be "programmed" once (eg. with an identifier). Many protocols allow to lock parts of the memory and therefore make them read only.

- Security related commands

  Some protocols contain security related commands. This involves then variants of the read and write commands, commands to write to the key storage (without read access) and authentication commands.

- Application related commands and memory organization

  Some protocols like ISO7816 define application identifiers, which can be registered and then allow to uniquely identify the purpose of a card or to even store multiple applications on a single card. For this to work, each application needs a separate memory region on the card.

Of special interest are cards which comply to ISO7816 (Identification cards). Not only does this standard define AIDs (Application Identifiers) to store a specific application (like Visa, MasterCard, Global Platform, ...), but it also defines "Files", which serve as data structure with access control. The NFC Forum speaks of ISO-DEP when referring to this standard. [7]

The digital specification of the NFC Forum[4] defines 5 different tag type definitions named T1 to T5 for the protocols mentioned above. For every protocol, the NFC Forum defines an unambiguous position to store data.

The data is then organized in so-called TLVs. TLVs are a very simple method to structure data. The acronym stands for "Type, Length, Value". The first byte denotes the type. And between zero and 3 bytes encode the length of the value. Finally, multiple TLVs are stored sequentially in the cards memory.

A TLV can contain a so-called NDEF (NFC data exchange format) message[11]. And NDEF messages can be used for many purposes. An NDEF message contains self-descriptive data. The type can be encoded as URI (Unique resource identifier), as MIME (multipurpose internet mail extension) or NFC-specific types. NDEF messages are a handy and very generic construct, which can be used to store text, pictures, http requests, to provide automatic Bluethooth pairing via NFC and much more.

2.4 Experiments, showing the communication

2.4.1 Normal NFC communication

Test setup:

The NFC communication with a NFC card is sniffed with a single loop antenna. Wireless charging is turned off for this setup. At the beginning the Request A (REQA) can be seen. It is transmitted with amplitude modulation with a modulation coefficient of 100%. After about $90\mu s$, the NFC card responds with an Answer to Request A (with passive load modulation).

[7] When writing a card emulation application for a mobile phone, usually work is done on this abstraction level.

This sequence is the starting point of a type A communication[8]. If this sequence works in presence of a charging field, the reader already learned, that there is a type A device in the field.

2.4.2 Distorted NFC communication

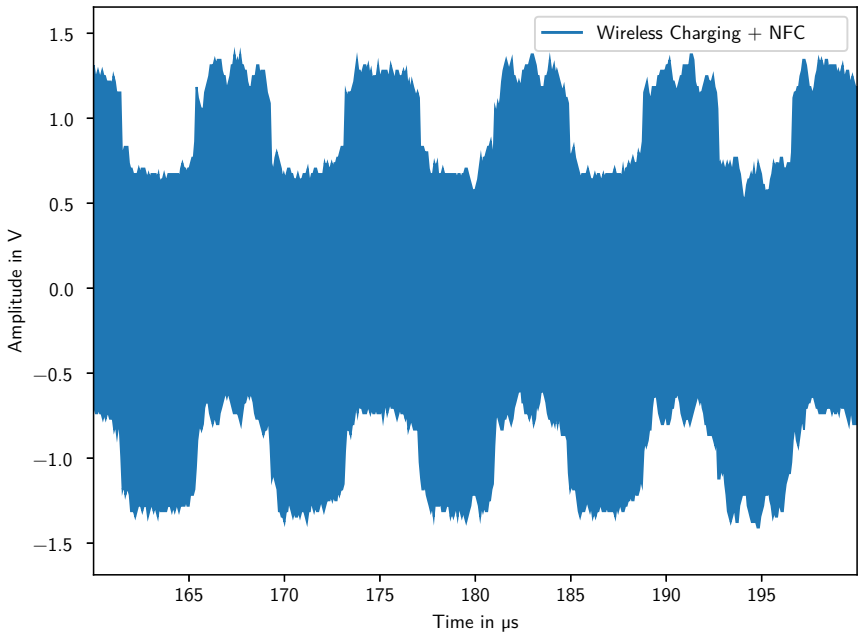

Figure 2.4: NFC field in superposition with a charging field

For this experiment, the wireless charging system and the NFC reader is active. To activate both, a mobile phone with support for both is placed on top of the combined setup. A pickup antenna is placed in between the combined wireless charging and NFC setup and the phone to record the field on an oscilloscope. The recorded voltage can be seen in figure 2.4. The rectangular wireless charging waveform can be seen in superposition to the NFC field. Also, the load modulation of the mobile phone is visible clearly.

2.5 Designs of NFC transponders

To investigate different error scenarios, the behavior of the counter part, the PICC, is of interest too. NFC transponders can be divided in two classes.

- Passive devices (cards and tags)
- Active devices (phones) with card emulation

[8]Instead, the reader may send the wake up command WUPA, which additionally wakes up cards, which were sent to the halt state.

2.5.1 Passive NFC devices

Banking cards, identification cards or passports are often NFC enabled. The layer with all electrical active components is called inlay. Usually, the antenna of these NFC cards are inside of the inlay. The antenna is a coil etched in a thin layer of aluminum or copper. Alternatively in some cards wire is used instead. The IC for NFC is connected to this antenna. In most cases the chip is a two terminal device.

To increase the efficiency, the circuit is designed to be resonant at about the carrier frequency of 13.56MHz[9]. Usually, this resonance is achieved with a capacity parallel to the NFC coil. In most cases it is realized without a separate capacitor component. This can be avoided, because already the IC and the NFC antenna have a certain capacitance.

In this document, the terms “NFC card”, “NFC tag” and PICC are frequently used. However, for most considerations the terms can be exchanged. The difference is, that tags usually can be sticked to surfaces, often have smaller form factors and use simpler protocols with cheaper NFC ICs.

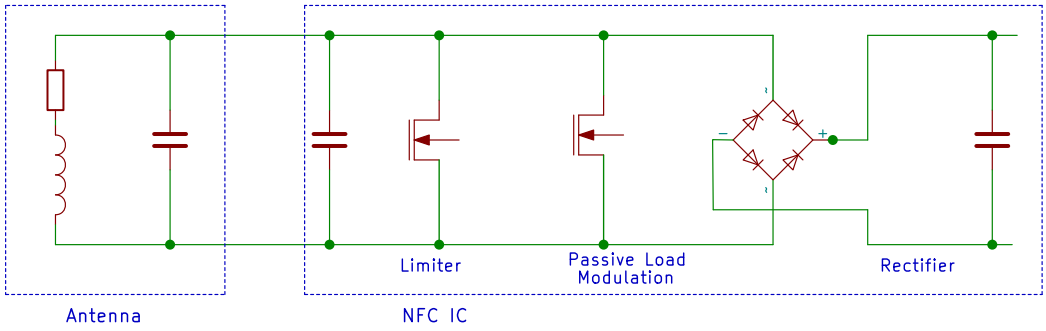

Figure 2.5: Equivalent circuit of an NFC card

Passive devices harvest the energy for operation from the magnet field. Therefore, they rectify the voltage at the input pins. The equivalent circuit of a typical NFC card can be seen in figure 2.5. At the left, the NFC coil with a series resistance and a parallel capacitance is shown. The integrated circuit has only two pins and adds additional capacity. To the right, a rectifier is shown, which creates a supply voltage for the chip.

The manufacturing process of the IC limits the maximum voltage, which is allowed at the inputs. But depending on the coupling between NFC card and reader, the induced voltage will vary. To force a reduction of a too high voltage, a transistor creates a parallel load. This transistor with an additional control circuit is called limiter.

To send data back to the reader, the field is modulated by a technique called “passive load modulation”. As delineated in figure 2.5, a parallel transistor shorts the inputs. The reader receives this modulation by detecting a change in the load (and therefore the current).

Not on the equivalent schematic are the demodulator and the clock recovery. In section 3, a possible topology for the second will be described.

[9]Usually a slightly higher frequency is chosen[16].

2.5.2 Active NFC devices (mobile phones, card emulation)

Active NFC devices like phones are supplied with power externally. They do not harvest energy from the field. This typically results in a greater area of operation. Besides, it allows to reduce the size of the NFC antenna.

However, with a reduced antenna size, the passive load modulation has less impact on the load impedance at the reader. This might impact the performance of the PICC to PCD communication.

As a countermeasure, most active devices use so-called "active load modulation". Instead of only changing the impedance, a current is actively driven through a coil to generate a NFC field in superposition to the carrier created by the reader.

If a device uses active load modulation, the modulation index seen at the reader is much bigger than with passive load modulation. However, different challenges with the synchronization appear as analyzed in [5].

It is not always possible to distinguish between active devices and passive cards or tags. There are some protocols, for which card emulation is not defined. If one of those protocols is detected, it is a passive card. If a device supports ISO-DEP ("Data exchange protocol"), it is a card. Otherwise, if it supports NFC-DEP, it is a device.

2.5.3 NFC charging

NFC energy harvesting can be used for charging small devices (wearables). Several considerations like efficiency and maximum power are analyzed in [15]. NFC charging is often used, when the form factor does not allow the integration of Qi wireless charging coils or if the power consumption does not justify the costs for integrating a QI system.

Besides NFC and Qi charging, there exist also other protocols for wireless charging.

2.5.4 Standardized card formats

ISO14443-1 standardizes different coil sizes. The geometries are not mandatory for card manufacturers. However, the test procedures and the maximum ratings for readers are defined for these devices [7].

The formats are named ID1 to ID6[10]. ID1 coils are the biggest and cover most of the area of typical cards. ID2 coils use about half of the width of the ID1 format. They are used for instance in debit cards, where the wire would be damaged by mechanically punching the numbers into the cards. The ID3 to ID6 geometries are intended for smaller cards and are popular for NFC Tags.

[10]ISO 7810 also defines card formats. There, the outline of the card it self is standardized. The geometries are called ID-1 to ID-3. However, they are not compatible with ID1 to ID3 from ISO14443.

2.6 Introduction into Qi charging

QI is a protocol for inductive power transfer in the low frequency region. The Qi standard distinguishes between several power classes. In this thesis, only the power class 0 is considered, which is used for charging phones. Among wireless charging options for phones, Qi is the most used protocol.

In the so-called basic power profile, up to 5W can be transmitted. For higher needs, the extended power profile was introduced. It supports power of up to 15 Watt.

The frequency in Qi wireless charging usually is varied between 100kHz and 200kHz. Moreover, the frequency may be used to adjust the transmitted power. However, for several reasons the frequency was fixed to 127774Hz for the setup.

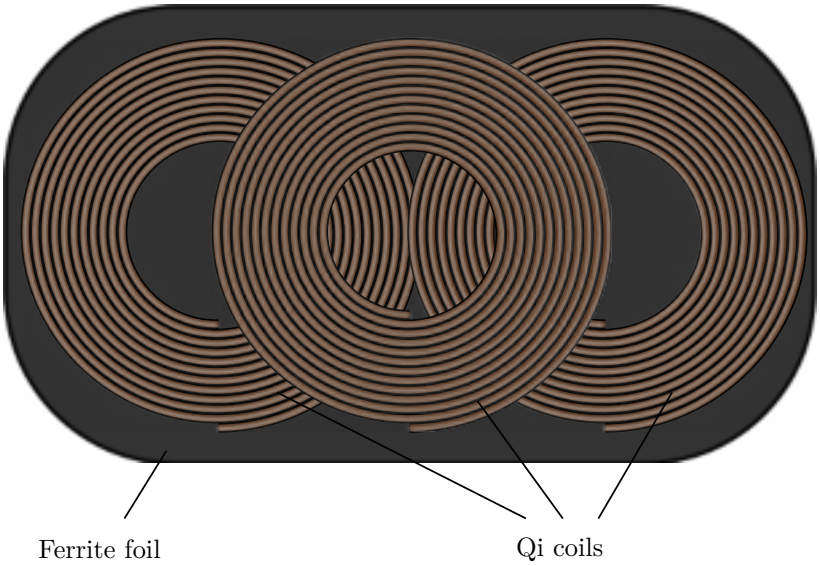

Figure 2.6: Sketch of the MP-A9 coil layout

The standard provides a set of reference antenna setups. In the application, the 3 coil setup MP-A9 was chosen. Figure 2.6 shows a sketch of the three charging coils on top of a ferrite foil, which is also defined by the Qi standard. The three partly overlapping coils allow to place the receiver more freely. Only the coil with the best coupling to the power receiver is activated for the power transfer.

2.7 Qi Circuitry

Figure 2.7 shows the principal behind the driver of a Qi charger. The circuitry with the four switched transistors, which is also called H-bridge due to its shape, is used to maximize the efficiency. The DC voltage V_{rail} is applied to the load with alternating orientation (first from the left to the right and then from the right to the left). In order to achieve this functionality, in the first half-period only T1 and T4 are switched on. Then in the second half-period, only T2 and T3 are switched on. Finally, the output is a pulse-shaped voltage signal.

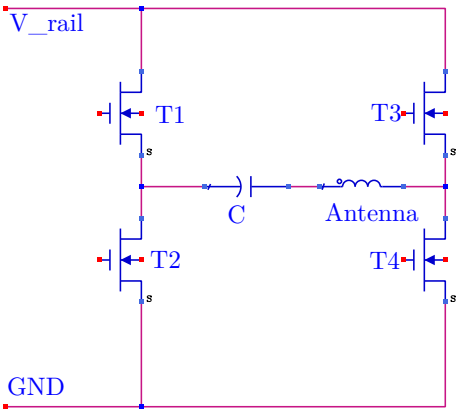

Figure 2.7: Wireless charging resonance circuit

In the basic power profile, often this signal is pulse-width modulated. However, in contrast to the usage in audio drivers, no oversampling is used in Qi charging. In order to avoid additional switching losses, the rectangular pulse signal is applied to the load directly with the charging frequency of 100 to 200kHz.

In the center of figure 2.7, a coil and a capacitor can be seen. The coil is used to generate the magnet field for the wireless power transfer. In order to increase the efficiency, the capacitor builds a series resonance circuit with the QI antenna. However, the resonance frequency of coil and capacitor[11] usually is lower than the operating frequency of the charger.

2.8 Qi communication

In contrast to NFC, the communication between power transmitter and power receiver is not used to create a data link, but only to establish the energy transfer and adapt to changes, eg. in the load of the power receiver (charging phases of a battery), in the coupling between the transmitter and the receiver or when foreign objects move into the operating area.

With NFC the reader, which provides the magnet field, is the master of the communication. In contrast, with Qi the power receiver is the master of the communication. First, always the receiver sends a request or information packet. Depending on the packet, the power transmitter might then answer this packet.

2.8.1 Modulation schemes and physical layer

Power transmitter to power receiver communication

The power transmitter sends information by modulating the magnet field using Frequency Shift Keying (FSK). The frequency of the magnet field is switched between two levels in order to encode the binary base band signal. Depending on the configuration, the period

[11] in the unloaded case without power receiver

of the two frequencies differs by up to 282ns. The data bits are encoded using a differential Manchester scheme (also called bi-phase encoding). Each bit is transmitted in 512 periods of the charging signal, resulting in a raw bit rate of about 250 bit/s depending on the frequency of the carrier.

Each byte is extended by a parity bit and a stop bit. Finally, a packet consist out of a header (1 byte), the message and a checksum (1 byte).

Additionally, three responses are defined, which require only one byte and neither contain start, stop nor parity bits. The responses are acknowledge (ACK), not acknowledge (NAK) and not defined (ND).

Power receiver to power transmitter communication

The power receiver communicates similarly to NFC cards by modulating the load. The power transmitter shall detect the load change by measuring the current and voltage at the primary coil.

The bits are again encoded in the differential Manchester scheme. Furthermore, the raw bit rate is defined to be 2 kbit/s. Again, every byte is followed by a parity and a stop bit.

A communication packet consist of a preamble, a header, the message and a checksum. The preamble are between 11 and 25 bits of ones. Header and CRC are both again 1 byte long.

2.8.2 Initialization

Analog Ping

Initially, the charger starts with a so called analog ping. Therefore, the charger sends a short pulse packet at the resonance frequency and records the current. If a metallic object is in the operating area, the LC resonance circuit will be detuned and the current will change. By comparing the current to a reference value, the charger can assess, if there are any objects in the magnetic field. This could be a power receiver (eg. a mobile phone) or a foreign object of an electrically conductive material.

The analog ping is a low power mechanism for detecting devices. Furthermore, it is one of the implemented foreign object detection methods (see section 2.8.4). However, the Analog Ping is not required by the QI specification. The principle of operation is similar to the “Low power card detection” feature of many NFC reader ICs.

Digital Ping

A so-called digital ping lasts for a longer duration than the analog ping and shall be answered by the power receiver (with a signal strength packet). When receiving an answer, the power transmitter (Qi charger) learns, that a QI receiver is in the magnet field, and that it is not heating up metallic objects, which moved in the field.

Identification and Configuration, Negotiation and Calibration

In the identification and configuration phase, the receiver informs the transmitter, how it wants to operate (eg. the maximum power expected by the power receiver and certain

minimum and maximum values for some parameters). The power transmitter derives a so-called power contract from that information.

In the extended power profile additional steps must be performed. In the so-called negotiation phase, the power contract is further negotiated. Therefore, the power receiver sends negotiation requests, which then can be accepted or denied by the power transmitter.

Another phase in the extended power profile is the calibration phase. In this phase, the power receiver measures and reports the power consumption at two different loading conditions. The power transmitter measures its power consumption as well. As a result, the transmitter can refine its model of the transmission losses. Therefore the Foreign Object Detection procedure gets more accurate.

2.8.3 Power transfer

During power transfer, the power receiver sends following packets:

- Control Error packet
- Received Power packet
- Renegotiation request

The control error packet informs the transmitter, if the receiver needs a higher or a lower voltage. Then the wireless charger is supposed to adjust its parameters accordingly. Depending on the power contract and the operating point it might adjust the frequency, the duty cycle or the amplitude of the pulse signal.

The received power packet contains information about the power at the power receiver. The transmitter can therefore calculate the losses. This information can be used for Foreign Object Detection (see next section).

The receiver is always the master of the protocol. It initiates every communication. The power transmitter only responds. During the power transfer the receiver is allowed to end the power transfer or in the extended power profile to renegotiate the power contract my sending a Renegotiation request.

2.8.4 Foreign object detection (FOD)

The energy transmitted with QI can heat up metal objects in the magnet field to a dangerous level. Two algorithms are implemented to detect foreign objects, which draw energy.

The first algorithm runs in the low power (stand by) mode and uses the analog ping described in section 2.8.2. This algorithm detects changes in the resonance frequency of the Lc series circuit. Detected are power receivers and magnetically active (mainly metallic) objects in the operating volume. However, NFC cards might not be detected, because they do not influence the charging system strong enough.

The second algorithm runs during the power transfer and works by monitoring the losses. This mechanism is important to protect the safety of the user, because foreign objects may heat up during wireless charging to a dangerous level.

This second algorithm works by detecting unexpected power losses. The power transmitter measures the current and the voltage. Therefore, it can calculate the input power. Furthermore, the power receiver measures those values at the receiver side too. It can

therefore calculate the output power. Because the receiver periodically informs the transmitter about the received power, the transmitter can calculate the losses.

In the basic power profile, the power transmitter has fixed formulas implemented, how much energy loss is expected at a certain loading condition. These formulas usually are calibrated once and then shipped with the wireless chargers firmware. For the extended power profile, a fine calibration of those formulas can be performed during the calibration and recalibration phases of the Qi protocol.

If during the power transfer the difference between the measured losses and the predicted losses gets bigger than a threshold value, then the wireless charging is stopped. These additional losses could be caused by a foreign metallic object, which heats up because of eddy currents. However, it was found that the losses in 13.56MHz NFC cards are often too small to be detected.

2.8.5 Power adjustment

Usually, the power receiver further regulates its output voltage or current eg. to meet the requirements for charging a battery. Therefore, the load draws a certain power independent of the magnet field. The power transmitter cannot force a different power level into the power receiver.

Theoretically, the maximal power is transmitted, when the load is matched to the source. That means, that the impedance of the load is the complex conjugate of the impedance of the equivalent voltage source. If the impedances mismatch, the received power drops. However, the circuit is not tuned to be impedance matched, because the source is very low ohmic. Moreover, if it was matched, the efficiency is already lower than 50%.

Therefore when speaking of power adjustment, then actually the voltage/current at the receiver is adjusted. The receiver can ask the transmitter to either increase or decrease the power, which actually means, that the induced voltage at the receivers coil will change.

Because the power receiver has control over the protocol, already the QI communication can be used to regulate the voltage at the receivers coil. So for instance, if the receiver uses a buck converter in order to generate 5V at its output, it might regulate the induced voltage to maybe 10V, whereas with an LDO (low dropout converter), it would target a value much closer to the 5V.

The Qi protocol foresees three possibilities to adjust the power.

- Frequency

  By changing the frequency, the proximity to the resonance frequency can be adjusted. Generally moving closer to the resonance increases the transmitted power.

  For the extended power mode in the product, the frequency is fixed to 127.774kHz. Therefore, adjusting the frequency is not allowed.

- Pulse width

  This mode is especially used when operating at lower powers. Because only AC parts of the signal contribute to the transmitted power, its amount is maximum for a duty cycle of 50% and decreases for lower and for higher values. By changing the duty cycle of the charging signal, the transmitted power can be adapted.

- Rail voltage

  The rail voltage is the DC voltage, which is then switched by the H bridge. Under the assumption that the system is linear, the rail voltage is proportional to the field strength and to the induced voltage in the power receiver. Adaption of the rail voltage is the method used in the extended power profile.

  For the wireless charger of the setup, the rail voltage is generated by a DC DC converter and can be adjusted up to 22V. Usually the value is below 10V with typical LDO based power receivers, as they are used by most phones.

  If the phone is misaligned to Qi charger and therefore the coupling is bad, the induced voltage would decrease. Because of the feedback system, the rail voltage is then increased to compensate this effect. Therefore, the critical case for compatibility between Qi charging and NFC is, when the phone is badly aligned on the charger.

Chapter 3

Analysis of challenges in combined Qi and NFC systems

In this section, two phenomena are analyzed. First, it was found, that when a device is being charged, NFC communication is not possible anymore or at least the performance suffers. In order to find the dominant failure modes, the interferences between the wireless charging system and the NFC system are analyzed. The motivation behind these considerations is to identify counter measures, which can be implemented to solve the coexistence problems stated earlier.

Secondly, the processes related to Qi-charging that cause damage to NFC cards are analyzed. The observations shall clarify, why cards are damaged. Ideally, this knowledge can be used to predict the risk of destruction and to design either save wireless chargers or resistant NFC cards. It was found, that the same effects that cause damages on the cards also have negative impact on the NFC communication. Therefore, both topics are investigated in the same section.

3.1 Influences between NFC and Charging system

There are several ways, how the charging system and the NFC system could influence each other.

- Common PCB

  Both systems are on the same PCB. There could be cross talk. For example switching noise on the power lines (ground bounce).

- Common area of fields

  Both systems transmit and receive in the same area. Unfortunately, all antennas couple. An expected effect is distortion of the communication. Over voltage could cause temporal or permanent failures. Furthermore, matching circuits are detuned.

  If there is a phone on the charger, it strongly effects the NFC field distribution.

  NFC cards can be permanently damaged by the charging field. Besides, the internal logic of the card could be distorted temporarily. Different error cases on the card side are analyzed in this section.

- Common ferrite

  Additionally, the ferrite foil below the charging coils has an effect on the NFC system. Ferrites are designed for a certain frequency range. The ferrites for wireless charging might be lossy for NFC frequencies.

  If the ferrite goes into saturation, it becomes non-linear.

The common area of the fields is expected to be the major source of malfunction. Furthermore, the setup with two boards already eliminates the first error source.

3.2 NFC Failure modes

In this section, the effects of the common area of the fields are discussed.

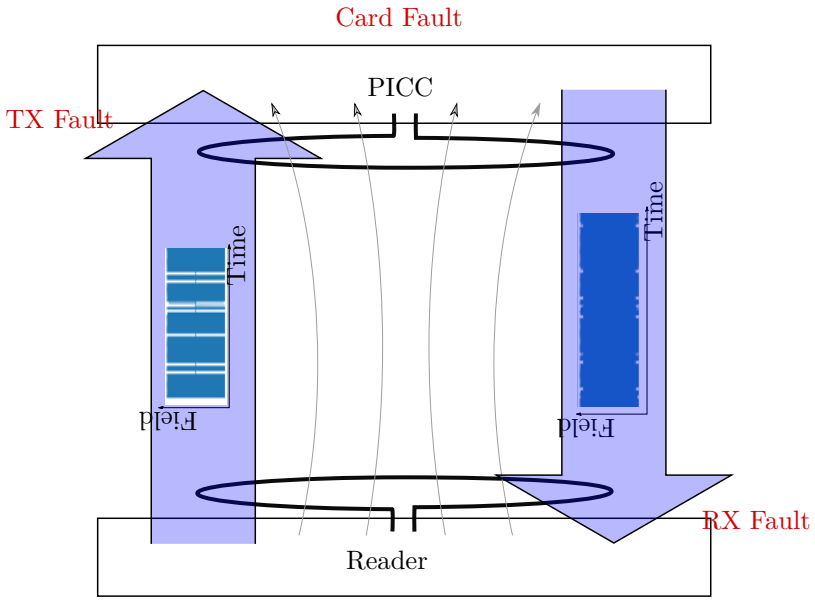

Figure 3.1: Graph for identification of error sources for NFC communication during wireless charging

One communication cycle is shown in figure 3.1.

Beginning at the bottom of the figure, the reader modulates the request on the field (here a Request A is shown). The card processes the request. After the frame delay time, it answers by modulating the field. The reader detects the sub carrier and derives the answer. (In the figure, an ATQA is shown.)

In red, the three major faults during communication are noted. Where could a failure in combination with wireless charging come from?

3.2.1 TX failures

Because of the charging field, the card cannot understand the requests anymore. It does not send any answer.

ISO14443 regulates the maximal settling times, maximal overshoots and the maximal deviation of the field strength for reader to transponder communication. Every card has to be able to operate with those deviations to be conforming to the standard [7].

However, those ratings cannot be applied on the distortions of the charging field. There are no specifications on the maximal noise level in the low frequency range.

The existence of TX failures therefore must be evaluated by experiments on real cards.

3.2.2 Card failures

ISO14443 does not specify, up to which charging field strength, a card has to operate. The value of $7.5\,\mathrm{A/m}$ (for the ID1 form factor) specified in ISO14443-2 is only valid for the carrier frequency of 13.56MHz. The charging field strength is much higher than this value.

Along with the NFC field, the charging field is modulated as well during load modulation. The card might fail to pull the necessary currents.

Typically, NFC cards have limiters to protect the IC from overvoltage. If the limiter starts to operate because of the charging field, then one half of the NFC carrier is shorted by the limiter. This effect, caused by the non-linearity of the limiter could be seen as mixing between the charging and the NFC signal. Moreover, it can confuse the clock generation of the card.

As a result, the load modulation can be invalid or weak. The state machine on the card (which is defined in various standards) could get corrupted.

3.2.3 RX failures

If a card manages to understand and answer the request, the reader still needs to understand the answer. The voltage induced by the fundamental charging field could act as an additional bias voltage to the ADC at the RX pin.

The harmonics could distort the communication. Certain frequencies close to the carrier could get misinterpreted as a sub carrier. Especially critical for the communication at the lowest bit rate are frequency components close to $13.56\mathrm{MHz} \pm 847.5\mathrm{kHz}$, because these are the main frequency components generated by the load modulation.

3.3 Analysis of the harmonics of wireless charging

The circuit of the wireless charging transmitter is simplified as shown in figure 3.2. The H-Bridge generates a differential signal, which is applied to a series resonance circuit. Resistive parts, parasitic capacities, transistors and the other coils are neglected for the considerations in this section.

The signal source is assumed to be a perfect rectangular voltage, neglecting slew rate and possible break before make issues[1]. For a duty cycle of 50%, the signal has no DC offset. For any other duty cycle, this property does not hold anymore.

$$v_{in}(t) = \begin{cases} +V_{rail}, & \text{for } 0 \leq t \leq T_1 \\ -V_{rail}, & \text{for } T_1 \leq t \leq T \end{cases}$$

[1] If in figure 2.7, T1 opens, before T2 closes, then the current has no path anymore. But, because the coil forces a continuous current, it closes over (parasitic) capacitors and creates huge voltage overshoots.

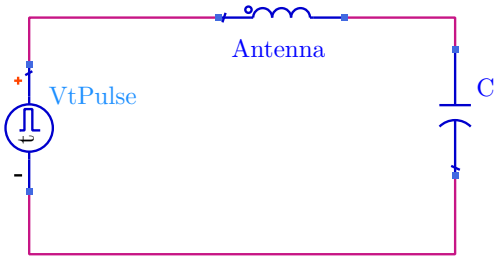

Figure 3.2: Equivalent circuit of the Qi power transmitter

3.3.1 Transformation into the frequency domain

The complex Fourier series becomes:

$$\begin{aligned} V_{in}[n] &= \frac{1}{T}\int_0^T v_{in}(t)e^{-jn\omega_0 t}dt \\ &= \frac{1}{T}\frac{1}{-jn\omega_0}(V_{rail}e^{-jn\omega_0 T_1} - V_{rail} - V_{rail} + V_{rail}e^{-jn\omega_0 T_1}) \\ V_{in}[n] &= \frac{V_{rail}}{jn\pi}(1 - e^{-jn2\pi\frac{T_1}{T}}) \end{aligned} \tag{3.1}$$

The $1/n$ in (3.1) causes the typical $1/f$ behavior of a rectangular pulse. For example, if the rail voltage is 10V and the duty cycle is the 99th harmonic at $f \approx 12.8$MHz has an amplitude of about 127mV.

The second term is a factor with an amplitude between 0 and 2. If the duty cycle is 50%, all even harmonics cancel, while for the odd harmonics the factor has the maximal value of 2. Also note, that the calculated values $V_{in}[n]$ are elements of the complex Fourier series. In order to get the amplitude of a sinusoidal wave, an additional factor of 2 has to be applied.

3.3.2 Filter effects of the circuit

Considering the circuit in figure 3.2, the transmission function between V_{in} and V_{ant} can be calculated for the unloaded case as

$$\frac{V_{ant}}{V_{in}} = \frac{sL_{ant}}{sL_{ant} + \frac{1}{sc}} = \frac{1}{1 + \frac{1}{s^2 cL_{ant}}} = \frac{1}{1 - \frac{1}{\omega^2 cL_{ant}}}$$

This function has a pole at the resonance frequency of the charging circuit. At higher frequencies, the ratio approaches 1. Therefore, higher frequency components are not filtered by the circuit and can be seen with identical amplitude on the active charging antenna.

It is also interesting to analyze the behaviour in the time domain. When the rectangular input voltage switches the sign, the voltage in the capacitor at first stays constant. Therefore, the full voltage jump lays on the wireless charging coil. This behaviour also could be observed with an oscilloscope.

3.3.3 Effects of the Qi signal on the NFC reader

The field strength generated by the wireless charger is proportional to the current through the coil. The voltage over the primary coil must be integrated to get the current. However, in order to calculate the voltage which is induced in the NFC antenna, again the derivative of the field is of interest.

The voltage at the NFC antenna (open condition) can be calculated as:

$$V_{NFC} = sMI_{WCh} = \frac{sMV_{WCh,ant}}{sL_{WCh}} \approx \frac{V_{in}M}{L_{WCh}} \text{for higher frequencies} \tag{3.2}$$

The distorting voltages are the harmonics of the rectangular charging voltage damped by M/L_{WCH}. As the antenna of the NFC reader is in a fixed arrangement with the charging coils, permanent reduction of this voltage can be achieved by minimizing the mutual inductance M.

This voltage (3.2) can be observed with an open NFC reader antenna. Because every consideration was linear so far, an equivalent circuit can be easily calculated. Figure 3.3 shows a T circuit (also used eg. in [12]), which is used to describe the magnetic coupling between wireless charging coil and NFC reader antenna. To simplify equations at higher frequencies, the wireless charging resonance capacitor can be neglected.

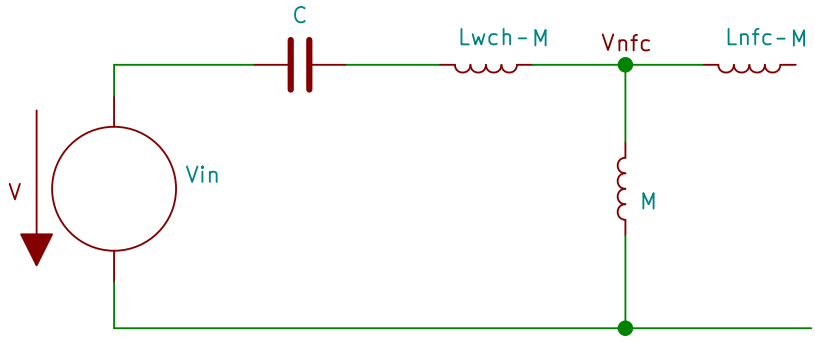

Figure 3.3: Equivalent circuit of the coupling situation between the NFC reader and the wireless charger

In figure 3.3, an equivalent T circuit for the coupling situation between charger and NFC reader is shown. It can be observed, that the T circuit is correct if the secondary side is open. Furthermore it can be verified, that it is correct, when the secondary side is shorted. It follows, that it is valid for any load.

The equivalent linear non-ideal voltage source has an internal impedance of

$$\begin{aligned} Z_i &= s(L_{NFC} - M) + \frac{sM(sL_{WCh} - sM + \frac{1}{sc})}{sL_{WCh} + \frac{1}{sc} - sM + sM} \\ &= sL_{NFC} - \frac{s^2M^2}{sL_{WCh} + \frac{1}{sc}} \approx sL_{NFC} - \frac{sM^2}{L_{WCh}} = sL_{NFC}(1 - K^2) \\ Z_i &\approx sL_{NFC}(1 - K^2) \end{aligned} \tag{3.3}$$

when neglecting the matching capacitor and the parasitic interconnects. In the equation, K is the coupling factor, which will be discussed in section 3.5 in more detail.

3.3.4 Effect of the harmonics on the RX pins

In this section it is analyzed, how the harmonics of the wireless charging signal affect the RX input voltage of the NFC reader. The NFC matching network acts as another filter circuit. For simplicity, the single ended circuit is analyzed.

During the reception phase of the NFC reader the transceiver still creates an NFC carrier in order to power the PICC. The effect of the carrier is not of interest for this consideration. Because of the linearity of the network, the TX pins must be shorted, when considering the effects of a different source.

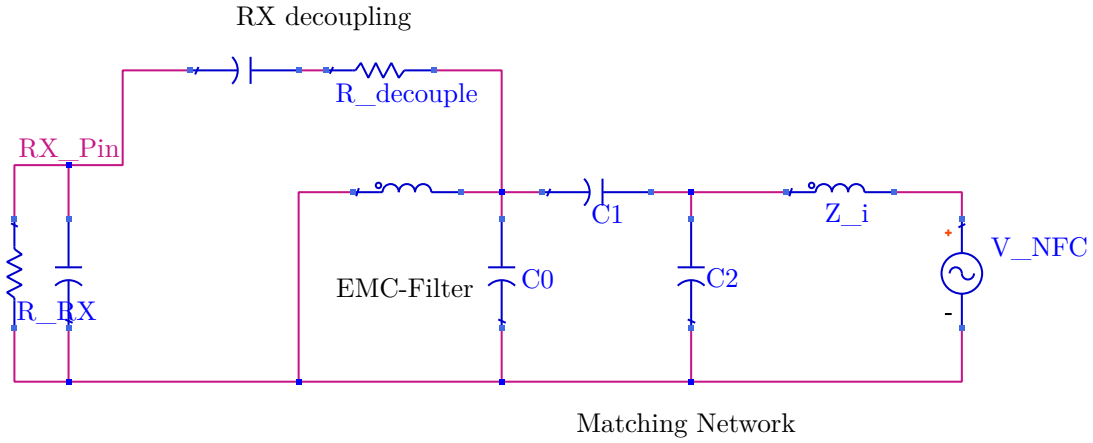

Figure 3.4: Equivalent circuit for calculating distortions at the RX pins

Figure 3.4 shows the matching network with the TX pins shorted. Furthermore, the input impedance of the RX pins of the IC is modeled as a resistor and a capacitor in parallel, which can be seen at the very left of the figure. The source is the voltage induced in the NFC antenna caused by the magnet field of the wireless charger on the very right of the figure. Finally the output is the voltage at the RX pins.

The distortions are induced in the NFC reader antenna and flow through the matching network to the RX pins. Over the same path, the load modulation of NFC cards gets transferred. Therefore, it is of special interest, what happens to signals in the frequency range close to the NFC carrier.

Coming from the right, first a low pass filter of second order can be seen. Its corner frequency is usually above the NFC carrier frequency.

The EMC filter is now a parallel circuit of C0 and the EMC coil. It is low ohmic for low and high frequencies. However, for frequencies close to the EMC frequency, the impedance tends towards infinity. For high frequencies, C1 and C0 build a capacitive voltage divider. At low frequencies, C1 and the EMC coil build a low pass filter of second order.

The RX decoupling capacitors on the top of figure 3.4 filter out the DC voltage. Because of the high capacitance, only very low frequencies are filtered by $C_{decouple}$ (even the fundamental charging frequency is not attenuated significantly). Very high frequencies are further attenuated by the parasitic capacity on the RX pins. However, for most frequencies

the RX decoupling only causes a constant damping because of a resistive voltage divider with the input resistance of the IC.

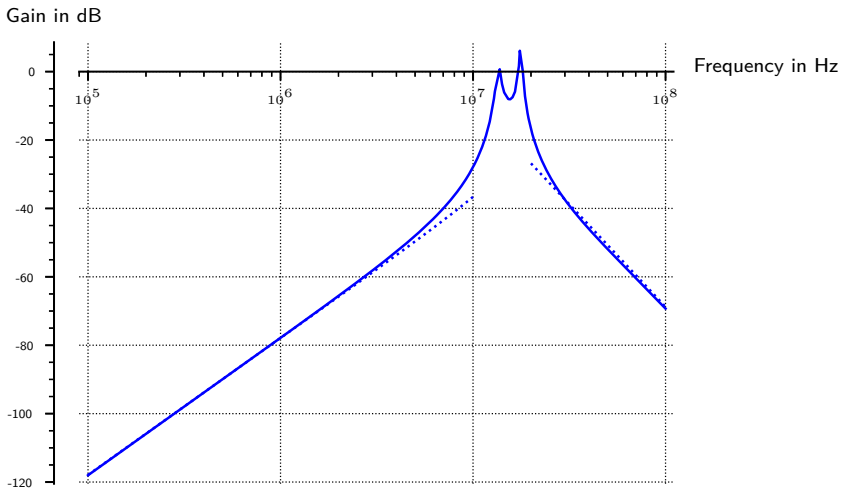

Figure 3.5: The transfer function of an NFC matching network from an induced voltage in the coil to the RX pins

Finally, for low frequencies, the attenuation can be described by a second order high pass filter characteristic. C1 and the EMC coil determine the cutoff frequency. In figure 3.5, a typical transfer function can be seen. The dotted asymptote on the left shows 40dB per decade.

High frequency components on the other hand are attenuated with -60dB per decade, caused by the low pass characteristic created by Z_i and C2 (2nd order) and by the low pass filter consisting of the chip capacitor and the resistors in the RX path. An additional damping is created by the capacitive voltage divider (C0 and C1). This behaviour can be seen at the dotted asymptote on the right in figure 3.5.

For frequencies close to the NFC carrier, the circuit can be seen as two resonance circuits (L_{EMC} with C0 and Z_i with C2), which are capacitively coupled by C1. In figure 3.5, the two resonances can be seen in proximity to the NFC carrier frequency. This structure causes a voltage gain for NFC frequencies.

For calculating the spectral components of the voltage at the RX pin, the gain from figure 3.5 must be multiplied by the spectral components derived in equations (3.2) and (3.1). The spectral components at the RX pins caused by the charger are expected to first increase with 20dB/decade (1/f signal filtered by a second order high pass). Close to the NFC carrier, the spectral components are high. Frequency components higher than the NFC carrier decay with -80dB/decade for high enough frequencies. The conclusion is, that low and high frequency components are attenuated by the matching network. However, signal components close to the NFC carrier fully affect the voltage at the RX pins.

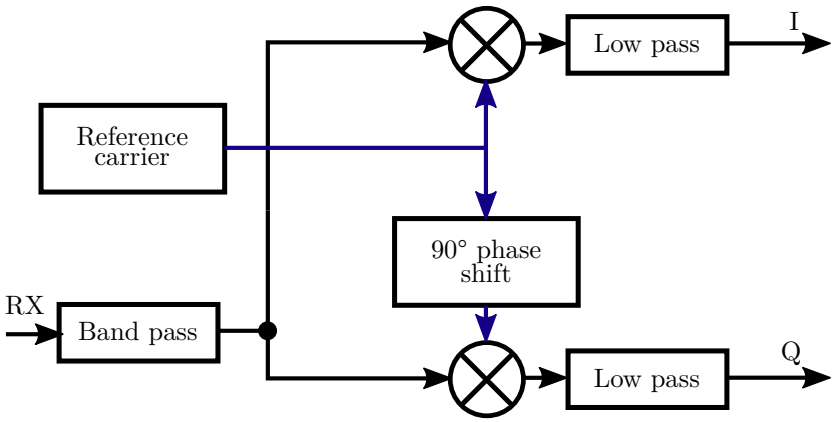

Figure 3.6: Block diagram of a quadrature demodulator

3.3.5 Intermodulation products

The signal at the RX pin is demodulated by the chip. Quadrature demodulation is the concept to mathematically describe this process. Figure 3.6 shows the principle of operation. First, the band limited signal is multiplied with the carrier and with a 90 degree shifted version of the carrier. Applying a low pass filter on the two signals yields the in-phase and the quadrature components from which the modulated sub carrier can be reconstructed.

First, the principle of operation is explained on regular NFC communication with a regular sub carrier created by a PICC in the magnet field of the NFC reader. Afterwards, the effect of harmonics of the charging signal on the signal after demodulation is investigated.

Effects of a regular sub carrier

For simplicity, only an unmodulated sub carrier is considered. Furthermore, the sub carrier is assumed to be a pure sine wave[2]. Moreover, the NFC carrier is assumed to be purely sinusoidal (cosine). The voltage at the RX pin in presence of a card is then proportional to:

$$V_{RX,card}(t) \sim cos(2\pi 13.56\text{MHz}t)(1 + \alpha sin(2\pi 847.5\text{kHz}t)) \tag{3.4}$$

α is the modulation degree and depends on the coupling to the card.

For shorter formulas $\omega_0 = 2\pi 13.56\text{MHz}$ and $\omega_1 = \omega_0/16$ are introduced.

If the reference sub carrier is in phase to the carrier at the RX pin, only the in-phase component I remains. Q is zero.

$$\begin{aligned} \mathcal{I}(t) &\sim LP\{V_{RX} cos(\omega_0 t)\} \\ \mathcal{Q}(t) &\sim LP\{V_{RX} sin(\omega_0 t)\} \end{aligned} \tag{3.5}$$

[2]In reality, it is a rectangular pulse

The LP operation stands for a low pass system[3]. When equation (3.4) for a regular, simplified sub carrier is inserted into (3.5), the I and Q values become:

$$\begin{aligned}\mathcal{I}(t) &\sim LP\{cos(\omega_0 t)cos(\omega_0 t)(1+\alpha sin(\omega_1 t))\} \\ &= LP\{\frac{1+cos(2\omega_0 t)}{2}(1+\alpha sin(\omega_1 t))\} \\ \mathcal{Q}(t) &\sim LP\{cos(\omega_0 t)sin(\omega_0 t)(1+\alpha sin(\omega_1 t))\} \\ &= LP\{\frac{sin(2\omega_0 t)}{2}(1+\alpha sin(\omega_1 t))\}\end{aligned}$$

Applying the low pass gives:

$$\mathcal{I}(t) \sim 1+\alpha sin(\omega_1 t) = 1+\alpha sin(2\pi 847.5\text{kHz}t) \tag{3.6}$$

$$\mathcal{Q}(t) = 0$$

However, Q still needs to be evaluated, because the reference carrier used in equation (3.5) might be shifted in phase. Moreover, due to the transfer function of the matching network the amplitude modulation might look like a phase modulation at the RX pins.

Effects of harmonics of the charging field

How do the harmonics from the charging field effect the demodulated signal? Every harmonic can be considered separately. That is valid, because despite the multiplication with the carrier, the system is still linear[4].

In the application, the frequency of the charger is fixed to 127.774kHz. Therefore, the harmonics are of the form:

$$V_{RX}(t) \sim sin(2\pi n 127.774\text{kHz}t) = sin(n\omega_c t)$$

$$\mathcal{I}_n(t) \sim LP\{cos(\omega_0 t)sin(n\omega_c t)\} = LP\{\frac{1}{2}(sin(\omega_0 t - n\omega_c t) + sin(\omega_0 t + n\omega_c t))\}$$

The low pass filter gives for n close to $\frac{\omega_0}{\omega_c} \approx 106$:

$$\mathcal{I}_n(t) \sim sin((\omega_0 - n\omega_c)t) \tag{3.7}$$

For the $n = 106th \approx \frac{\omega_0}{\omega_c}$ harmonic of the wireless charging signal, the resulting sine wave has a very low frequency. It can be considered as a slow shift of the DC level. For $n \ll 106$ or $n \gg 106$, the low pass filter of the demodulator gets active and therefore those components are uncritical. Furthermore, the damping of the matching network damps the signal significantly for those harmonics.

[3]The filter has to pass frequencies lower than sub carrier frequency (848kHz) plus the bandwidth required to decode the base band signal. It hast to block frequencies above 13.56MHz.

[4]For a fixed reference carrier the system stays linear. However, the system is not time invariant anymore.

Especially critical are the cases with $n \approx \frac{(16\pm1)\omega_0}{16\omega_c}$.

$$\begin{aligned}\mathcal{I}_{99}(t) &\sim sin(2\pi 910\text{kHz}t)\\ \mathcal{I}_{100}(t) &\sim sin(2\pi 783\text{kHz}t)\\ \mathcal{I}_{112}(t) &\sim sin(2\pi 751\text{kHz}t)\\ \mathcal{I}_{113}(t) &\sim sin(2\pi 878\text{kHz}t)\end{aligned}$$

These signals get added to the constant I value from the carrier and can be hardly distinguished from a regular sub carrier (see equation (3.6))!

This noise may lead to a sub carrier being detected, even if there is none. In case a sub carrier exists, it may cause the chip to consider the modulation to be incorrect or it might consider it as collision of two modulating cards.

It could be also verified experimentally, that signals with frequencies close to $13.56MHz\pm 848kHz$ distort NFC communication strongly, whereas other frequencies (also frequencies close to 13.56MHz) have less impact.

Identified measures against this error are:

- Reduction of the rail voltage
- Bandwidth reduction of the matching circuit
- Analogue filters (see section 4.4.5)
- Improvements on the demodulator (bandwidth reduction)
- Reduction of the coupling factor between charging and NFC reader antennas (see section 3.5 and 4.4.1)
- Optimize the detection success rate for the higher noise level (see section 4.3.6).
- Predicting the noise and removing it

3.3.6 Effects on an NFC card

Figure 3.7 shows an equivalent circuit for the coupling between the wireless charging transmitter and an NFC card. A T circuit of the mutual inductance, the inductance of the charging coil and the inductance of the NFC coil is introduced like in section 3.3.3. The capacitor on the left is the used for the wireless charging resonance. The capacitor on the right is the parasitic capacity of the NFC antenna plus the capacity of the NFC chip. On the very right the IC of a card is show, which is an active element unlike the other elements. According to section 2.5.1 and later analysis in section 3.6.5, the rectifier and the limiter can be seen as non-linear loads, whereas the modulator is active.

Equation (3.2) and (3.3) from section 3.3.1 and 3.3.2 can be used to derive an equation for the induced voltage in NFC cards in an analogue way. The equivalent voltage source includes the effects to the left of the dashed line in figure 3.7.

$$V_{eq} \approx V_{in}\frac{M}{L_{WCh}} = V_{in}K\sqrt{\frac{L_{NFC}}{L_{WCh}}}$$

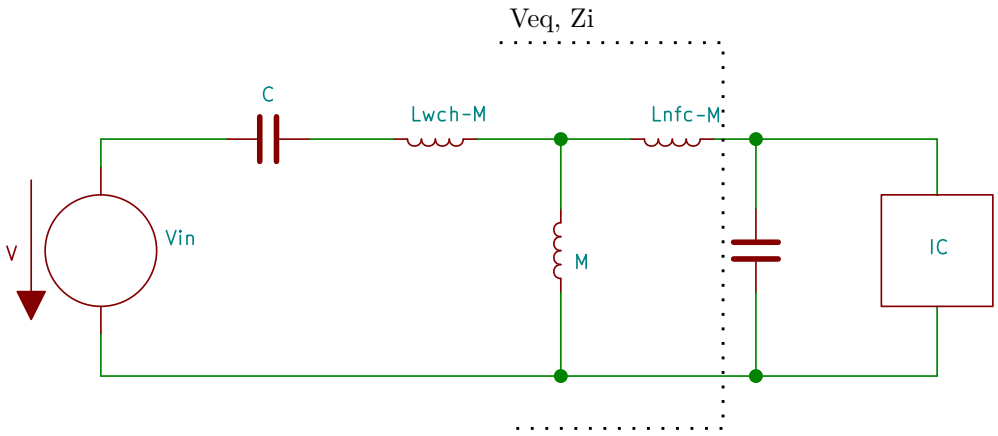

Figure 3.7: Equivalent circuit for the coupling situation between the charging system and an NFC card

The impedance of the equivalent circuit can be approximated as:

$$Z_i \approx sL_{NFC}(1 - K^2)$$

Now, there are different error sources possible. First the signal components with a frequency close to the NFC carrier could distort the NFC receiver of the card. And the card then could not understand the NFC requests anymore. However, the amplitude of those signal components is already significantly smaller than those of an NFC carrier. Also the experiments in section 3.4 lead to the conclusion, that this is not the issue.

When considering the low frequent charging signal, the impedance Z_i is very little. In like manner, the parallel capacity of the equivalent model has only little impact. Therefore, low frequency components can affect the card very strongly.

These low frequency components have a direct influence on the card. In section 3.6, the destructive effects of the wireless charger on cards are investigated. But even, when the signal level is too small to damage the card, still the modulation scheme of the card could be corrupted, as shown in section 3.4.2.

Finally, there are also mixing effects caused by the non-linearity of the card. As mentioned in the introduction in section 2.5.1 cards usually contain a voltage limiter, which gets conductive, if the voltage exceeds a certain threshold. In section 3.6.2 the DC behaviour of the limiter of several cards is also measured. This behaviour is highly non-linear. If the card was linear, then the voltage at the card ICs terminals could be expressed as $V_{NFC+Qi} = V_{NFC} + V_{Qi}$. However, the IC is not linear, but can be viewed as compression function.

Simulating the mixing behaviour failed due to instabilities and convergence issues. However, to explain why the signals get mixed, the simplified schematic network in figure 3.8 can be used. The magnetic fields of NFC and Qi charging induce voltages in the PICC. The IC is represented by a resistive load in parallel to its limiter. The limiter is simulated with two ideal Zener diodes and a series resistivity.

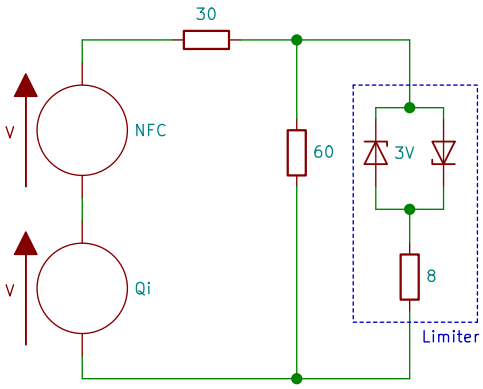

Figure 3.8: Schematic network to explain mixing behaviour caused by limiters of NFC cards

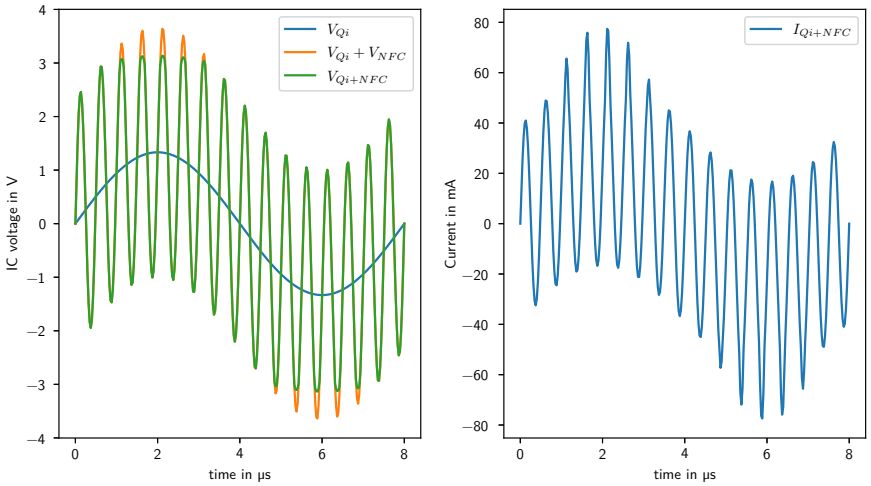

Figure 3.9: Voltage and current signals to explain mixing at an NFC card

Figure 3.9 shows the shapes of voltage and current of the network shown in figure 3.8. On the left the voltages at the IC can be seen. The effect of the Qi charging is shown by the blue curve. There the limiter is not active at all. The orange signal shows the hypothetical voltage at the IC, if Qi and NFC could be calculated independently and then added together (linear system assumption)[5]. Finally, the green curve on the left shows the actual voltage, which is stronger compressed by the limiter on the card in some regions. The effect can be seen even better on the right side of figure 3.9, where the current through the IC is plotted. At the maxima of the Qi signal, the amplitude of the NFC current is increased. This effect mixes the Qi signal onto the NFC signal. Finally at the NFC reader, this effect is very similar to the load modulation of cards and may cause RX failures (according to the classification in section 3.2). The frequency of this mixed signal

[5]Both, graph and schematic are only for explanation, but do not represent real values. The NFC signal is at a frequency of 2MHz in order to obtain a nice graph.

is twice the frequency of the magnetic field of Qi.

In section 3.4.3 the effect of non-linear objects in general is discussed based on real observations.

3.3.7 Low pass and band stop filters

In section 4.4.4 and 4.4.5 different filter structures are investigated for the wireless charging signal. This section gives some insights, which effects can be expected from low pass and from band stop filters on pulse shaped signals. However, this section contains only idealized simulations. Filter structures and measurements can be found in section 4.4.4 and 4.4.5.

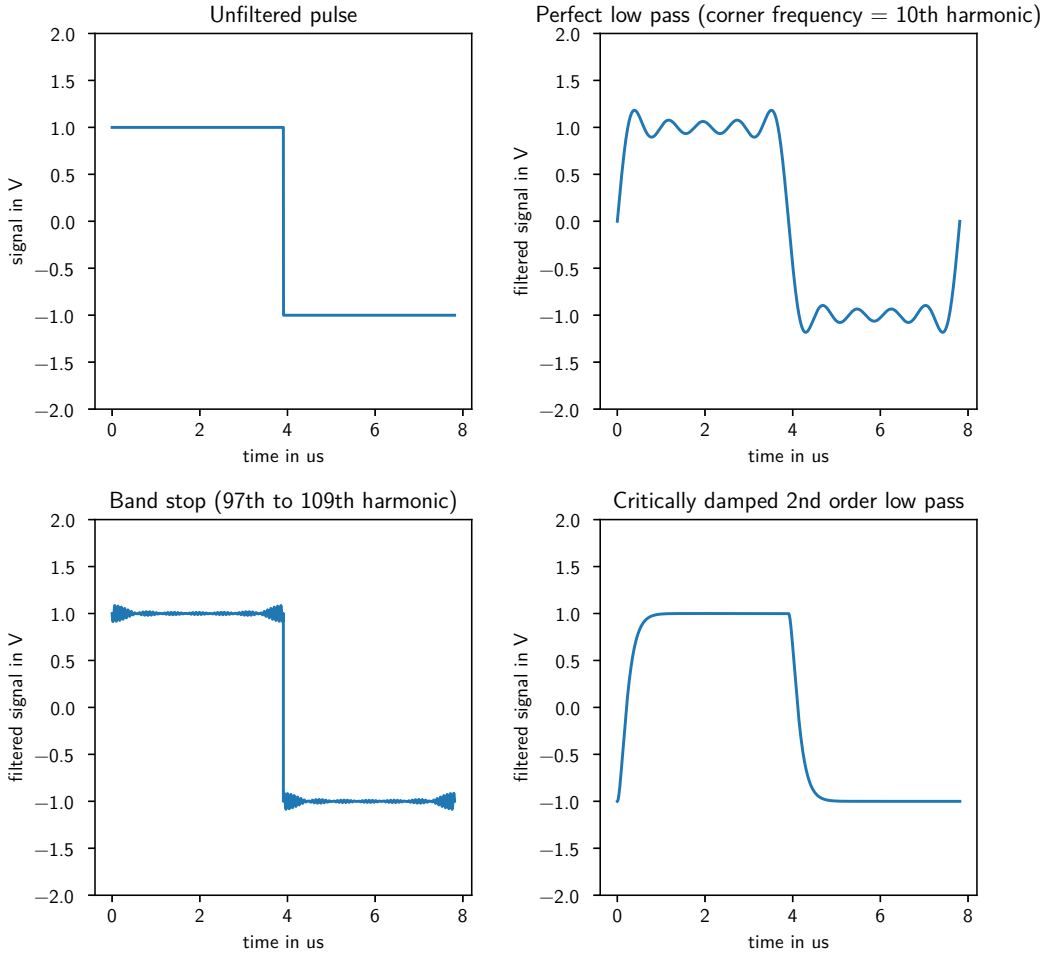

Figure 3.10: Comparison of step responses of filters

The effects of different filter types can be seen in figure 3.10. The figures shows a periodic pulse signal with different filters applied. The plots are derived from idealized mathematical models and show, what can be expected from a notch filter implementation and how it is different from a low pass filter. In the upper left one period of the unfiltered signal can be seen. To the right of it the effect of a perfect low pass filter can be seen.

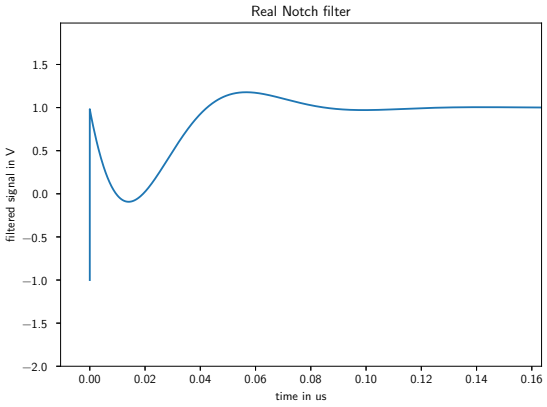

Figure 3.11: Time response of a realizable notch filter

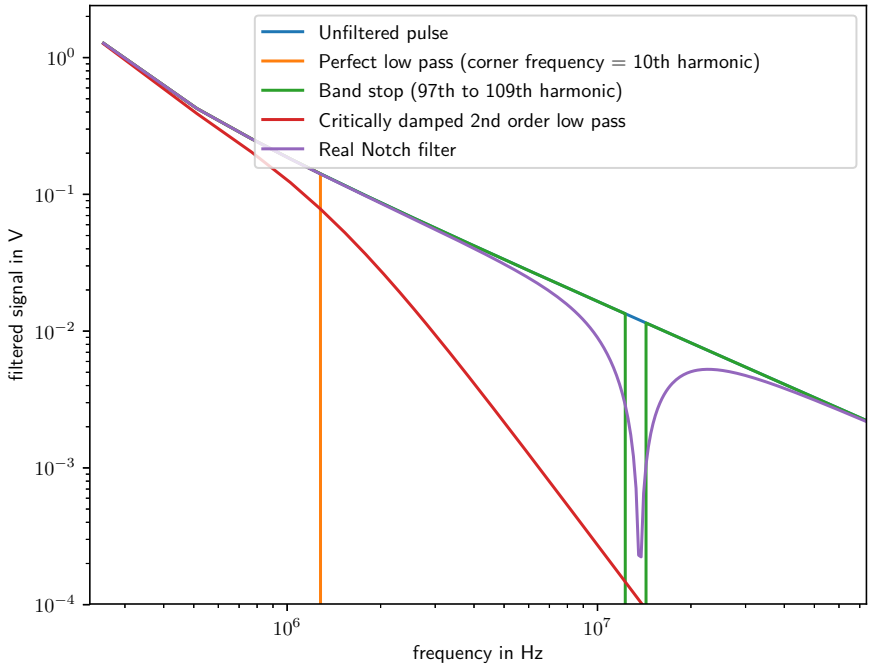

Figure 3.12: Comparison of step responses of filters in the frequency domain

However, this kind of filter cannot be realized, because it is a-causal. The flanks of the filtered signal are flatter and a ripple remains in the high and low phases.

The plot on the lower right of figure 3.10 shows a critically damped second order low pass filter. In contrast to the perfect filter from before, this one can be realized. Moreover critically damped filters show no overshoot or ripple. The effect of the filter is, that the flanks are flattened.

On the lower left of figure 3.10, a perfect band stop filter can be seen. The signal looks noisier than the unfiltered signal. However, a Fourier analysis shows, that the spectrum of the signal around the NFC frequency is zero. Again, this is an ideal band stop, which

cannot be built, because it is a-causal.

The response of a realizable notch filter can be seen in figure 3.11. At the signal edge the response looks again worse than the one of the unfiltered signal. Still, the Fourier transform in figure 3.12 shows, that also this filter improves the spectre of the signal.

Figure 3.12 shows the discrete Fourier transform of the filtered signals on a double logarithmic scale. Plotted are only the odd harmonics, because all the even ones are zero (see section 3.3.1). The unfiltered signal is a straight line with -20dB/decade. The perfect low pass zeros out all components with $f > f_c$. In contrast the perfect band stop zeros out only all components in a small frequency band and is identical to the curve of the unfiltered signal otherwise. Even the realizable filters (red and purple curve) in this graph do not amplify any frequency component.

As a conclusion it can be stated, that low pass filters flatten the signal edges. Notch filters (and other band stop filers) on the other hand do not flatten the signal edges. Interestingly in the time domain the band-stop filtered signals look even more noisy than the unfiltered one.

3.4 Experimental investigation on NFC failure modes

Distinguishing, which failure mode is present, is an important step to decide on countermeasures to take. Unfortunately, it was sometimes difficult to unambiguously determine the fault origin.

For example the effect of a TX error is, that the card does not respond. That can be easily verified by inspecting the field. However, the effect of a card failure could be a missing response as well. Therefore an unambiguous distinguishing of TX and card failures is not possible with a regular and unmodified card within a single experiment.

3.4.1 Measurements of NFC operation with a regular charging field

In this setup, a charging field with an adjustable field strength was generated. An NFC reader simultaneously polled for type A cards. The NFC reader gave a binary feedback. Either an REQA was detected, or not. A type A NFC card was placed in the field at different positions. To verify the existence of load modulation, a sense coil is placed below the card.

Measurement 1: maximal charging field

In this setup, the limit for successful NFC communication of the magnetic field strength of the wireless charger was evaluated. Several NFC cards were placed with maximal coupling on the charger. The setup can be seen in figure 3.13. The ID1 NFC card is aligned to the middle charging coil and then offset by about 1cm to obtain the maximal coupling between the two coils. The magnetic field strength produced by the middle charging coil was increased, until the NFC reader reported no valid responses anymore.

The results were diverse. With some cards, already the minimum rail voltage of 1.7V was too much for successful communication. Other cards stopped responding at 4.6V. Furthermore, no relation to card size or number of turns was found.

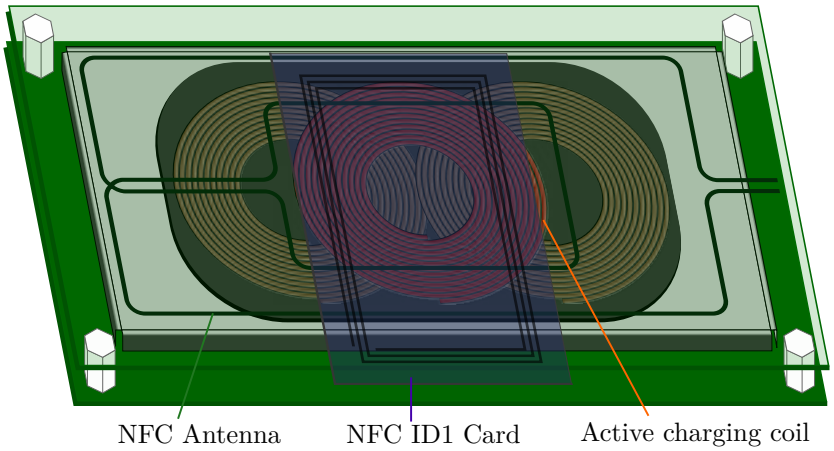

Figure 3.13: Setup with maximal coupling between charging coil and card antenna

For all cards still a back modulation could be seen on the oscilloscope, when the reader reported no response anymore.

From this experiment, it can be concluded, that there exists a region, where NFC cards answer, but either the reader does not understand the answer, or the answer is incorrect (see section 3.4.2). However, from the oscilloscope plots it was not possible to verify, if the response is valid.

The setup showed, that already at moderate field levels, the response is not understood anymore if the coupling between card and charging coil is strong. Possible error sources are RX faults and Card faults.

Measurement 2: low coupling of the card to the charging field

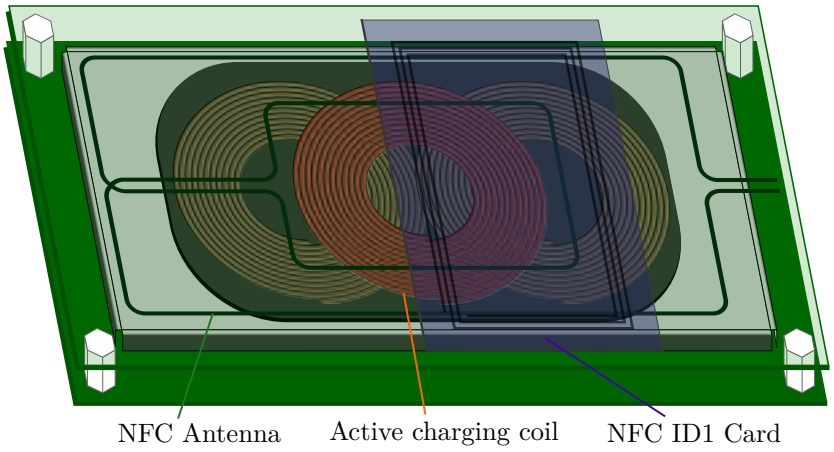

Figure 3.14: Setup with no coupling between charging coil and NFC card

In this setup, the charger generated a strong charging field. The total magnetic flux through the card depends on the positioning of the card. There are even spots, where the card is completely decoupled to the charging field. Figure 3.14 shows such a setup. The

NFC card with ID1 dimensions is offset by about one half to the charging coil in order to reach zero coupling.

However, the NFC reader antenna still saw the full charging field. Because now the card sees the NFC field without Qi distortions, it should properly understand the NFC reader (no TX faults) and should be able to properly answer the requests (no card faults). Therefore, this setup can be used to isolate RX faults.

When the card was located in a spot with no coupling to the charging coil, it answered the requests, it received independent of the magnetic field strength of the charger. An interesting result is, that the NFC reader understood the answers with a certain success rate. This success rate did not vary much with the field strength. So even at the maximal rail voltage of 22V, the answers to the requests could be decoded.

A theory to the result of a certain success rate is, that possibly the phase relation between charging and NFC answer plays a role. Maybe the NFC reader is more susceptible to noise for example when starting to decode, than during decoding. If this was the case and the start of decoding coincidently matches an edge of the charging signal, then a receiver error would occur.

The result can be interpreted, that the RX error mode does not play a great role for type A cards. However, the RX error mode seems to exist and to decrease the success rate by a factor.

Measurement 3: low coupling of an NFC card to the NFC reader

In this setup, the TX error mode was investigated. The card was positioned to couple weakly to the NFC reader antenna and strongly to the charging coil. At a certain charging field, the position was searched, at which the card did not understand the request anymore. Theoretically, this happens, because the NFC modulation of the reader is so small, that the distortions dominate the RX channel.

However, no significant difference in the critical positions for different charging fields could be observed. That the card did not respond anymore seems to be caused by the inability to harvest enough energy from the NFC field. Still, a clear statement, that there are no TX errors, cannot be made.

Measurement 4: influence of a power receiver

The previous measurements were performed without a power receiver on the charger. The charger was set up to use a certain voltage to drive the resonance circuit. Therefore, a magnet field was present, but as no receiver was in the field, no power was consumed.

In the intended operation, there is a mobile phone on top of the charger. The question arises, if the measurements from before shall be performed with a load.

The problem with including a power receiver in the measurement setups is, that the complexity of the setups would increase significantly. Between the four coils (power transmitter, power receiver, NFC reader, PICC) there are 6 mutual inductances, 5 of which depend on the positioning of PICC and power receiver. Therefore isolating one effect becomes difficult.

A mobile phone on the charger causes three effects. Firstly, because it brings additional ferrite foils and metallic housing, it changes all inductance values and changes the distribution of field lines and therefore the coupling situation.

Secondly, the receiver's circuitry is coupled into the transmitters circuity and therefore changes the tuning of the circuits (including the NFC circuits). Because of these two effects, the mobile phone must be considered during the NFC reader antenna matching (see section 2.2).

Thirdly, it draws energy. How does the power consumption affect the NFC systems?

For this consideration, a constant AC voltage at the chargers coil and good coupling is assumed. According to the transformer principle, a voltage is induced in the receiver's coil. Therefore additional currents flows in the primary and the secondary coil. This two currents create fields in opposite direction. Therefore, the net magnetic field stays the same as without receiver! In a good coupling condition, the net field strength depends on the coil voltage. Furthermore, because the law of magnetic induction $V = -\frac{d\Psi}{dt}$ must stay true, the net field over the chargers coil still depends only on the coil voltage, even if the power receiver and the charger are not well aligned. However, when the coupling is weak, local peaks in the magnetic field could occur.

The measurement 2 was repeated with a reference QI charging receiver, which pulls up to 15W. In the measurement setup, the power receiver is well coupled with the charger. With a sense coil the field strength, a well coupled ID1 NFC card would see, is captured. For the measurement the load is changed between 0W and 15W. Meanwhile, the charging voltage is kept constant. The effective, induced voltage increased by 1.7% when changing the load from 0 to 15W. As expected, the field only changed only slightly.

In a second measurement setup, the power receiver is badly coupled to the charger. Furthermore, the pickup coil is placed with decreased coupling to the charger's coil, but badly coupled to the receiver's coil. Again, the voltage is kept constant and the load changed from 0 to 15W. The effective, induced voltage increased by 15% when adjusting the load to 15W. As expected, the current has more effect, when the receiver is misaligned.

The rectangular shape of the induced voltage became more triangular, when the load was increased. Also in the frequency domain a reduction in the harmonics could be seen with higher loads.

Comparing different power receivers is difficult, because many of them do not charge, if only a magnet field of constant amplitude is supplied without any Qi communication. However it was observed, that different receivers have opposite effects. Some power receivers cause an increase in the reported coil current compared to the case without receiver. Whereas others even caused a decrease at the same rail voltage!

To reduce complexity, it seems reasonable to perform measurements without a power receiver. If a power receiver is included, the positioning plays a critical role, because there are many coupling situations to be considered.

3.4.2 Measurement of NFC operation with a sinusoidal charging field

As previously shown, the charging system creates a reasonable amount of harmonics. These harmonics could cause TX and RX failures. Furthermore, they could create card faults, if the card is not able to recover a correct clock from the NFC field.

To distinguish the effects of the fundamental and the harmonics, parallel operation was tested with a purely sinusoidal voltage. A three coil QI MP-A9 configuration was fixed below of the NFC reader antenna. The distance between the charging and the NFC coils was fixed to 3mm. Directly on top of the NFC antenna, a pickup coil and a type A

ID1 NFC card were fixed with maximal coupling to the reader antenna. The pick up coil was connected to an oscilloscope.

The circuitry for creating the sinusoidal charging field can be seen in figure 3.15. An arbitrary waveform generator was used to generate a sine wave. An RF Amplifier was used to amplify the available power. It drives the charging coil and a series capacitor.

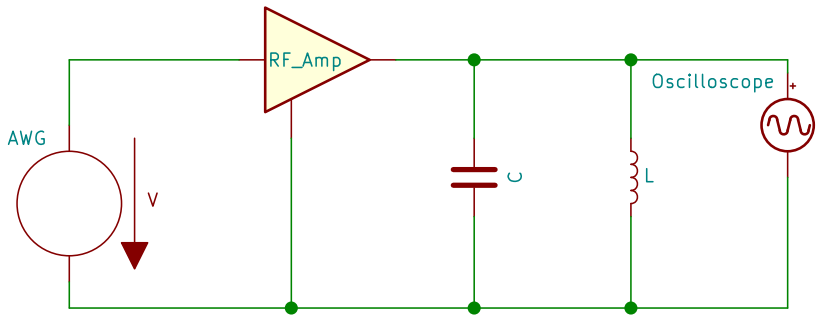

Figure 3.15: Circuit for creating the sinusoidal charging voltage

The parallel capacitor was used to compensate the reactance. Because of the high quality factors of coil and capacitor, the remaining impedance at the resonance frequency was much higher than the 50 Ohms, which would be optimal to match the output of the RF amplifier. The one capacitor design was used because of its simplicity.

The value of the capacitor was 120nF. By sweeping the frequency, the maximal voltage was found to be at 158kHz (verified with the oscilloscope). An LCR meter reported a resonance frequency of 155kHz.

In figure 3.16, the gain of the amplifier was adjusted to get 3 volt peak to peak at the oscilloscope. This voltage was measured across the charging coil. The NFC sub carrier, which was created by the card under test, can be clearly identified in the oscilloscope data from figure 3.16. Furthermore, the NFC reader could decode the answer successfully.

In the experiment the voltage was increased, until first communication failures occur. At about 18 Volt peak to peak, first failures could be observed with the card under test. At 20 Volts, the communication was completely broken. However, still a sub carrier could be seen on the oscilloscope record (figure 3.17).

However, the sub carrier does not look valid anymore. Figure 3.18 shows a section of the oscilloscope trace, where the low phase of the sub carrier lasts for 20 NFC periods. This is an illegal response. To be conform to the type a protocol, the low phase of the sub carrier must contain 8 periods of the NFC carrier. Or if the low phase corresponds to an unmodulated phase, it must be 64+8=72 periods of the NFC carrier. The graph is an indicator for errors happening in the card.

Possible error sources include:

- The card is not capable of switching the transistor for load modulation
- The clock recovery fails

  This seems likely, because of the framing error, mentioned above.
- The limiter pulls so much current, that the parallel transistor for load modulation is ineffective

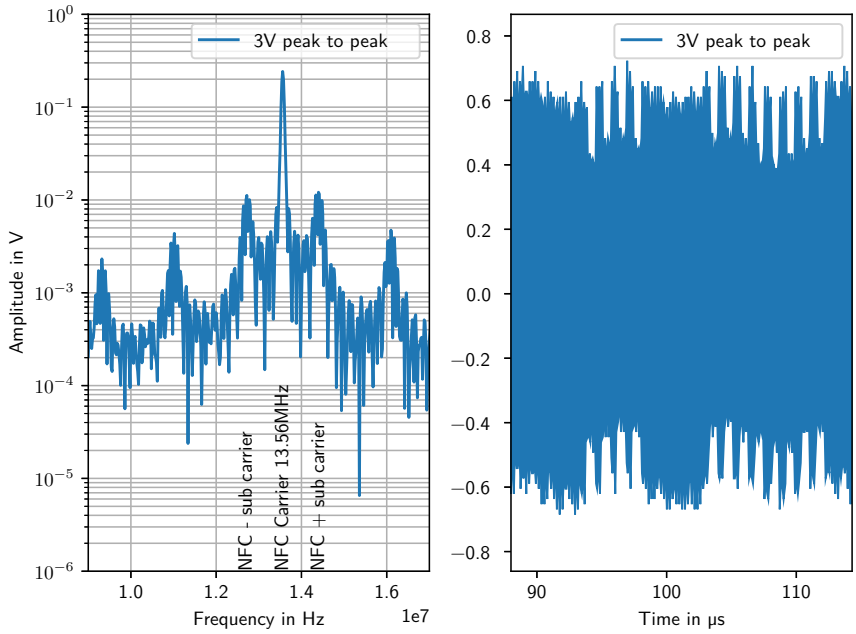

Figure 3.16: Plot of an NFC field with a sub carrier with a weak sinusoidal charging field in superposition

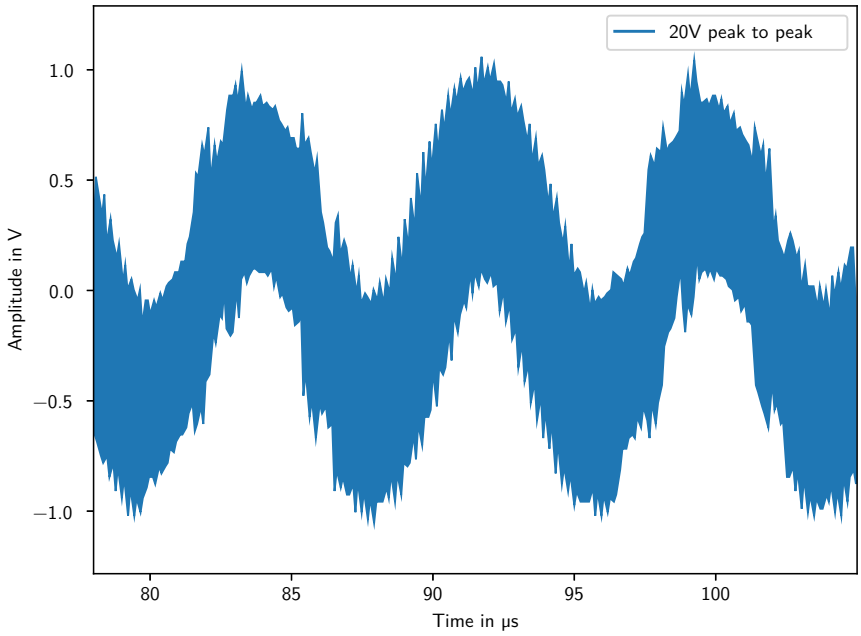

Figure 3.17: NFC field with a stronger sinusoidal charging field in superposition

To conclude, even with a pure sinusoidal charging voltage, relatively low voltages across

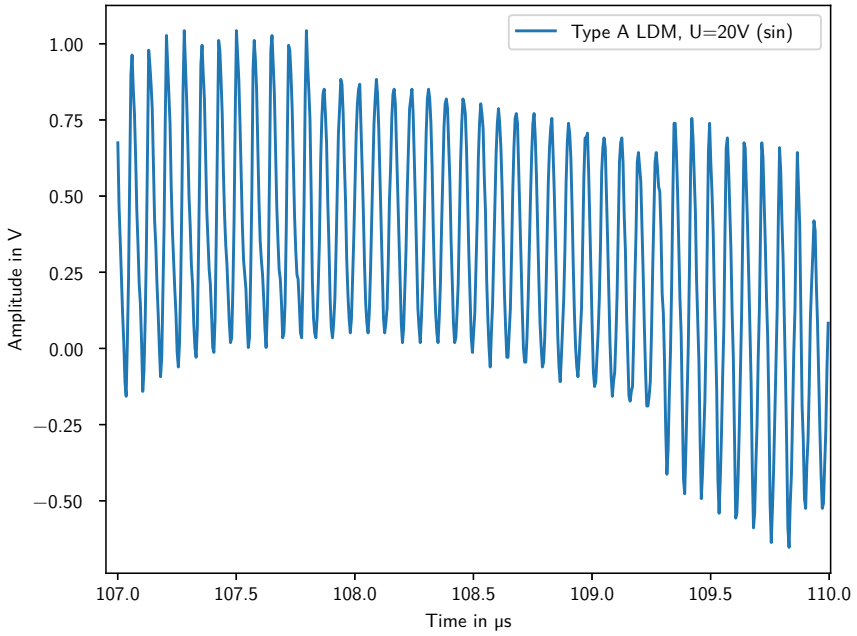

Figure 3.18: Illegal Framing of a type A card during sinusoidal charging with 20V peak to peak coil voltage

the charging coil cause card failures. (20V peak to peak are around 7V rms, $\frac{20\text{V}}{2\sqrt{2}} \approx 7.07\text{V}$.) This is a voltage level, which is often reached during normal charging operations. As a conclusion, it can be said, that true parallel operation of NFC cards and wireless charging is not possible. Cards may stop working properly when exposed to strong charging fields, even if the charging signal was filtered.

3.4.3 Measurement of the influence of non-linear NFC loads

A theoretical explanation of mixing issues caused by NFC cards can be found in section 3.3.6. However, this section focuses on observations made with an field strength indicator card.

During the development of countermeasures, an interesting observation could be made. When the magnet field of the charger was on and no PICC was in the field, the RX circuitry of the NFC reader works fine. Even at higher field strengths, the chips almost never wrongly identified a sub carrier.

However, if an NFC card is moved in the two magnet fields, then even without sending any NFC commands, the RX path discovers a sub carrier, occasionally. The effect can be reproduced very easily with a LED field strength indicator card[6].

In figure 3.19, the percentage of detected sub carriers can be seen, when a led indicator card was in the field with maximal coupling to the charging coil. This measurement was done without a power receiver.

[6]The major argument for using such cards was, that they were not damaged by the charging field. Besides, the effect is stronger, than with regular NFC card.

V_{Rail}	sub carrier
0V	0 %
2V	100 %
5V	100 %
10V	100 %
20V	100 %

Figure 3.19: Statistic of wrong sub carrier detection caused by LED field strength indicator card

It can be seen, that already at very small rail voltages, the NFC chip was reliably convinced, that a sub carrier exists. If the coupling between the indicator card and the charging coil is reduced, then also the influence on the sub carrier detection rate is much smaller.

To investigate the effect, internal signals were recorded and analyzed.

Figure 3.20 shows the BPSK-Sum[7] in different conditions. With the NFC field, but no card and no wireless charging, the sum is zero (upper left of figure). With a type B card in the field, single spikes can be observed (upper right of figure). Each peak indicates a phase jump of the modulation. It can be observed, that, as expected, the peaks have a distance of 1/106kHz $\approx 10\mu s$ or a multiple of it.

With 12V rail voltage at the charging coil and no non-linear devices, the BPSK-Sum shows a significant amount of spikes (figure 3.20 middle row on the left). But still no sub carrier was reported.

When the charging field was off, but the field indicator card was placed on the NFC antenna, the number of spikes increased as well. However they were smaller than with wireless charging only, and they came in packs (middle row on the right).

Finally, when the wireless charger was active (with 12V rail voltage) and the indicator card was laying on top, a sub carrier was detected[8]. Compared to the plot with wireless charging only, the peaks are higher.

However, no visible relation of the BPSK-Sum and the shape of a voltage in a pick-up coil could be observed. When measuring the voltage in a pick up coil with an oscilloscope, it could be seen, that the NFC field gets stronger distorted by the indicator card when a charging field is present.

An explanation for this phenomena is, that due to the non-linearity of the load, the operating point plays a role. The low frequent wireless charging signal acts as a shifting operating point for the higher frequent NFC field. Due to this offset, the upper and the lower half wave of the NFC signal are differently compressed by the non-linear device. Therefore, the harmonic distortion of the NFC carrier increases.

The measurement was performed with a LED indicator card. It is unlikely, that such a device is used by the end customer. Nevertheless, these observations are useful, because NFC cards are non-linear as well. Furthermore, a mobile phone could cause several non-linear influences on the field.

[7]The BPSK-Sum combines the in-phase and quadrature components of the binary phase shift keying demodulated signal.

[8]For this measurement, the coupling between wireless charging coil and field indicator card was not maximized. Therefore, such a high rail voltage was necessary to get the sub carrier.

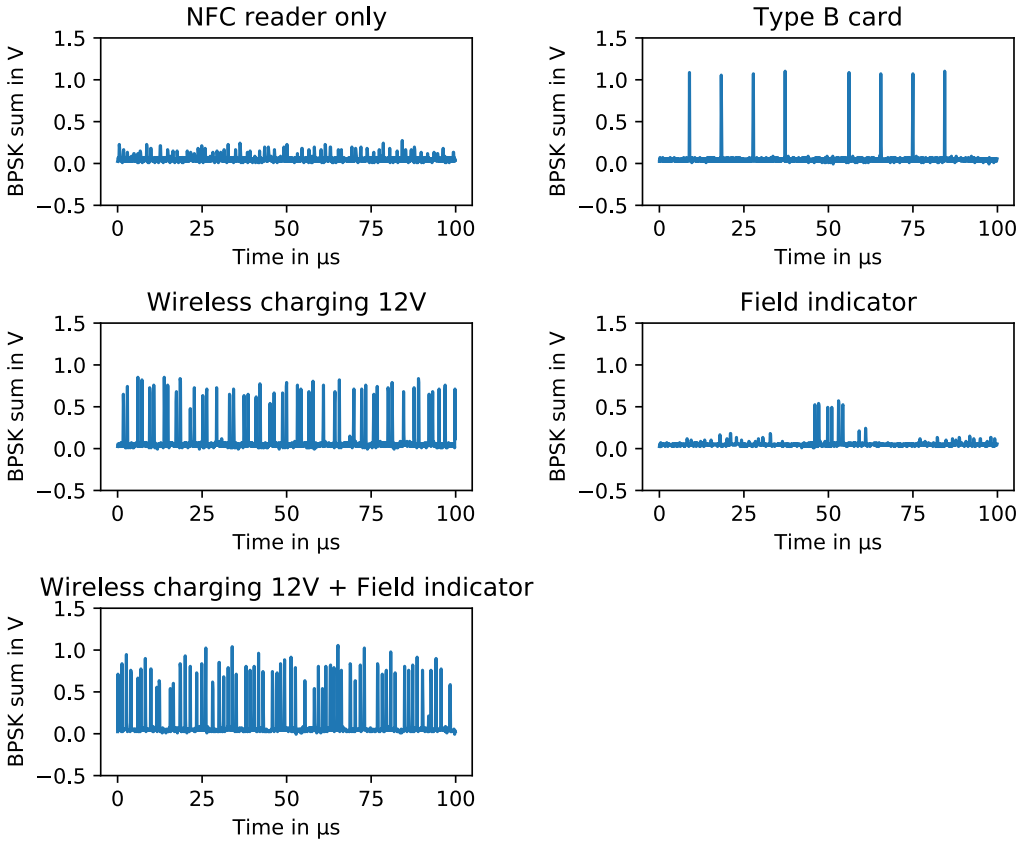

Figure 3.20: Plot of the BPSK sum signal for different setups

3.5 Analysis of inductive coupling

3.5.1 Definitions

The third and fourth Maxwell's equations are the basis of the phenomena of mutual and self inductance.

$$\oint_C \mathbf{E}d\mathbf{r} = -\frac{d}{dt}\iint_A \mathbf{B}d\mathbf{A}$$

where C is the border of the area A. Usually, C is chosen at the wire of a coil (which is only approximately closed). If additionally, the field is homogeneous and orthogonal to the area, the formula simplifies to:

$$V_{ind} = -\frac{d}{dt}BAN = -\frac{d\phi}{dt}$$

with N being the number of turns.

The fourth Maxwell equation when neglecting the dynamic part becomes:

$$\oint_l \mathbf{B}d\mathbf{l} = \iint_A \mu\mathbf{J}d\mathbf{A}$$

l is the border of the area A. J is the current density. For simplification line currents through the Area are assumed. By choosing l to be a trajectory of the magnetic field, the formula simplifies to

$$Bl = \mu \sum_i I_i = \mu N I$$

When a trajectory is found, the field strength can be easily calculated.

The inductance between two coils is now defined as the ratio

$$L_{1,2} = \frac{\Psi}{I}$$

where Ψ is the total magnetic flux through the coil 2, caused by the current I through the coil 1. The current through the coil 2 is zero. As long as μ is constant, L is independent of the current and is proportional to $N_1 N_2$.

By using the Laplace transform, the differential operator vanishes. This form is interesting especially for sinusoidal signals:

$$\frac{V_2}{I_1} = sL_{1,2} \text{ under the condition that } I_2 = 0$$

This form can be used to calculate an inductance from measurements.

For coil 1 $\neq$ coil 2, usually the symbol $M_{1,2}$ is used and the inductance is called mutual inductance. If the coils are the same, the symbol L_1 is used omitting the second index.

Interestingly, $M_{1,2}$ is always equal to $M_{2,1}$!

The coupling factor is defined as $K_{1,2} = \frac{M_{1,2}}{\sqrt{L_1 L_2}}$.

Air only setup

The actual setup has a ferrite foil below the charging coil. Furthermore, the circuitry is protected by a metal shield. Before considering the complete setup, it is interesting to first investigate an air only setup. Without ferrite foils and metal sheets, the major sources for asymmetry are eliminated.

Planar setups

For theoretical analysis, sometimes all currents are assumed to be in the same plane. This is a simplification, because in reality, the middle charging coil is about 1mm higher than the others. Moreover, the readers NFC antenna is separated from the charging coils by about 3 millimeters.

When all currents are in one plain, and additionally it is an air only setup, the field lines intersect the plain orthogonally (see figure 3.21).

3.5.2 Analysis of antenna shapes

In this section, the effects of the layout and positioning of coil setups are discussed. Different strategies for decoupling are developed. In the following graphs, there is a red and a blue coil. The red coil is always the primary coil and driven with a certain current. The blue coil is the secondary coil and therefore open.

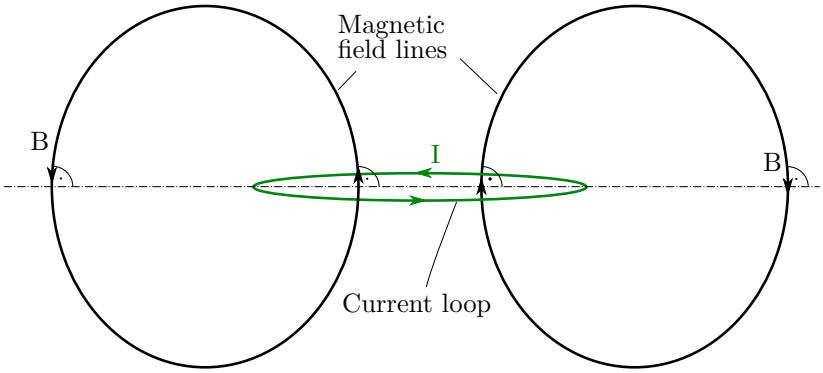

Figure 3.21: Sketch of the field lines in a planar air only antenna setup

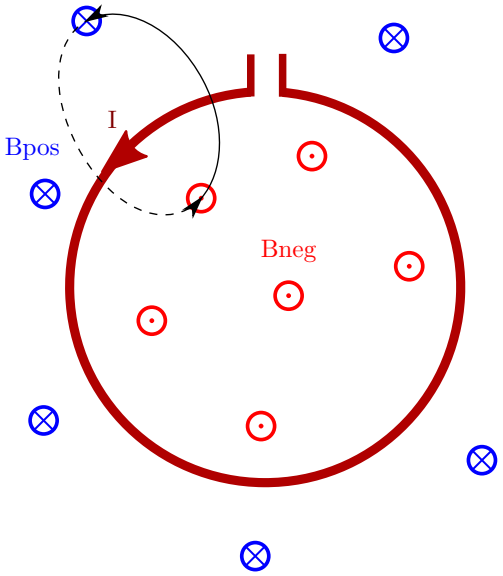

Figure 3.22: Sketch of a single coil in a planar air only setup

For the following examples a planar setup is assumed.

A current through a coil produces a magnet field. In an air only setup, the field is orthogonal to the plain of the coils. The field lines enter and leave the plain perpendicularly.

Inside of the coil, the field lines come out of the plain. These field lines are said to have negative direction. Outside of the coil, the field lines go into the plain. They are in positive direction.

In figure 3.22 a single coil produces a positive field inside and a negative field outside. The closer the field lines are to the loop, the stronger the field gets. Because all field lines

are closed, they exactly compensate each other.

$$\iint_{-\infty,-\infty}^{\infty,\infty} \mathbf{B}d\mathbf{A} = \iint B_{pos}dA - \iint B_{neg}dA = \Phi_{pos} - \Phi neg = 0$$

Coupling of overlapping coils

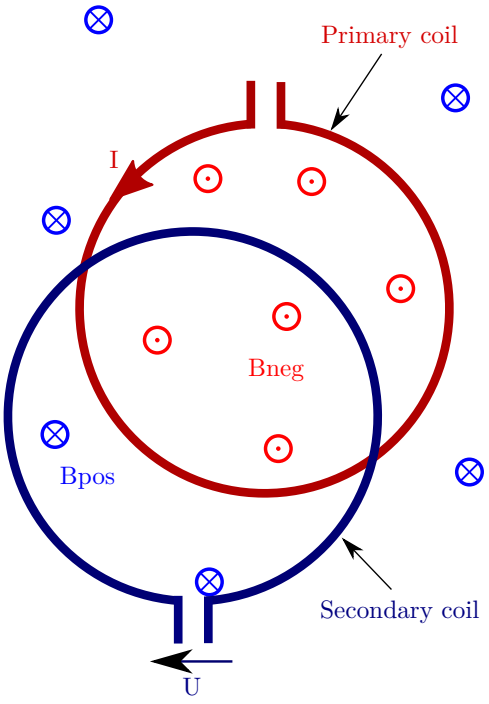

Figure 3.23: Visualization of two overlapping coils in a planar setup

On figure 3.23 a secondary coil was added. The voltage at the second coil can be calculated as

$$V_2 = -\omega\Phi_2 = -\omega \iint_A \mathbf{B}d\mathbf{A} = \omega(\Phi_{2,neg} - \Phi_{2,pos})$$

It can be seen, that the mutual inductance can be positive or negative. When the positive portion and negative portion of the magnetic flux are equal, the two coils are completely decoupled and no voltage is induced.

Coupling of different sized coils

In figure 3.24 the secondary coil contains the primary coil. The complete positive flux is captured but only part of the negative flux is captured. The flux through the secondary coil is the same as the flux outside the secondary coil with opposite sign.

$$\Phi_2 = \iint_A B_{pos}dA - \iint_A B_{neg}dA = -\iint_{Plane\setminus A} B_{pos}dA$$

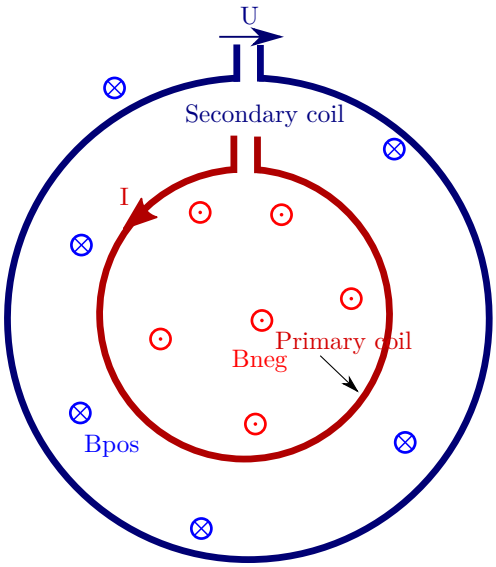

Figure 3.24: Visualization of decoupling with a big secondary coil

The coupling never reaches zero, but can be made arbitrarily small by making the secondary coil bigger. The downside is, that the secondary coil only induces a very weak field in its center. This follows directly from the law, that $M_{1,2} = M_{2,1}$.

Reducing coupling by removing area

The mutual inductance can be reduced as well by excluding areas from the inside of the primary coil. The flux outside of the secondary coil can be exactly compensated by removing some effective area in the negative field area.

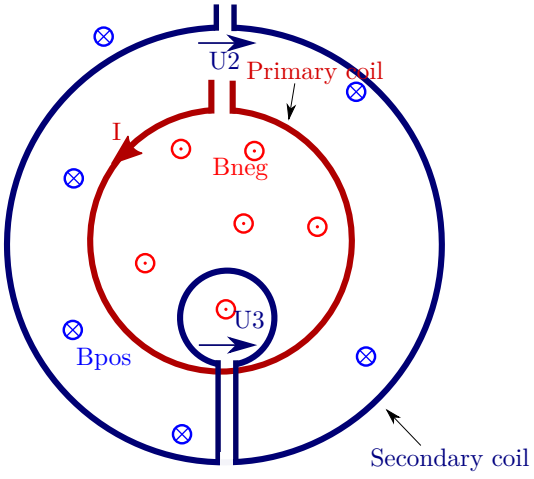

Figure 3.25: Sketch of two coils, which are decoupled by removing inner area

In figure 3.25, two secondary coils can be seen. By connecting the dotted lines, they

are put in series. Note, that the third coil is connected clock-wise.

$$\Phi_2 = -\Phi_{\text{outside coil 2}}$$

$$\Phi_3 = \iint_{A_3} \mathbf{B} d\mathbf{A}$$

$$V_{total} = V_2 + V_3 = \omega(-\Phi_2 + \Phi_3) = \omega(\Phi_{\text{outside coil 2}} + \Phi_3)$$

Complete decoupling can be achieved, when the flux inside the compensation coil is equal to the flux not covered by the first secondary coil with different sign.

Reducing coupling by adding area

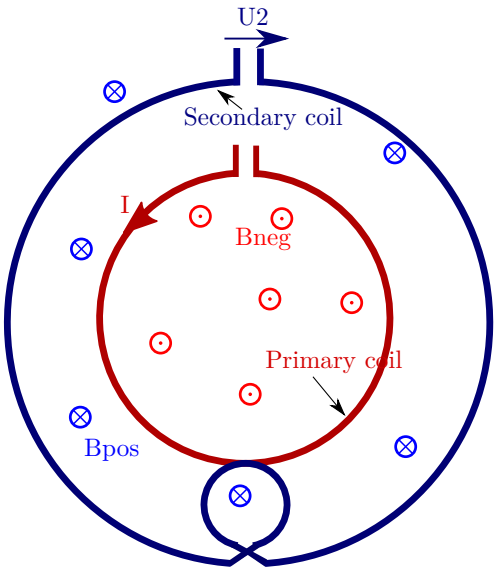

Figure 3.26: Sketch of two coils, which are decoupled by adding outer area

Instead of adding a clockwise compensation loop inside the negative field zone, a counter clockwise loop can be put outside the coil in the positive field zone. This can be seen in figure 3.26.

Decoupling and blind spots in planar setups

A blind spot is a position for a specific NFC PICC, where the antenna of the NFC Reader and the antenna of the PICC decouple. Blind spots within the operating volume are unwanted and shall be avoided at least for all standardized geometries.

For this section a planar setup is assumed. The charging coils, the reader antenna and the PICC lay all in the same plane.

If a charging coil is decoupled from the reader antenna, there are automatically blind spots between the NFC reader antenna and some PICC antenna geometries. This result is independent of the strategy used, as long as the setup is planar. The reason is, that $M_{1,2} = M_{2,1}$.

The charging loop is coil 1, the reader antenna is coil 2 and the coil 3 is of the PICC. If $M_{1,2} = 0$ then likewise $M_{2,1} = 0$. If the coil 3 has the same dimensions and the same position as the charging coil, then $M_{2,3}$ is zero too! A blind spot.

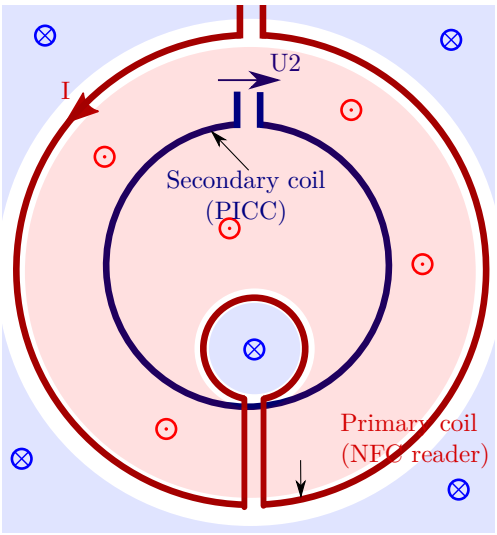

Figure 3.27: Sketch visualizing the Blind spot problem

Figure 3.27 shows the setup as in figure 3.25. Here the current flows through the outer, reader NFC coil with the compensation loop. When the setup is completely decoupled, the total magnetic flux through the QI coil must be zero. Either the magnetic field in the whole area covered by the QI coil is zero, or there are areas, where it is positive and areas, where it is negative. In both cases, there are many possible antenna forms and positions, where the positive and negative fields cancel out.

So in planar setups NFC cards with Qi coil size have always blind spots in the middle of the antenna setup. However cards, which are significantly bigger than the charging coils, might not gain additional blind spots within the operating volume. The NFC antenna could be designed to ensure, that there are no ID1 sized areas, where the positive flux is fully compensated. However, if the NFC reader antenna shall be decoupled from multiple charging coils, then blind spots seem unavoidable even for ID1 cards.

Ideas for non-planar setups

The issue with blind spots and decoupling arises, because an NFC card with an antenna with Qi size can be placed directly above the charging coils. Because the NFC reader antenna is decoupled to the charging antenna, it is then also decoupled to the NFC card.

However, NFC card, NFC reader antenna and Qi charging coils are not exactly in one plain. Theoretically, the spatial separation could be utilized to ensure, that only the Qi coils and no NFC cards are decoupled from the NFC reader antenna.

In this section, two ideas are presented, how such a setup could look like. Unfortunately, they do not appear to be practicable and no further investigation was done on them.

Figure 3.28 shows a non-planar setup, where the compensation loop is added on a

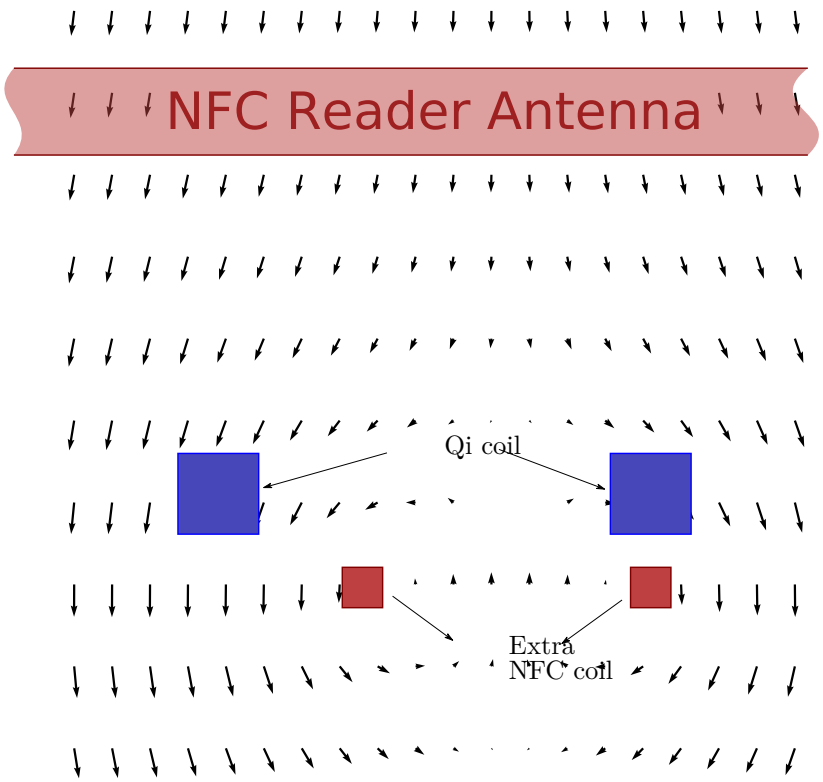

Figure 3.28: Decoupling of a charging coil and the NFC reader coil with a compensation loop in parallel to the antenna plain

plane parallel to the NFC reader plane. Because the compensation loop is smaller, the effect on the field is more local. The effects above the main NFC coil are so small, that no cancellation of the magnetic fields occurs there.

A problem with this approach is, that the distance between the charging and the reader NFC coil has to be big enough. However, ideally the distance is kept short for efficiency reasons.

By rotating the compensation loop by 90°as shown in figure 3.29, the distance problem can be reduced. The field lines above the NFC reader coil are mainly horizontal and do not influence the mutual inductance to PICCs.

Designing such a structure for production is difficult. Another downside is the increased the self impedance of the NFC reader coil, which results in reduced coupling to cards.

3.5.3 Analysis of ferrite foils

Physical properties

Ferrites are usually ceramic materials often containing iron. The main reason for using ferrites is, that they are ferrimagnetic. Therefore, they can be used to guide the magnetic

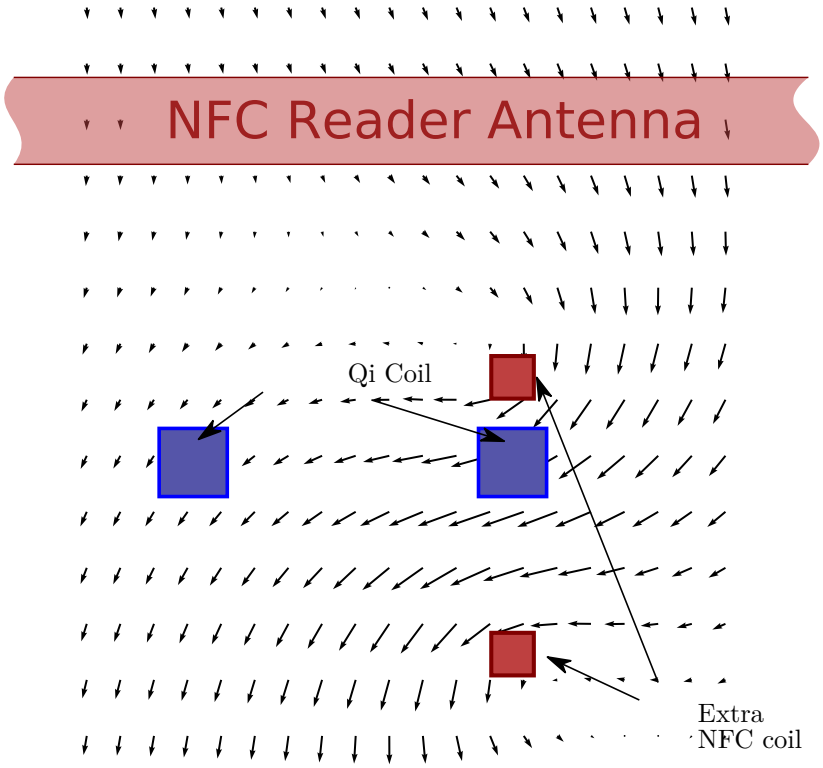

Figure 3.29: Decoupling of a charging coil and the NFC coil with a vertical compensation loop

field, to increase the inductance and to guard sensitive areas from magnet fields.

The second major property is, that they are bad electrical conductors. If a normal conducting object is inside of a magnet field, voltages are induced inside. The resulting currents are called eddy currents. They cause losses in the material.

Ferrites can be designed to either have high or low coercivity. A high value is favorable for magnetizing the material permanently. For guiding fields with little losses, a low coercivity is preferred. For wireless charging, the ferrite foils fall into the latter category.

The relative permeability μ_r can be designed in the manufacturing process and often has values between 100 and 10000. Usually, this measure has a strong dependency on the frequency and the temperature.

There are different reasons for losses within a ferrite. One is the hysteresis. If the fields get too strong, the magnetization becomes non-linear. When reducing the field again, the field strength over the H-field is on a different curve. When integrating the power, it can be observed, that energy is lost. Another reason are eddy currents, as discussed before. Moreover, aligning the Weiss districts of the material creates losses.

Per convention the losses are summarized in the imaginary part of the permeability. The real part is then called μ', the imaginary part μ''.

For theoretical considerations in this thesis, sometimes the ferrite is assumed to be

perfect. Such a perfect ferrite has a μ value of $\infty + 0j$. Therefore, the magnetic resistance is zero.

Simulation of the coils in air or vacuum is computationally cheap. Still analytical calculations usually are not possible, but approximating formulas exist for various coil geometries. However, this is not the actual scenario. In the real setup, there are many metal components and dielectrics. The charging coils have a ferrite foil attached to improve the magnetic behavior. The foils channel the magnetic flux away from lossy material. Furthermore, they reduce the field line length in the air. Therefore, they reduce the magnetic resistance and increase the magnetic field. Moreover, they change the distribution of the field and therefore the coupling factors.

The power receiver usually contains another ferrite foil between the wireless charging coil and its circuitry. Moreover, different geometries for charging coil, NFC coil and ferrite foils are possible on the phone side. Because the concrete setup depends on many unknowns, it is difficult to define an unambiguous simulation setup.

Additionally, ADS with Momentum as solver cannot simulate arbitrary dielectric shapes. A dielectric material can be only defined as substrate, which makes it infinite. However, simulating the actual size of the ferrite foil is important and the next three sections explain, why it is important. Simulation of NFC fields with ferrites was already performed for example in [9] using ADS with HFSS.

One infinite ferrite foil

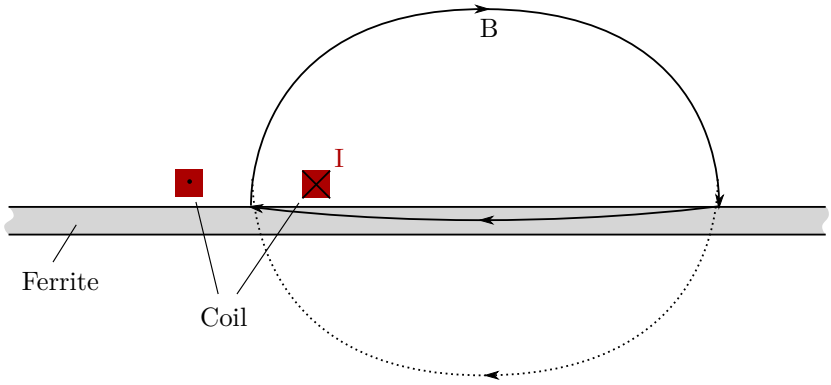

Figure 3.30: Effect of one infinite ferrite foil below a charging coil

In figure 3.30, an infinite ferrite foil is added below a charging coil. One field line is drawn, which orthogonally intrudes the foil.

When comparing this setup to an air only setup, the field distributions above the charging coil are similar, if the distance between foil a coil can be neglected. The dotted line shows, how the field line would close in an air only setup.

By considering the symmetry, it can be seen, that the air distance with an infinite ferrite foil is about half the air distance as without. Therefore, the magnetic resistance is expected to reduce by a factor of two. Furthermore, the field strength and the inductances double. This could be verified with simulations in ADS. Moreover, measurements of the

inductance showed the factor of two as well. Finally, simulation shows no significant change of any coupling factors between charging and NFC reader antenna when simulating with and without ferrite.

Placing an infinite ferrite foil just below the charging coils increases the field strength and inductance by a factor of approximately two, but the field distribution above the coil is not changed significantly.

Two infinite ferrite foils

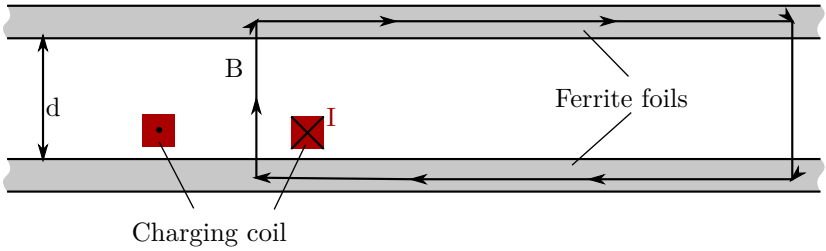

Figure 3.31: Sketch of a charging coil with two infinite ferrite foils

A power receiver usually contains a ferrite foil as well. Figure 3.31 shows a setup, where it is modeled infinitely.

Again the magnetic reluctance inside the ferrite is neglected. The reluctance per square meter is:

$$R' = \frac{d}{\mu_0}$$

The reluctance inside the coil becomes:

$$R_{inside} = \frac{R'}{A_{coil}}$$

The reluctance of the return path is zero with a perfect ferrite. R' is a measure for the density of the field lines and it is constant. Therefore, the field outside of the coil is very weak, because the flux spreads over a huge area.

Decoupling would be impossible in such a setup. Also simulations show higher coupling factors with two infinite ferrite foils.

Two finite ferrite foils

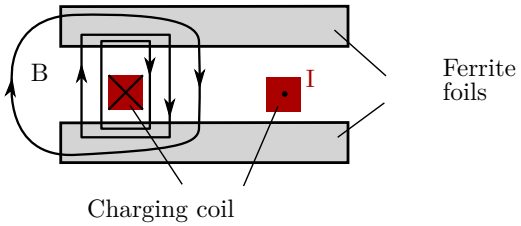

Figure 3.32: Sketch of a charging coil with two aligned ferrite foils

Figure 3.32 shows as setup with two finite ferrite foils. The ferrite foils provide paths for the magnetic flux with short air distances. Therefore, the field is focused in the regions with overlapping ferrites. Outside the field decays quickly. As a result, the ferrite foils help to decouple the charging coils from the NFC reader antenna. By adding the foils, the self impedances grow quicker, than the mutual inductance does.

When neglecting edge effects, the reluctance can be calculated as

$$R = \frac{(\frac{1}{A_{coil}} + \frac{1}{A_{ferrite} - A_{coil}})d}{\mu_0}$$

Unfortunately, finite foils cannot be simulated with ADS and Momentum and the infinite foil scenarios both fail to approximate this scenario. To the contrary: with two infinite layers the field lines move further away, instead of focusing closer to the charging coil. The conclusion is, that from theoretical point of view it is not a valid approach to simulate a foil as substrate layer. Therefore, it is currently not possible to properly simulate the coupling situation in ADS with Momentum.

3.5.4 Magnet field calculations

In order to model the effects of wireless charging on PICCs, the coupling between the charging coil and the PICC's coil is required. In this section, the field distribution is calculated and used to assess the worst case coupling situation. However, the effects of the finite ferrite foil cannot be considered properly.

Charging coils

First, the charging coils on their own are analyzed. The field distribution of the coil is estimated as two times the field distribution in air (without ferrite). It was calculated numerically from the Biot-Savart equation.

For the MP-A9 layout, two coils are directly on top of a ferrite foil. A third coil sits on top of the two bottom ones. The top coil has 12 turns and a nominal inductance of $9.8\mu H$. The bottom ones have only 11 turns. Because of the proximity to the ferrite, the inductance of $10.2\mu H$ is still bigger than of the top coil. Unless otherwise noted, the value of the middle coil is used in calculations.

The charging coil creates a certain magnetic flux. From the definition of the inductance follows:

$$L = \frac{\Psi}{I} = \frac{\iint_A B dA}{I}$$

The area is bounded by the spiral coil. The areas overlay. B field components inside the middle coil are counted N (11 or 12) times. The spiral coil can be modeled as N concentric loops. If they had the same size and would couple 100%, the magnetic flux could be calculated as:

$$L = \frac{\Psi}{I} = \frac{N\Phi}{I} \rightarrow \Phi = \frac{LI}{N}$$

Because the turns have different radii, the field does not always constructively add. The inductance for a fixed Φ/I ratio gets smaller. The total $\Phi := \iint_{\text{coil plane}} \max(B, 0) dA$ gets bigger than $\frac{LI}{N}$.

In [18] an approximation formula for the inductance of a spiral coil is given as

$$L = 31.33\mu_0 \frac{n^2 a^2}{8a + 11c} \tag{3.8}$$

with $a = \frac{r_{min}+r_{max}}{2}$ and $c = r_{max} - r_{min}$. Assuming a perfect infinite ferrite, the inductance becomes twice that value (see section 3.5.3). The calculated value is $10.6\mu H$ for the bottom charging coils and matches the actual value very well.

To calculate the distribution of the magnetic field, the Biot-Savart (3.9) integral was solved numerically. This law states, how the field strength caused by a current loop can be calculated, in situations without magnetically active objects.

$$\mathbf{H}(\mathbf{r}) = \frac{1}{4\pi} \int_C \frac{I d\mathbf{l} \times (\mathbf{r} - \mathbf{l})}{|\mathbf{r} - \mathbf{l}|^3} \tag{3.9}$$

H is the three-dimensional vector of the magnetic field. r is the position, where the field is observed. C is the curve of the wire, through which the current flows. I is the current through the wire. dl is the infinitesimal long distance vector along the curve C. l is the position on the curve, which is the argument of the integrand.

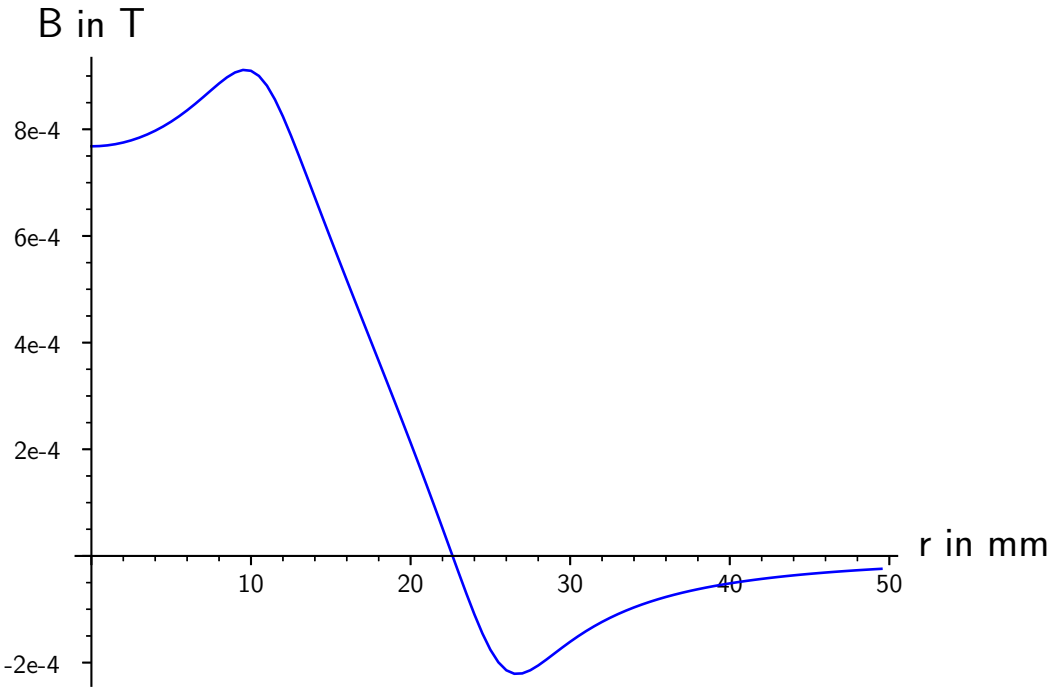

Figure 3.33: Field distribution of a charging coil (calculated)

The integral in (3.9) can be solved numerically for one specific point r. Summation

over all turns gives the total H field in that point (see equation (3.10)).

$$H_z(r) = \sum H_{z,i}(r)$$
$$H_{z,i}(r) = \frac{I}{4\pi} \oint_{C_{\text{turn},i}} \frac{Id\mathbf{l} \times (\mathbf{r} - \mathbf{l})}{|\mathbf{r} - \mathbf{l}|^3} \tag{3.10}$$

Figure 3.33 shows the B field component in z direction with respect to the radial distance from the center. The values were calculated for a current of one ampere through one of the lower charging coils. To consider the ferrite, the resulting field amplitude is doubled. In order to match the physical setup, the distance in z direction is set to 3mm.

Coupling to NFC cards

In order to analyze the damaging of cards, the mutual inductance between the active coil of the wireless charger and the PICC must be known. This measure depends on many unknowns. In this section, first the worst case shape and size for the PICC antenna is calculated. Then the worst case positioning of ID1 cards is analyzed. This section focuses on the coupling and not on the mutual inductance. The effect of the number of turns are therefore not considered yet.

A concentric loop with radius ρ in the plain at a certain distance captures a magnetic flux of

$$\Phi(\rho) = \iint_{r_x^2 + r_y^2 < \rho, r_z = const} \mathbf{B}(\mathbf{r}) d\mathbf{A} = \int_0^{\rho} 2\pi r B_z \begin{pmatrix} r \\ 0 \\ r_z \end{pmatrix} dr \tag{3.11}$$

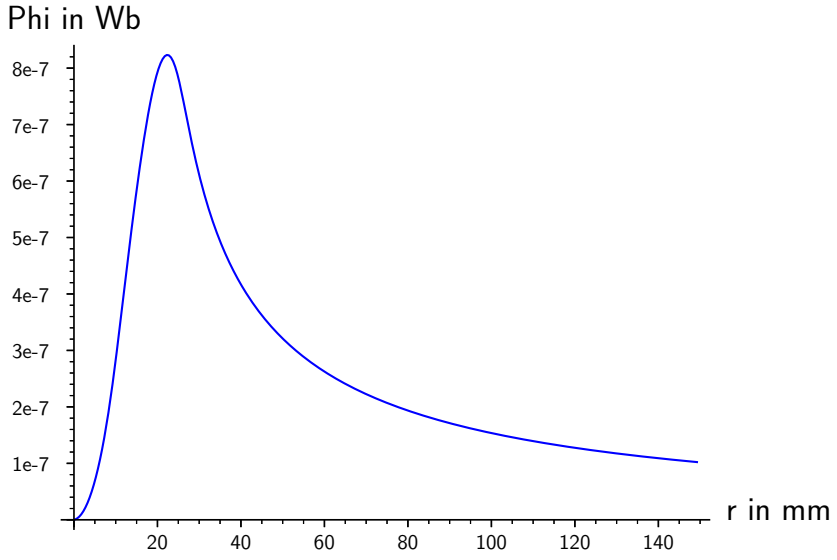

Figure 3.34: Simulated magnetic flux of MP-A9 setup in a concentric coil in 3mm distance

Figure 3.34 shows the numerical calculation of (3.11) in a distance of $r_z = 3$mm.

To calculate the worst case coupling between the wireless charger and any PICC antenna in the $z = 3$mm plane, the total flux with positive z component must be calculated. This flux is the maximum of equation (3.11) shown in figure 3.34. By investigating this figure, it can be found that a concentric circular loop with the radius of 22.3mm maximizes the coupling to the charging coil[9].

$$\frac{\Phi_{total}}{I_{coil}} = 2\mu_0 0.32763 = 823.4\frac{\text{nWb}}{\text{A}} \tag{3.12}$$

Because of the charging field, a voltage is induced in the NFC coil of a card. The voltage in the coil is[10]

$$V_{ind} = -\frac{d\Psi}{dt} \approx -\frac{N d\Phi}{dt}$$

The maximal effective flux, which can flow through the card's antenna, is the Φ_{total} calculated in equation (3.12).

$$\begin{aligned} V_{\text{ind,max-K}} &= N\frac{d\Phi_{tot}}{dt} = N823.42\text{nWb}\,\text{A}^{-1}\frac{dI_{\text{WCh,coil}}}{dt} \\ &= N823.42\text{nWb}\,\text{A}^{-1}\frac{V_{\text{WCh,coil}}}{L_{\text{WCh,coil}}} \\ \frac{V_{\text{ind,max K}}}{V_{\text{WCh,coil}}} &= N77.68^{\text{mV}}/_{\text{V}} \end{aligned} \tag{3.13}$$

Equation (3.13) allows to quickly calculate the worst case voltage at the card from the number of turns and the voltage at the wireless charging coil. The value of the inductance used in the equation is the approximation from equation (3.8).

The positioning of the PICC plays a crucial role. If the PICC antenna is overlapping with the charging coil by approximately 50%, almost no voltage is induced and the card can withstand any charging fields. Using the equations for the magnetic flux density, the total flux through an ID1 sized loop can be calculated for a certain positioning. For calculating the flux, the area of a 40mm x 70mm ID1 card is divided into ring segments with equal magnetic flux density. The complete flux is then the sum of the flux densities times the areas covered.

By least squares optimization, the position with maximal coupling is calculated. When the card is offset by 14mm from the center aligned position in the direction of the longer side of the PICC's antenna, the coupling is maximized. The simulated magnetic flux is then $642\text{nWb}\,\text{A}^{-1}$ times the coil current. This can be also expressed as $60.6\text{mV}\,\text{V}^{-1}$ times the coil voltage.

The most important findings of this section was the calculated maximal coupling between a lower coil of the MP-A9 charging coils and a PICC. The worst case is 77 68mV/V for round coils with $r = 22.3mm$. For ID1 cards, the ratio is 60 6mV/V.

[9]The only remaining unknown for calculating the coupling factor K is the wire thickness of the secondary coil. Changing the number of turns does not change the coupling factor, because the mutual inductance grows linear and the self inductance quadratically with the number of turns.

[10]The approximation assumes, that the N turns of the card overlay each other. Then every turn sees the same magnetic flux Φ and induces the same voltage.

3.5.5 Measurement of coupling and comparison with calculated values

In the last section, the field distribution of the charging field and several coupling situations were analyzed numerically. To supplement the results, in this section measurements are presented, which cover the calculated scenarios. In order to assess the effects of a charging field with the MP-A9 setup on cards in section 3.6, formulas are derived to calculate the voltage induced in a card's antenna. Several measurements are performed to assess influences of the amplitude, distance between the charging coil and the card and of the Qi power receiver.

The results of the last section are quite accurate for the lower charging coils only, because the middle coil has a greater distance from the ferrite. To compensate for the greater distance, the middle coil has an extra winding. For most experiments, the middle coil was used.

In the simulations of the last section, the coupling was assessed by calculating the field for a current of 1A in the primary wireless charging coil. As from a theoretical point the coupling is independent of the frequency, the signal shape was not analyzed. However, for the measurements of the induced voltage, the field was generated by the regular charging circuit. In order to compare the results, the signals are decomposed in their frequency components. The fundamental frequency is used to assess the coupling.

Harmonics and RMS values of the wireless charging current

The current through the coil can be easily calculated in the frequency domain. Because the signal from the H bridge has a duty cycle of 50%, the formula for the nth harmonic becomes:

$$\hat{I}_n = \frac{V_{in}[n]}{Z(n\omega_{0,WCh})} = \frac{2V_{rail}}{jn\pi} \begin{cases} 0, & \text{if } 2 \| n \\ 2, & \text{else} \end{cases} \quad \frac{1}{jn\omega_{0,WCh}L + \frac{1}{jn\omega_{0,WCh}c}}$$

For the schematic values, the formulas for the fundamental and the third harmonic become $|\hat{I}_1| = 2.678mSV_{rail}$ and $|\hat{I}_3| = 18.8mSV_{rail}$. The RMS value can be calculated as the sum of squared absolute values of I_n. Unfortunately, no analytical solution to the infinite sum could be found. But a numerical approximation gives:

$$I_{rms} = \sqrt{\sum_{i \in \mathbb{N}_+, 2 \nmid i} \frac{|\hat{I}_n|^2}{2}} \approx 189.9mSV_{rail} \tag{3.14}$$

The value was calculated for $L = 9.8\mu H$, $c = 400nF$ and $\omega_{0,WCh} = 2\pi 127774Hz$.

The purpose of the first measurement is to verify, if the voltage at the charging coils behaves as expected. For this measurement, the middle charging coil was used. The rail voltage of the charger was set up to 5V. The voltage across the charging coil is measured with an oscilloscope. The comparison of the spectre to the expected, calculated values can be seen in figure 3.35. For the fundamental, an error of 5% could be observed. The measured value is 9.952V, whereas the simulation gives 10.51V. A possible error source could be parasitic inductances.

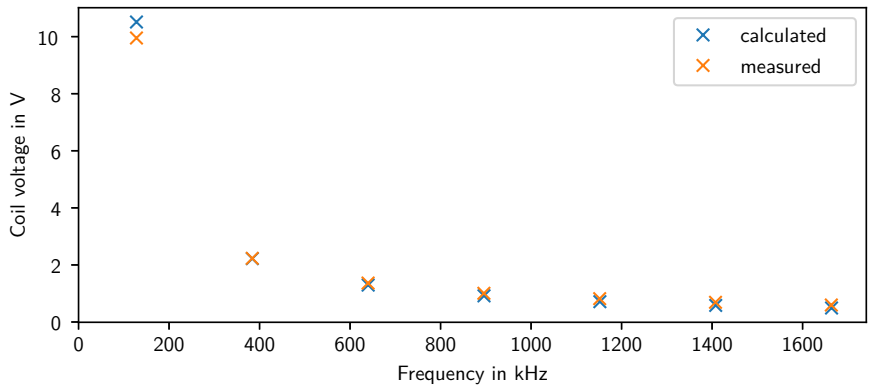

Figure 3.35: Visualization of the calculated spectre of the coil voltage versus the measured spectre.

Maximum coupling between charging coil and circular coil (measurement)

Next, the maximal coupling between the charger and a secondary coil was determined empirically. The charger was set up to produce a field with 5V rail voltage at 127.774kHz. A circular coil was placed concentrically to the charging coil in a distance of 3mm. The induced voltage is recorded with an oscilloscope. The size of the loop was adapted to maximize the induced voltage.

The coupling was maximized with a circular antenna with a circumference of 145mm. The radius is 23mm, which validates the calculated 22.3mm. The fundamental amplitude of the measured voltage is 674mV. The ratio of the induced voltage to the coil voltage therefor is $674mV/9.952V = 67.73^{\mathrm{mV}}/\mathrm{V}$. The theoretical value found in simulation is $77.68^{\mathrm{mV}}/\mathrm{V}$. Because the outer coils were simulated, but the middle coil was measured, a deviation is expected.

The analysis of the maximal coupling is interesting as the worst case measure especially for small antenna forms. Next, the maximal coupling to an ID1 card is assessed experimentally.

The wireless charger is set up to use a rail voltage of 5V and to use a frequency of 127.774kHz. A wire loop in ID1 shape (40mm x 70mm, as simulated in section 3.5.4) is connected to an oscilloscope to assess the coupling to the charging coil in 3mm distance. The position of the wire loop was adapted to maximize the induced voltage. The maximal fundamental amplitude of the induced voltage was 559mV. The maximum ratio of the induced voltage in a one turn ID1 card to the coil voltage is therefore $559mV/9.952V = 56.17^{\mathrm{mV}}/\mathrm{V}$. The calculated value was $60.6^{\mathrm{mV}}/\mathrm{V}$. This value is used to calculate the mutual inductances in section 3.6.5.

Using equation (3.14) for calculating the RMS current, the RMS magnetic flux can be calculated from the rail voltage of the charger:

$$\Phi_{tot,rms} = 78.2\frac{\mathrm{nWb}}{\mathrm{V}}V_{rail} \tag{3.15}$$

Equation (3.15) allows to quickly calculate the worst case voltage at the card from the number of turns. The inductance used for the numerical value is the calculated inductance

from equation (3.8).

Measurement of linearity of the wireless charging circuit

With the next experiment, the linearity of the charging coils is assessed. The position of the ID1 loop is fixed, and the rail voltage is changed from 5V first to 10V and then to 20V. The spectre of the induced signal is supposed to increase constantly over all frequencies by 6dB.

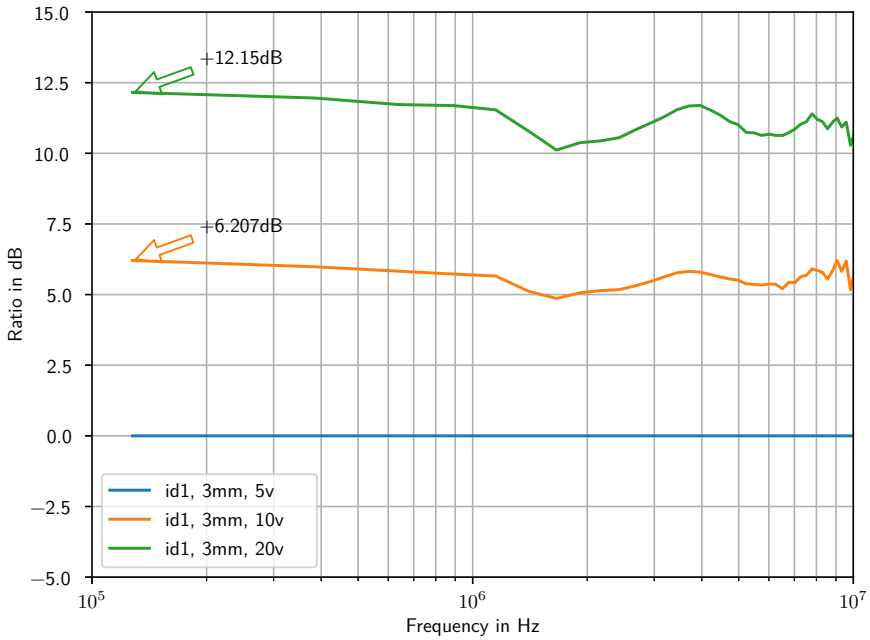

Figure 3.36: Comparison of the induced voltage in an ID1 card at different rail voltages

Figure 3.36 shows the effect of the rail voltage over the frequency. The values are normalized to the setup at 5V. As expected, the curve for 10V rail voltage is about 6dB above the 5V signal. The curve for 20V is about 12dB above. The deviation from the expected values for the fundamental is with 0.2dB or 2.3% relatively small. For higher frequencies, the deviation gets bigger. In the NFC frequency range, the increase by a factor of 4 of the rail voltage resulted in an increase of a factor of only 3.2 of the induced voltage. There exist many possible reasons for this behaviour. For example any limitation of the slew rate of the output stage of the charger could cause such a behaviour.

Measurements of effects of the distance between charging coil and PICC

Figure 3.37 shows the difference of the induced voltage when directly on top of the charging coil, in 3mm distance and in 6mm distance. All curves are normalized to the spectra of the recorded signal at 3mm vertical distance. It can be seen, that the field increases by 3 decibels, if the distance is reduced to zero. When increasing the distance to 6mm, a reduction of only 1 decibel could be observed. This plot suggests, that increasing the distance to the charging coils has only little impact on the induced voltage in cards.

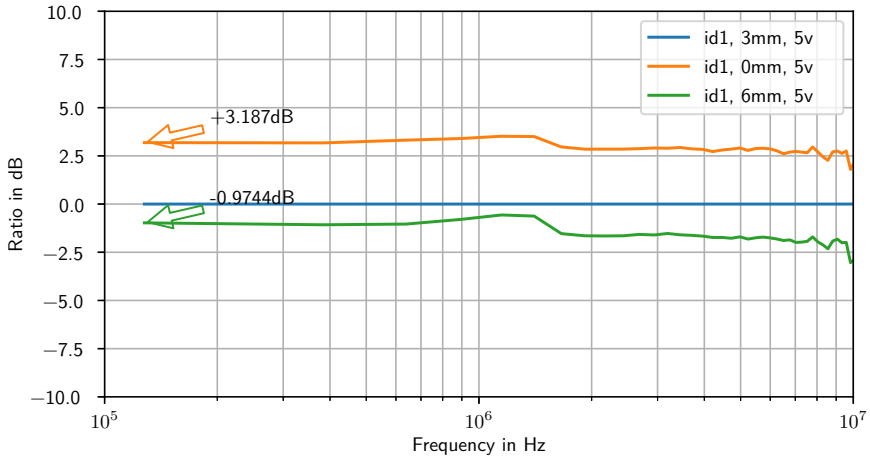

Figure 3.37: Influence of the distance on the maximal coupling of an ID1 card

Measurement of the influence of a Qi power receiver

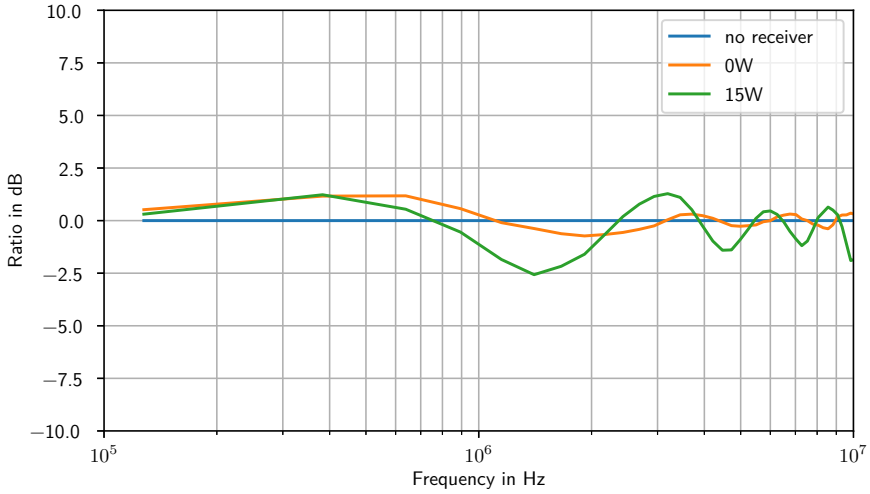

Figure 3.38: Effects of a power receiver on the induced voltage in a card

So far, all the setups did not include a Qi power receiver. The next experiment was performed to evaluate the effects of a power receiver. The wireless charger was set up to use a fixed rail voltage of 12V.

Figure 3.38 shows the spectral components without a power receiver, with a power receiver but without any load connected to it and with a power receiver, which constantly pulls 15W. The field was recorded with a round loop with a diameter of 45mm. In contrast to the former setups, the position is fixed and not optimized to yield a maximal voltage. The pickup coil is positioned between the power receiver and the charging coil, resulting in high coupling values. The curves are again normalized, so that the signal without a power receiver (blue) is at 0dB. According to the formula (3.14) derived earlier in this section, the

RMS current at 12V rail voltage without receiver should be $I_{RMS} = 189.9\text{mS}12\text{V} = 2.28\text{A}$. The internal current measurement reports a coil current of 2.19A.

The orange signal was recorded in presence of a QI power receiver without any load connected. It can be seen, that the spectral components change their amplitude only marginally by up to 1.3db. The current reported by the internal coil current measurement circuit is 1.72A. So even less, than without a receiver[11]!

Finally, for the green signal the receiver is loaded with a resistor. To cover the maximal load in the extended power profile, the resistor was designed to have 1.66Ω and dissipate 15W at the 5V output of the receiver. The realized value is higher, resulting in only 13W to 14W of dissipated power. It can be seen, that the induced voltage mainly depends on the rail voltage and not on the loading in this setup. The coil current measurement circuit reports 2.73A.

For all three measurements, the rail voltage was fixed at 12V. The power receiver used is configured to operate, even though the charger does not communicate the QI control packages in this mode. A comparison of different power receivers is difficult, because many of them do not operate with a fixed rail voltage.

Omitting a power receiver for measurements yields a reasonable number of well reproducible setups. In contrast, when measuring with a receiver many unknown parameters influence the reproducibility of the setups negatively:

- Power consumption

  If a phone is used as power receiver, it cannot be controlled, how much power the phone draws.

- Magnetically active materials

  Different phones have different influences on the magnetic field lines. Ferrites guide them. In metallic objects, additional losses occur.

- Positioning and Coupling situation

  Without a phone, there is one coupling condition between Card and charging coil to take care of. With a phone, there are several mutual inductances, which have to be considered.

- Rail voltage, frequency, duty cycle

  As the power transmitter is supposed to adjust its parameters according to the receiver's need, one looses control over at least one of these three parameters.

Concluding from these observations, for further experiments a setup without power receiver is chosen.

To summarize, in the last sections following worst case ratios were measured for the

[11] This behaviour is not consistent across receivers. Some power receivers cause the current to rise.

MP-A9 wireless charging setup for the middle coil and NFC cards:

$$\frac{I_{rms}}{V_{rail}} = 190mS,$$
$$\frac{\Phi_{rms}}{V_{coil}} = 78.2\frac{\text{nWb}}{\text{V}} \text{ for the total magnetic flux,}$$
$$\frac{V_{ind}}{V_{coil}} = 67.7^{\text{mV}}/_{\text{V}} \text{ worst case for antennas with r=23mm,}$$
$$\frac{V_{ind}}{V_{coil}} = 56.2^{\text{mV}}/_{\text{V}} \text{ worst case for ID1 antennas}$$

These equations cover the major influences of wireless charging on PICCs. Other influences were identified but not modeled. In the next section, the topic of card destruction by wireless charging fields is investigated using these ratios.

3.6 Analysis of card damaging by charging fields

It was found that the strength of the charging field, in which cards are permanently damaged, varies widely between different cards. In order to understand these differences, this section aims to explain the processes and to derive formulas for assessment, whether a card will be damaged, or not. It is important to understand the effects, which cause the damage on the cards. Interestingly, it was seen, that cards can be operated far beyond the absolute maximum ratings before they get permanently damaged. In order to find the point, where limits are exceeded, it is necessary to express the relations mathematically. Furthermore, the gathered knowledge could be used in future to develop robust cards, which can withstand the wireless charging fields.

First, the process of card destruction is investigated experimentally. The limits together with key parameters of several cards are summarized.

Secondly, the limiters of different cards are measured. These simple measurements give insight in the source of the problem. It allows to create a simplified model of a card, which is later used for simulations.

Next, the thermal aspect is enlightened. Therefore, the relation between power dissipation and over-temperature is discussed. The maximum temperature and the maximum power dissipation are investigated. Then, the effects of over-voltage and over-current are discussed.

Finally, the measurements, the numerical and the theoretical considerations from the previous sections are combined in a model of the system. The system is simulated for different rail voltages.

3.6.1 Experimental investigations on card destruction

In this experiment, the robustness of different cards against wireless charging fields is evaluated. The coupling between a card and the middle charging coil is maximized as described in section 3.5.4 and the rail voltage of the charger is increased step-wise. No power receiver is used. Instead, the charger is set up to apply a constant charging field. After applying the field for 30 seconds, an NFC reader is used to assess, if the card is still responsive. The rail voltage at which the card got incapacitated is recorded.

DUT	Size	Turns	Card material	Rail Voltage	Frequency	Coil Voltage
1	ID1	3	Plastic	>15	100	>38.8
2	ID3(circle)	4	Plastic	12	110	23.8
3	ID1	5	Plastic	9.4	127.774	14.6
4	ID2	5	Plastic	10	100	25.8
5	ID2	8	Paper	14.9	127.774	23.2
6	ID1	7	Inlay only	8.7	127.774	13.5

Figure 3.39: Comparison of the destruction levels of different cards

In figure 3.39, the destruction levels of six different PICCs are shown. The table shows different NFC cards with their chip, card material, antenna size and number of turns. The rail voltage and the frequency is noted at the point at which the card permanently stopped to respond. Different models of different manufacturers were used. Their names are not disclosed. Instead, they are named "DUT 1" to "DUT 6" in the whole document. The last column shows the calculated RMS voltage at the charging coil. It makes the measurements with different frequencies comparable.

Most cards were measured with 127.774kHz. However, some cards could not be destroyed with that frequency. For them, the frequency was reduced in order to increase the induced voltage in the card.

In the next sections the phenomena is discussed in more detail.

3.6.2 Analysis of power dissipation in PICCs

As explained in section 2.5.1, cards usually contain a limiter, which protects the integrated circuit from over-voltage. There are several concepts of limiters, which all behave similar from the outside. When the voltage exceeds a threshold, the limiter becomes conducting (like a Zener diode) and prevents the voltage from rising any further.

When the limiter gets active, the majority of the power is dissipated there. The power consumption of the remaining chip is neglected for the considerations in this section.

During regular operation, the limiter clips an NFC field at 13.56MHz. Fortunately, all limiters under investigation also work at lower frequencies and even with DC. The load curves of the chips of several NFC cards were measured by applying a DC voltage to them. Both, current and voltage were measured.

In figure 3.40, the DC voltage over current curves of several NFC cards chips can be seen. All the devices despite DUT 1 show a very flat curve. The limiter restricts the voltage as described before by creating a shunt current.

The lowest clipping voltage is 3.3V measured with DUT 6. Figure 3.39 shows, that this tag has a high number of windings and is already permanently incapacitated at low rail voltages.

On the other end, there is DUT 1, which is very robust against Qi charging. It's antenna has only three turns and the limiter tolerates higher voltages.

The currents and the power in the measurement are higher, than the maximum ratings in the data sheets. The curves for 200mW and 500mW are there for orientation. 200mW is a typical data sheet value. However, for some chips more than 1W was required to

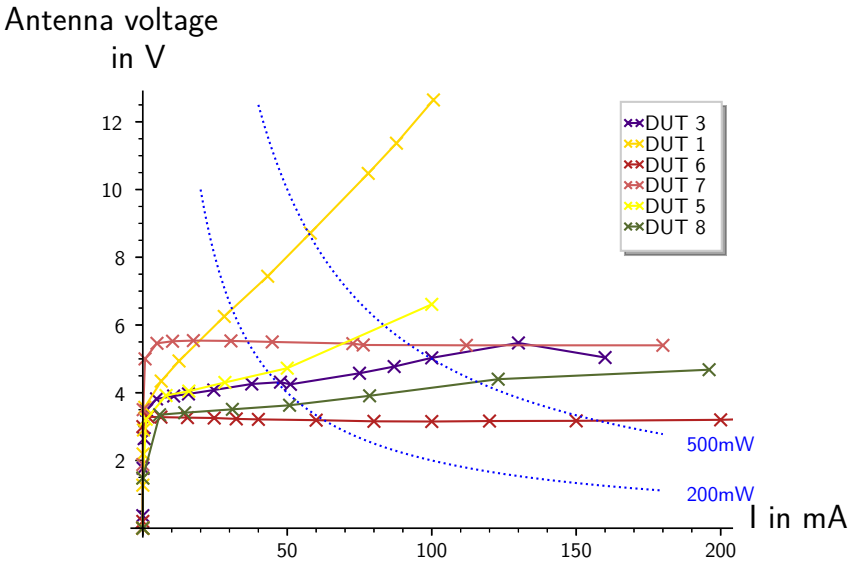

Figure 3.40: DC load characteristic of NFC chips (limiter)

incapacitate them. Moreover, 200mA are far more, then the absolute maximum ratings of the ICs allow.

3.6.3 Analysis of thermal degradation

When cards are placed in a strong charging field, power is dissipated in the limiter and the chip heats up. The rate depends on the heat capacity. It was found, that a steady temperature is reached after about 15 seconds, depending on the card. The final temperature depends on the heat resistivity.

Figure 3.41: Picture showing thermal degradation of an NFC card

Figure 3.41 shows the thermal effects on a PICC. The plastic in the region of the chip melts and discolors. The card was still functional.

Unfortunately, no suitable measurement equipment was available for assessing the temperature of the chip properly. Measurements with an infrared thermometer suggest, that the temperature at the surface of the card was above 150°. For comparison, Card ICs

produced by NXP usually are specified for ambient temperatures up to 70°. Furthermore ISO 7810 specifies, that identity cards must not show delamination or discoloration at temperatures below 50°C.

As shown in figure 3.41, plastic cards may start to deform in the region close to the chip. Moreover, smoke could be observed on some cards. Fortunately, no cases of ignition of paper cards are known. The auto ignition temperature of paper is above 200°C.

The power dissipated in the chip $P = VI$ has to be transported to the environment. The thermal resistance between chip and environment determines the temperature difference $\Delta T = R_{th}P$.

Assuming an infinitely extended card with the heat source in the middle, the lines of equivalent temperature are concentric circles. The thermal resistance of a cycle with radius r can be described with infinitesimal thermal resistances and conductances (see figure 3.42).

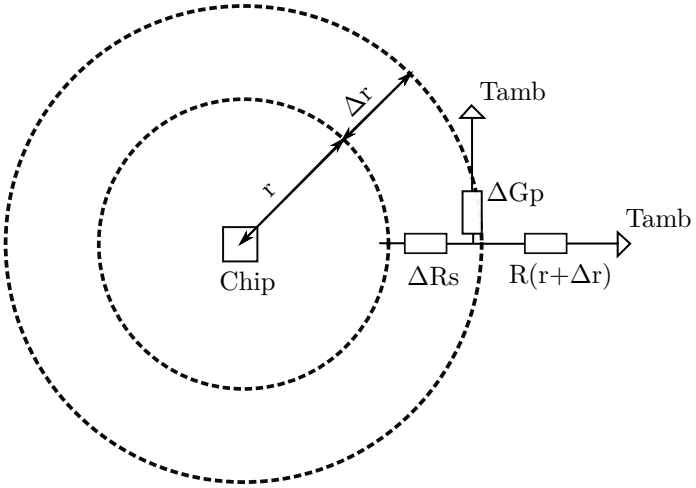

Figure 3.42: Model of the thermal resistance of an infinite card

The model from figure 3.42 can be used to calculate the thermal resistivity R(r) between a circle with the radius r and the ambient temperature potential. The model partitions the card in rings with a certain width Δr. By replacing Δr with the infinitesimal small dr, R(r) can be expressed implicitly by a differential equation.

ΔR_s is the series thermal resistivity of the ring. It is caused by the thermal conductance of the material of the card. It can be calculated as:

$$\Delta R_s = \frac{\Delta r}{2\pi r d k}$$

d is the thickness of the card and k is the specific thermal conductance, which is a material constant.

ΔG_p is the parallel thermal conductance. It is a measure for the heat dissipated into the air or another material, which surrounds the card. It is assumed, that the top side

dissipates energy by convectional heat transfer, while the bottom side conducts the heat. It can be approximated by:

$$\Delta G_p = 2\pi r \Delta r(\alpha_{\text{convection}} + \alpha_{\text{conducted}})$$

$\alpha_{\text{convection}}$ is the heat transfer coefficient of the top side. It depends on the medium (air), the geometry and the temperature difference. For natural convection, a typical value is $10\text{W}\,\text{m}^{-2}\,\text{K}^{-1}$. When the card lies on top of the charger, heat is dissipated by conductance to the charger on the bottom side. In the calculations, a value of $\alpha_{\text{conducted}} = 100\text{W}\,\text{m}^{-2}\,\text{K}^{-1}$ was used.

$R(r + \Delta r)$ is the resistivity of the outer circle towards infinity.

Now $R(r)$ can be calculated as:

$$R(r) = \Delta R_s(r) + \frac{1}{\frac{1}{R(r+\Delta r)} + \Delta G_p(R)}$$

$$\frac{R(r)}{R(r+\Delta r)} + R(r)\Delta G_p(r) = \frac{\Delta R_s(r)}{R(r+\Delta r)} + \Delta R_s(r)\Delta G_p(r) + 1$$

$$R(r) + R(r)G_p(r)R(r+\Delta r) = \Delta R_s(r) + \Delta R_s(r)\Delta G_p(r)R(r+\Delta r) + R(r+\Delta r)$$

$$\Delta R(r) = R(r) - R(r+\Delta r) = \Delta R_s(r) + \Delta R_s(r)\Delta G_p(r)R(r+\Delta r) - R(r)G_p(r)R(r+\Delta r)$$

Taking the limes ($\lim_{\Delta r \to 0}$) gives the differential equation.

$$dR(r) = dR_s(r) - \underbrace{dR_s(r)dG_p(r)R(r)}_{\to 0} - R(r)^2 dG_p(r)$$

After inserting the equations, the regular differential form in equation (3.16) can be observed.

$$\frac{dR(r)}{dr} = \frac{1}{2\pi r dk} - R(r)^2 4\pi r \alpha \tag{3.16}$$

Unfortunately, an analytic solution to the equation could not be found. In figure 3.43, the solution for (3.16) can be seen for specific values for α and k. If the radius of the heat source is 2mm, it heats up by about 605K for paper and 426K for plastic cards per Watt according to this graph.

With high temperatures, heat transfer by radiation occurs. The formula for the power depends on the temperature to the power of four. For a perfectly black object with a certain temperature, the energy radiated becomes $P = \rho A T^4$. Likewise, the environment radiates and heats up the object. The net power becomes:

$$P = \rho A(T^4 - T_{ambient}^4)$$

ρ is the Stefan-Bolzmann constant. When considering radiation, the relation to the temperature becomes non-linear. For example with 100K over temperature, about $1450\frac{W}{m^2}$ or $14.5\frac{W}{Km^2}$ are radiated. With 200K over temperature, the value becomes $3540\frac{W}{m^2}$ or $17.7\frac{W}{Km^2}$. It can be concluded, that for realistic temperatures, the effect of radiation is significantly smaller than the effect of conducted heat transfer to the charger. Therefore, it is not considered any further for the model from figure 3.42.

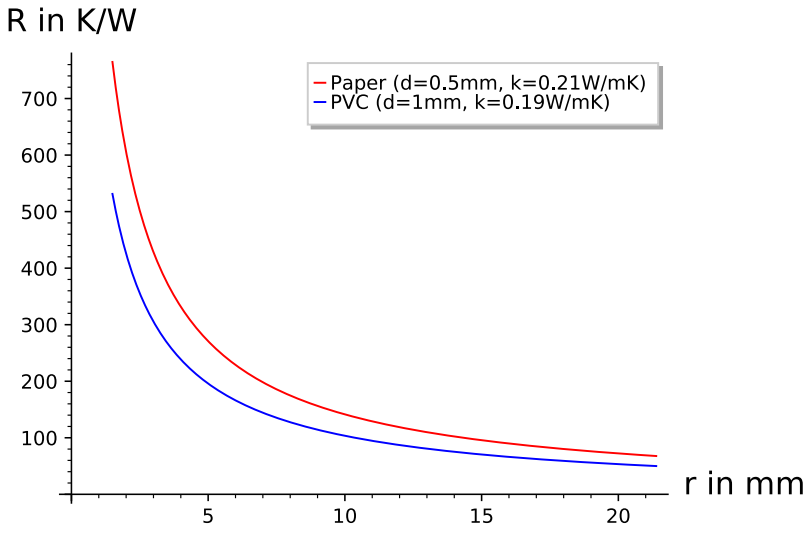

Figure 3.43: Simulated, thermal resistance over the size of the heat source (homogeneous card, without radiation)

The analysis shows, that paper cards are more susceptible to thermal degradation than plastic cards. The difference is in the order of 30% less temperature difference with plastic cards.

Because this numerical solution is based on assumptions, it can be only used as an indicator. For giving correct predictions, the thermal resistance has to be simulated for the setup of interest including the antenna shape and the package of the IC. This is out of scope for this thesis.

Instead, the temperature of the card in proximity to the IC of DUT 3 was measured with an infrared thermometer while increasing the dissipated power. The antenna of the card was cut and the NFC chip connected to an adjustable DC power supply. Current through and voltage at the chip was measured with a multimeter.

Figure 3.44 shows the temperature of the card on the ordinate and the power $P = UI$ on the abscissa. By curve fitting, a linear approximation of the data was found.

$$T = T_0 + R_{th}P = 23.8° + 131^{\mathrm{K}}/\mathrm{w}P$$

The thermal resistance observed in the experiment is significantly smaller, than the values found numerically for equation (3.16).

A reason for this difference could be the measurement equipment. The infrared thermometer captures the heat radiation in a certain radius. Because of this averaging, the observed thermal resistance is smaller, than the real value. Also the resistance in figure 3.43 drops within 1cm to about $100^{\mathrm{K}}/\mathrm{w}$.

As a conclusion, it can be stated, that cards may be operated significantly out of their specification, before they break. Current, power and temperature limits were exceeded significantly. The relation between power and temperature is linear, but for the thermal resistance only rough estimates could be made.

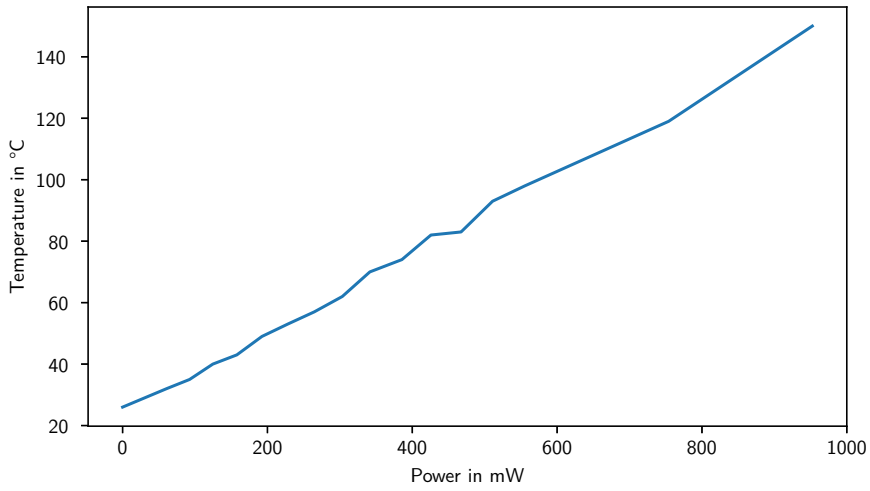

Figure 3.44: Measurement results of temperature in DUT 3 over dissipated power

3.6.4 Analysis of destruction by over voltage or over current

If the voltage across the two pins of the chip exceeds the maximal gate source voltage of the process of the chip, CMOS gates can break through. Therefore, the peak value of that voltage is of special interest.

First, the effects of the switching of the H-bridge are investigated. Therefore, the step response of the voltages and currents is analyzed. Afterwards, the voltages and currents are analyzed, if the induced voltage in the card's antenna gets bigger than the activation voltage of the limiter.

For simplicity the resonance capacitor of the QI circuit is neglected. The rectangular voltage causes a ramp shaped field. The ramp shaped field causes again a rectangular voltage being induced in the NFC card's antenna.

As analyzed before (section 3.3), the induced voltage at the card becomes

$$V = V_{\text{H-bridge}} \frac{M}{L_{WCh}}$$

and the inductance of the antenna is reduced by the factor $(1 - K^2)$.

The antenna and the capacitance across the IC's pins form a parallel resonance circuit. At the flanks of the rectangular voltage, overshoots occur. The height of the overshoots depends on the operation of the IC. Without IC and parasitic resistances, the step response can be calculated directly using the Laplace transform.

$$V_{IC} = \underbrace{\frac{1}{s}}_{\text{unit step}} \underbrace{\frac{\frac{1}{sc}}{\frac{1}{sc} + sL}}_{\text{LC filter}} = \frac{1}{s(s^2 Lc + 1)} = \frac{A}{s} + \frac{B + Cs}{s^2 + \frac{1}{Lc}}$$

Equating coefficients gives:

$$V_{IC} = \frac{1}{s} + \frac{s}{s^2 + \frac{1}{Lc}}$$
$$v_{ic}(t) = 1 + cos(\frac{t}{\sqrt{Lc}})$$

First, the inductance gets loaded. The current reaches the maximum, when the voltage across the capacitor reaches the induced voltage. The current in the coil further loads the capacitor up to twice the induced voltage. Considering, that the voltage jumps from $-V_{ind,\sqcap\!\sqcup}$ to $+V_{ind,\sqcap\!\sqcup}$, the peak voltage at the IC is even three times the peak value of the induced voltage.

If the limiter of the IC was a perfect clamping element, which gets conductive (shorts) just above the amplitude of the rectangular voltage, it would take over the current of the coil:

$$\begin{aligned} \hat{I}_{IC} = \hat{I}_L &= \sqrt{\frac{2\hat{W_{L/c}}}{L(1-K^2)}} = \sqrt{\frac{2c(2V_{ind,\sqcap\!\sqcup})^2}{2L(1-K^2)}} \\ &\approx 2V_{ind,\sqcap\!\sqcup}\sqrt{\frac{c}{L}} = \frac{2V_{ind,\sqcap\!\sqcup}c}{\omega_{card}} \end{aligned} \tag{3.17}$$

To give an example, values of c=20pF and $L = 6.5\mu H$ at an induced voltage of 5V result in a current peak of 18mA. This current peak prevents the voltage from reaching 15V. If the limiter is too slow, the voltage could rise to 15V, and possibly damage the IC. This current seems harmless, but if the capacitor is bigger, also the current gets bigger. Component values of c=70pF and $L = 1.8\mu H$ cause a peak current of about 62mA. If the limiter is already active, for example because of an NFC field, this current peak could get problematic. Common absolute ratings (data sheets values) of card ICs are around 30mA.

So far, the effect of the edges was discussed. However, if the induced voltage becomes greater than the activation voltage of the limiter, much bigger currents may flow. Then the current flows during the complete period and not just at the transitions.

At 125kHz, the impedance of the NFC coil inductance is small. For instance a $3\mu H$ coil has an impedance of about 2.5Ω. This is part of the reason, why the NFC cards have problems with limiting the voltage.

The charging field ramps up and down, and causes a voltage at the NFC coils, which is rectangular in first approximation. The limiter of the IC pulls the voltage at the chip to a lower level. The difference lies on the inductance of the card's antenna and on parasitic resistances. By neglecting the resistances, the formula for the current becomes:

$$\frac{dI}{dt} = \frac{V_{ind,rec} - V_{limiter}}{L}$$

As the current has to be free of any DC components, the term to the right can be integrated for a quarter of a wireless charging period ($\approx 8\mu s/4$) to get the peak current.

$$\hat{I}_{IC} = \int_0^{8\mu s/4} \frac{V_{ind,rec} - V_{IC}}{L} dt = \frac{2\mu s(V_{ind,rec} - V_{IC})}{L}$$

For example, if $V_{ind,rec} = 6\text{V}$ and $V_{IC} = 5\text{V}$ and $L = 3\mu H$, then the current through the IC becomes $\hat{I}_{IC} = 0.67\text{A}$. This current exceeds the maximum absolute ratings by far. Therefore, the metal traces in the IC probably will break.

However, if the limiter does not pull this current, instead the voltage at the IC would rise. The limiter can allow this only to some extent, because else the chip gets disabled by over voltage. As a conclusion, card destruction by over voltage and by over current are linked by the limiter. If the limiter fails in presence of strong wireless charging fields, over voltage might occur. If it operates correctly, high currents will occur.

To assess the susceptibility of a card, the following parameter need to be evaluated:

- Maximum magnetic flux Φ_{max}, which can be fetched by the antenna.

  Typically, form factors close to the size of a charging coil behave worst. Bigger antennas have some field lines in opposite direction, canceling each other. For worst case values see section 3.5.4.

  Small antennas have another disadvantage. They often need more turns to achieve the required voltage level or the required inductance.

- Number of turns.

  Together with the maximal field and the frequency, this determines the maximal voltage at the antenna.

  $$V_{ind} = -\frac{d\Psi}{dt} = -N\frac{d\Phi}{dt}$$

- Inductance and capacitance.

  In order to reduce the current through the PICC, according to formula (3.17) the inductance of the cards antenna shall be high and the capacitance low. Increasing the number of turns would result in a higher inductance. However, keeping the number of turns low is more important, than a high inductance. To increase the value, the area of the antenna can be increased or the diameter of the wire/track reduced.

  Because the resonance of the NFC card shall be slightly higher than 13.56MHz, the inductance and capacitance cannot be changed independent from each other. The capacitance partly comes from the IC. The remaining part then can be tuned by creating overlaps in the antenna layout.

  Parasitic resistances would also reduce the current, but decrease the quality factor too.

- Maximal ratings of the IC (current, voltage, power, temperature).

  Assuming, that the limiter is operating properly, the voltages and currents at the IC can be calculated. These values could be compared to the absolute ratings of the IC. The next section shows, that the real limits are much higher, than the data sheet values.

3.6.5 Comparison of NFC cards

This section summarizes some measurements on actual cards. The theoretical considerations of the last sections shall be supported by measuring the point, where cards stop to work.

Figure 3.45: Comparison of different NFC Chips for cards

In figure 3.45, different packages and methods of mounting on the card can be seen. One reason for the greater robustness might be the better heat transportation. Figure 3.43 shows, that increasing the effective size of the heat source has a considerable impact on the thermal resistance and therefore on the temperature of the chip. As many degradation processes speed up exponentially with the temperature, even small differences could be essential.

The DUT number 1 has only 3 windings. Therefore, the induced QI voltage is much smaller, than with the other cards.

Estimation of losses

The limiter is simplified as an ideal voltage clamping device plus a resistor for the remaining steepness. Curve fitting gave the values for the two measures. The resistance of the antenna is measured with a multimeter. The inductances of the antennas are calculated based on their geometry. For completing the model, the capacitances are calculated for a resonance at 13.56MHz.

The induced voltage at the limiter is calculated according to the analysis in section 3.5. For the calculation, the measured voltage of $45.5^{\mathrm{mV}}/\mathrm{v}$ per turn on the charging coil is used. After some experiments, PySpice with ngspice as solver was used to simulate the circuit because of the scripting capabilities. Unfortunately, the current version does not support steady state simulations (like harmonic balance) yet. Therefore a transient simulation was used instead. The boundary conditions for a steady state can be expressed for a half period by exploiting the point symmetry:

$$I_{L,NFC}(0) = -I_{L,NFC}(\frac{\tau}{2})$$
$$V_{IC,NFC}(0) = -I_{IC,NFC}(\frac{\tau}{2})$$

Figure 3.46 to 3.48 show the maximal currents (peak), maximal voltages (peak) and average power dissipation in the card, found during simulation. On the ordinate, the rail voltage can be seen.

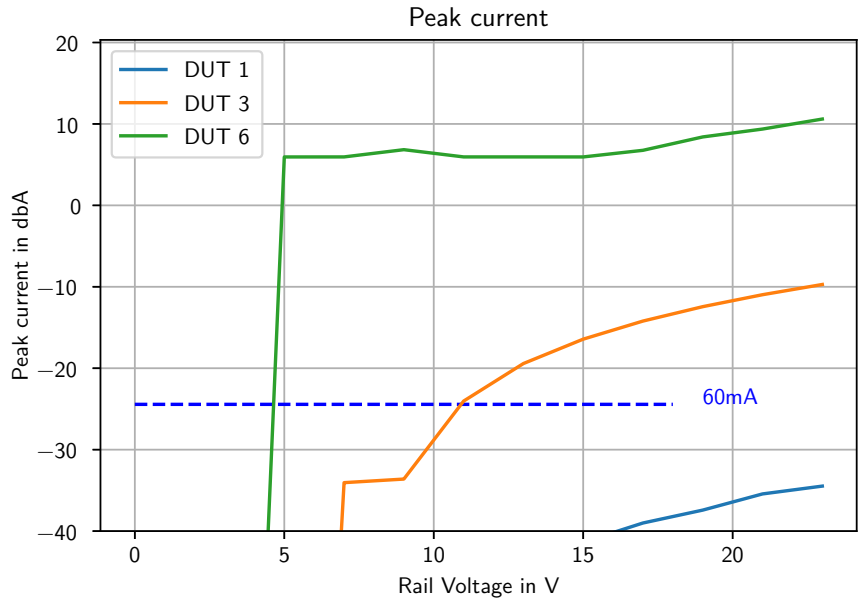

Figure 3.46: Simulated maximal peak current in cards during charging

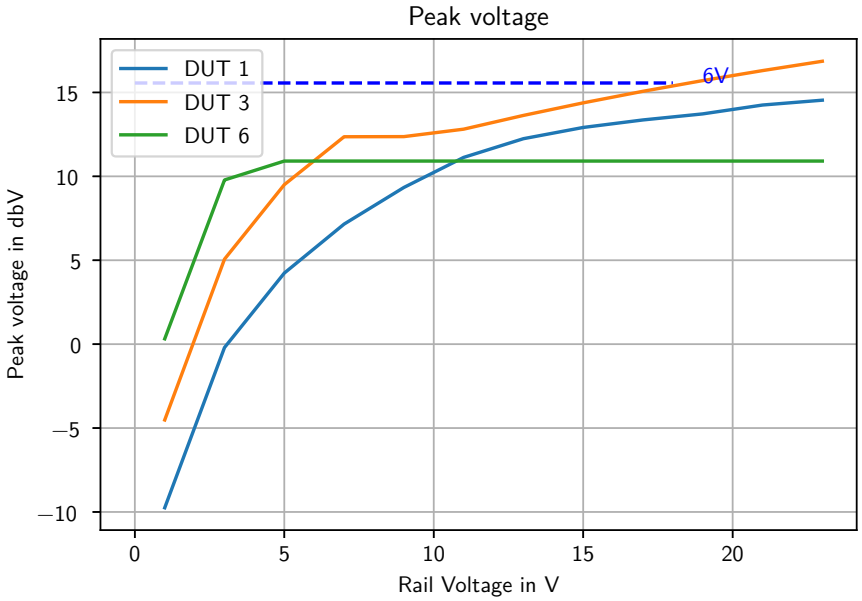

Figure 3.47: Simulated maximal peak voltage in cards during charging

Critical values are marked with dotted lines. 60mA is a typical design decision for dimensioning on chip tracks. 375mW was the power, at which destruction due to over heat is expected[12]. The voltage level, at which the gate breaks through, could be 6V.

[12]Assuming a maximal over temperature of 250°C.

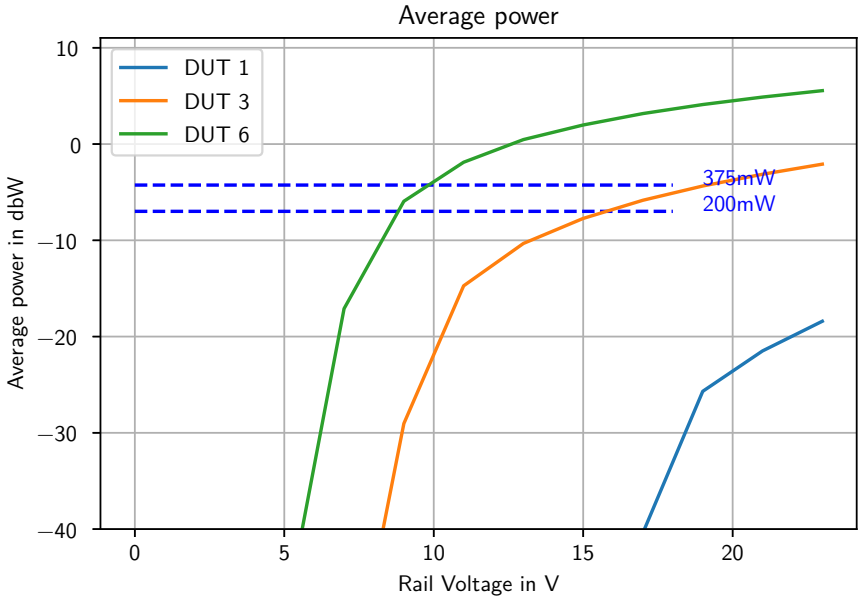

Figure 3.48: Simulated average power dissipation in cards during charging

It can be seen, that the design decisions for DUT 6 are unfortunate for coexistence with wireless charging. Because the number of turns is high and the voltage of the limiter is small, the limiting operation already starts at lower field strengths. Once the induced voltage is bigger, the current and the power rise quickly. When comparing the curves to the table 3.39, it can be seen, that the rise of the losses should start much earlier. At 8.7V, DUT 6 gets already destroyed. And at 5.5V, the IC already becomes warm.

When an IC is destroyed, an interesting question is, how it behaves then electrically. It could be a short, an open or some voltage dependent behavior. All cards, despite DUT 6, which were investigated during the experiments, were found to be electrically open when incapacitated. The chips still looked fine, but the cards did not respond anymore.

After destruction, DUT 6 shorted the antenna with a remaining resistivity of about 4.5Ω. There might be a risk of igniting paper cards with this IC.

To summarize the findings of the investigations on the topic of card damaging by Qi wireless charging, it can be stated, that as long as the induced voltage in an NFC card stays smaller than the limiters threshold value, no damage is to be expected. Formulas for calculating the worst case induced voltage are given in the latest sections. However, if the induced voltage exceeds the limiter voltage, the limiter gets active and the chip might be damaged. Several equivalent circuit of cards were simulated to show the influence of the major parameters.

In this chapter, first different failure modes were identified. Then the effects of the Qi charging magnet field on the NFC sub system were investigated to get a better understanding of the challenges. With the theoretical foundation, the failure modes could be successfully isolated. Next the magnetic coupling between the coils of Qi charging and NFC was investigated. In this section, important ideas for counter measures were developed. Finally the topic of card destruction was investigated and modelled. Most

mathematical derivations in this chapter were verified by measurements and vice versa.

Chapter 4

Evaluation of ideas for improvements

4.1 Overview and classification

In this section, possible countermeasures against card destruction and approaches to improve communication quality during parallel operation are listed. In the following sections, they are described in detail.

4.1.1 Time slot approaches

The idea is to create pauses for NFC communication during QI charging. There are several possibilities to implement this:

- Running an application on the phone, which suppresses notifications
- Informing the power receiver (protocol changes)
- Only reducing the rail voltage during the time window
- Let the charging system continue in free oscillation (PWM freeze)

4.1.2 Software approaches

Software approaches have the advantage, that no additional components are required. Much can be achieved by software only.

- Optimized loop for parallel card detection
- RX threshold adaption to reduce noise

One major task of the software is, to distinguish between NFC cards and card emulation by the phone.

4.1.3 Hardware approaches

- Custom antenna designs for the NFC reader to decouple from the charging coils
- Analog filters in the NFC circuit or in the charging circuit
- Changes to the NFC matching network
- Increase robustness of cards

4.1.4 Card detection and parallel communication

Some of the approaches discussed above target parallel NFC communication during wireless charging. Parallel communication can be further divided into parallel communication with phones and parallel communication with cards.

Some phones support parallel operation of NFC and QI charging. Others deactivate the NFC circuitry while charging wirelessly.

Parallel communication with cards is problematic. Not only are they are damaged in the field, but they already show different failures before this point. Unfortunately, a minimum of communication is required to detect the card. If the mobile phone, which is being charged, supports NFC in parallel, the reader needs to distinguish card and phone.

If the phone being charged does not support NFC while charging with QI, NFC is disabled or an application on the phone deactivates NFC card emulation for some periods, card detection is simplified. In that case, it is enough to detect any NFC load modulation to be sure, that a card is in the field.

In figure 4.1 the three conditions, “NFC card” present, “NFC card emulated device” present and “QI power receiver” (mobile phone) present, are visualized by three circles. The text in the intersections of the circles shows the intended operation for the scenarios. If no phone with support for wireless charging is present, normal NFC operation is possible. If an NFC card is in the field, charging has to be rejected. During charging, parallel card detection has to be performed. If the mobile phone additionally supports NFC card emulation (CE), then an extended card detection procedure is required.

The term “parallel communication” in the Venn diagram (4.1) is used for NFC communication with the phone during wireless charging.

4.2 Evaluation of time slot approaches

When a phone is being charged, it might be impossible to communicate with an NFC card, which moves between charger and phone (see section 3.2 and 3.4.3). By creating time slots for NFC communication, a quasi parallel communication and charging scheme could be established. With timeslots without wireless charging all error sources according to section 3.2 could be mitigated.

4.2.1 Proposal for a Qi protocol change

A clean solution for time slots ensures, that the receiver is aware of the charging pauses. Therefore, the QI protocol has to be enhanced by some packets.

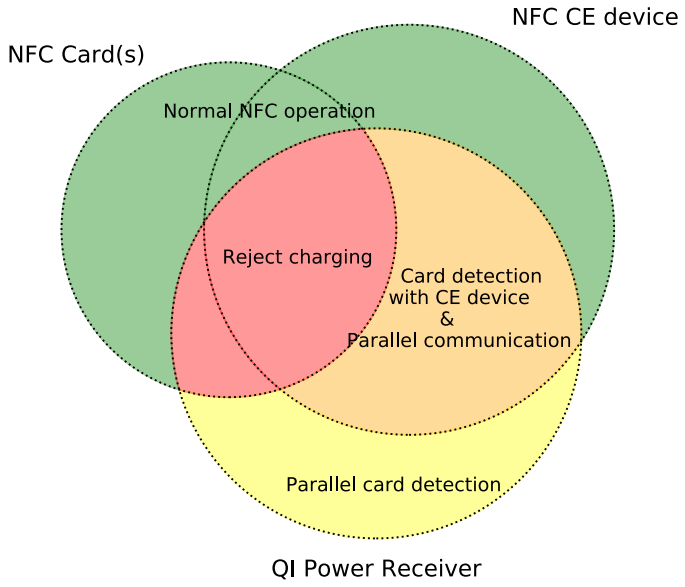

Figure 4.1: Venn diagram of situations and required actions

The proposal is to add a negotiation packet "Allow Pauses". A power receiver, which supports NFC time slots will send this packet within the configuration phase. The packet contains the information on the maximal duration, the transmitter is allowed to pause, to still ensure smooth operation of the phone and the battery.

If the power transmitter receives such a packet, then it is allowed to create a charging pause of up to the specified duration anytime outside of active QI communication.

If the duration of the pauses are in the order of several milliseconds, they can be utilized for different NFC tasks like card detection.

A downside of this approach is, that is does not work with current receivers. The receivers, which do not support it, have to be covered differently.

4.2.2 Create Time Slots without informing the receiver

In the current Qi standard, there is no possibility for the charger to introduce time slots with the receiver. The alternative is to stop charging without informing the receiver.

The problem is that the receiver is not able to provide any power to the phone. Once, the field is present again, the power receiver requires running through the QI initialization procedure again.

A phone will, depending on the software, notify the user, that the charging stopped. This is a potential safety risk in a car during driving. If time slots without informing the

receiver are used, a software application on the phone could be used to suppress these notifications.

As charging is fully stopped and continues only after a considerable delay in the order of a second, this approach is not suited for card detection. It might be used for different tasks, though. If an authentication procedure runs via NFC over the mobile phone, the car could sporadically create a time slot to verify, that the phone is still placed on the module.

4.2.3 PWM freeze

The idea behind this approach is to create a time slot, which is short enough, that the receiver continues to charge. The phone does not see an interruption of the power supply.

During operation, the charger drives the antenna with a pulse-with modulated voltage. Instead of discharging the coil and disconnecting the coil, the current state of the H-bridge is frozen for the duration of the time slot. The effect is that the field will oscillate freely.

After freezing the transistors, the field strength is a damped sinusoidal and contains no switching noise anymore. Because no new energy is provided, the energy in the resonance circuits will be dissipated by the receiver quickly.

However, when looking into the receiver a rectifier and a DC DC converter can be found. The capacitors of the rectifier must have a reasonable high capacitance in order to successfully communicate with the QI protocol.

Once the charging voltage is frozen, the voltage of the rectifier capacitors reduces, because they drive the load.

Usually, the voltage will be regulated to about 5 volts to load a battery. The regulator can be a buck, a boost or an LDO converter.

For the PWM freeze approach, a boost converter is optimal, because most of the energy in the rectifier capacity can be used before the output voltage drops.

A buck converter allows to discharge the rectifier capacitors to a level close to the required output voltage of 5 volts. If the rectifier capacitor was for example charged to 20V, about 90% of the energy can be consumed before the converter stops working. ($\frac{E_{5\mathrm{V}}}{E_{20\mathrm{V}}} = \frac{5\mathrm{V}^2}{20\mathrm{V}^2} = \frac{1}{16} \approx 7\%$ is the energy, which cannot be used.)

The difference of an LDO and a buck converter is, that the LDO works optimal for input voltages close to the output voltage. If the receiver is designed with an LDO, the voltage at the rectifier capacitor will be significantly lower than the 20V from the example above. Therefore, only a small portion of the stored energy can be utilized before the LDO stops working. For example, if the voltage may reduce from initially 6V to 5V before the wireless charging interrupts, then $\frac{5\mathrm{V}^2}{6\mathrm{V}^2} \approx 70\%$ of the energy cannot be used by the PWM freeze.

The charging phases of batteries are another topic, which plays a role. For instance lithium ion cells are first charged with a constant current. Once the voltage reaches a certain maximal value, a constant voltage is applied. This phase is called saturation phase.

If the charge controller is included in the receiver, it will regulate the current, if it is in the constant current phase and otherwise regulate the voltage. All my experiments were performed with the receiver configured in the constant voltage mode with a resistive load. Colleges from Czech Republic analyzed the influence in more depth.

Depending on the load, the slot duration, which is possible with freezing the PWM, is in the order of 100µs. That is by far too little to fit a NFC request and the answer. Even fitting only the complete answer of the PICC is not possible. For type A cards, the duration of an ATQA is about 150µs. Experiments showed, that still the communication could be improved by putting a 100µs freeze period over the ATQA.

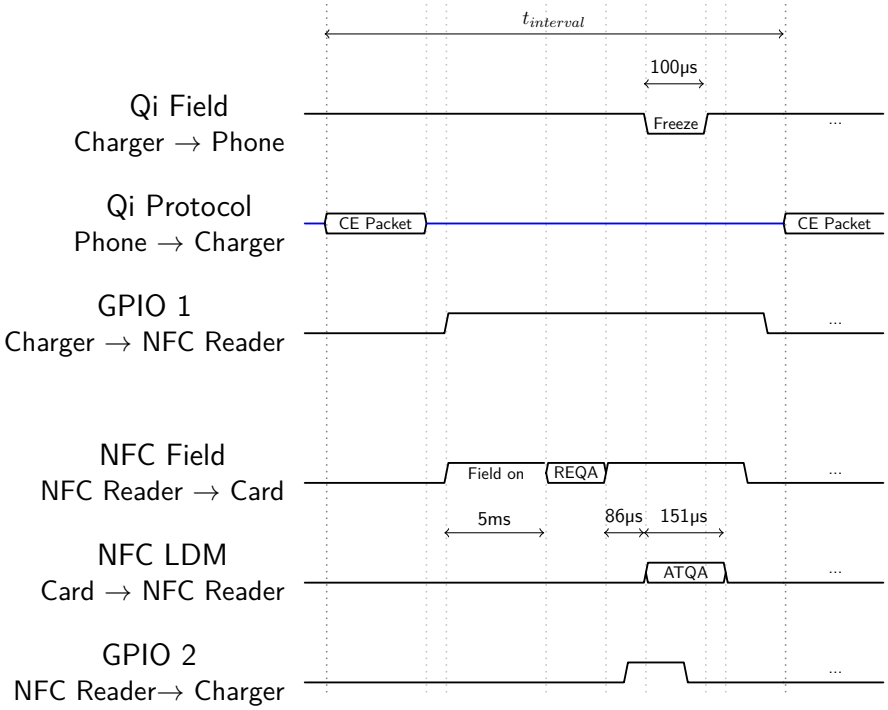

Figure 4.2: Timing diagram of the most important timings for the PWM freeze

Figure 4.2 shows the most important timings for the PWM freeze. The first row in the figure shows the magnetic field of the Qi charger. As shown, the field stays constantly on until the freeze is triggered and the field is off for 100µs.

To not disturb the QI protocol, the freeze can be performed only between the QI communication blocks. During the power transfer the power receiver periodically sends a control error packet. The second row in figure 4.2 shows these packets. The charger does not answer these packets, but only adapts the parameters according to the power contract negotiated earlier.

Ideally, the receiver shall send such a control error packet every 250ms. However, the Qi protocol gives some tolerances. Therefore, the exact time of the next packet cannot be predicted by the charger.

When making worst case assumptions, a total duration of only 11.5ms is available for the freeze ($t_{delay}^{(min)} + 11\frac{1}{f_{CLK}}$ according to the Qi specification). Fortunately, this duration is enough to fit a Request / Answer to Request pair for ISO14443-A proximity cards.

Nevertheless, the timing has to be accurate. Good results were achieved by connecting two GPIO pins the wireless charging and the NFC processor[1]. The third row in the middle

[1]Using a protocol like SPI or I2C might add additional jitter in time.

of figure 4.2 shows one of the two signals, which is set by the wireless charger to indicate the end of an control error packet to the NFC unit.

After the rising edge of GPIO 1, the NFC unit puts on the NFC field, sends a REQA, and before activating the receiver circuit, it sets the second GPIO signal to trigger the actual freeze. The last row of figure 4.2 shows the GPIO signal to activate the PWM freeze. If the timing of this second GPIO signal was inaccurate, then the freeze of the charging field would be outside of the load modulation. Therefore, it was tuned precisely to cover the beginning of the ATQA.

As soon as the microprocessor for wireless charging receives the second GPIO signal, it freezes the output stage for 100µs, which can be seen on the first row in the figure. Ideally, the card starts to send the ATQB simultaneously by load modulation of the NFC field, which can be seen on the second to last row in figure 4.2.

It was already mentioned, that the maximum duration of the freeze is only about 100µs. Unfortunately, another issue is the frequency, the slot can be created. The frequency of the freezes is the frequency of the control error packets. Unfortunately, the power receiver may send this packet only three times per second ($t_{interval,max} = 350$ms).

For type A cards, an improvement of the success rate of NFC request/response pairs could be observed using this PWM freezing method during wireless charging. Other protocols than 14443-A define much longer times for their initialization responses.

To summarize, this approach can be used to improve the detection rate of type A cards. It can reduce RX failures and card faults (according to the classification in section3.2). However, because of the short maximal duration, it is not suitable for other NFC packages and protocols.

4.2.4 Time slots with reduced power

Instead of completely turning off the power, the field could only be reduced to some compatible level.

Theoretically, this technique could be used for enhancing the duration of the PWM freeze.

For longer periods, reducing the power will result in the same problems with LDO converters as before. The field is reduced, so the induced voltage is reduced as well. The voltage after the rectifier will reduce. If it drops below 5V, the receiver cannot work properly anymore[2].

4.3 Implementation of software approaches

Various software approaches were investigated in order to improve communication and to protect NFC cards from charging fields.

4.3.1 Parallel card detection strategy

Often, detecting cards does not require a full discovery loop. Depending on the situation, a very simple algorithm can be used.

There are three possible situations regarding the phone and NFC:

[2]With an LDO and 5V output voltage

- The phone does not answer requests. Either NFC is not supported or turned off or card emulation is not supported or turned off.
- The phone answers NFC requests, but deactivates NFC during wireless charging.
- The phone answers NFC requests even during QI charging.

In the first two cases, it is possible to run a simplified parallel card detection loop. For the simple detection loop, for each protocol a request is sent. Then the reader tries to detect a response. If any device is detected, the charging process is stopped.

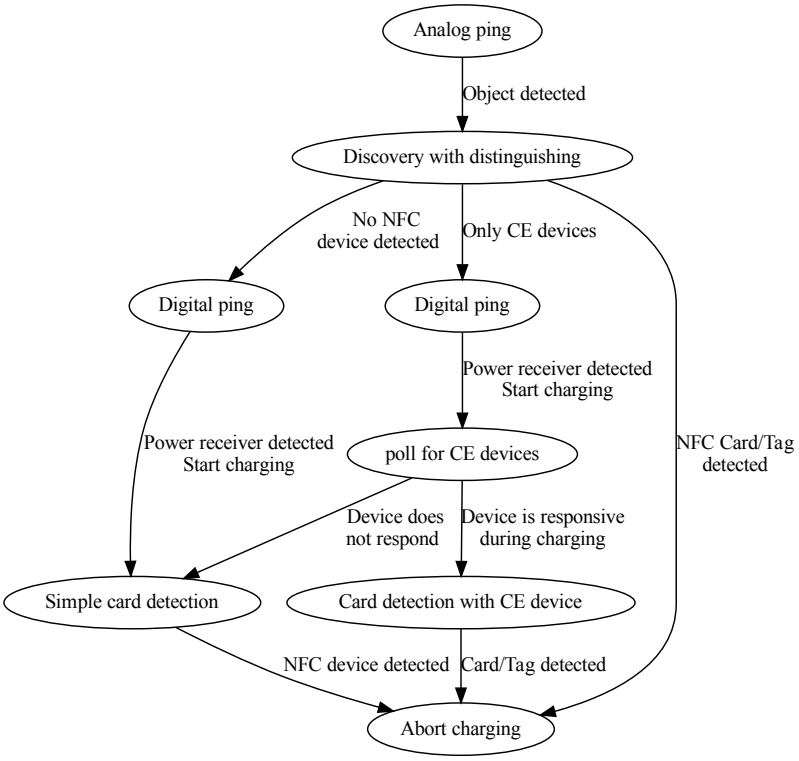

Figure 4.3: Flow chart of different parallel detection loops

The parallel detection loop can integrate the other software concepts as well.

4.3.2 Card and Device distinguishing

Some strategies for distinguishing a phone with card emulation from NFC cards or tags were discussed in the WPC and were added to the QI specification as a recommendation. One strategy is to poll for different technologies in different orders.

When the phone being charged is set up to emulate cards, it often answers to more then one of the three protocols 14443-A/B and Felica. However, when responding to one type, it does not respond to other types before the NFC field is reset.

Most NFC cards and tags only support one protocol. There are special multi-mode communication cards (dual interface cards and hybrid cards)[2], but they usually implement only one NFC technology and for example magnetic-stripe.

When polling for the different technologies in different orders, the card emulating device will always answer the first request. Distinguishing by this procedure works, if the phone supports at least two technologies. However, if a mobile phone supports only one NFC technology, there are several other properties, which can be used to still identify it as a card emulating device.

4.3.3 Simple card detection algorithm

This algorithm is used, when no card emulating device is in the field. The idea is, that if any NFC response is detected, it must be a card.

As shown in figure 4.4, the different technologies are polled for sequentially. In each technology the required initial request is sent. Afterwards, the NFC controller is put into receive mode. Any response will abort the detection loop.

Once per loop, the NFC field will be turned off for slightly longer than 5ms. By doing so, all cards in the field will respond in the next loop.

A complete loop covering the protocols ISO 14443-A/B, Felica and ISO 15693, takes about 25ms.

4.3.4 Parallel card detection algorithm with card emulating device I

As noted in section 4.3.2, the polling sequence determines the technology, a card emulated phone answers during a poll cycle without reset.

This can be used to define a different card detection procedure by polling for the different technologies in different orders. The phone will always answer the first request.

Algorithm 1 implements this strategy. This implementation follows the proposal of the WPC, which is found in Annex E of the Qi specification. First, vicinity cards are detected, for which no card emulation is defined. If a card is detected, the algorithm returns and charging is aborted. Then, the physical protocols are polled for in two different orders A, B and F and F, B and A. The number of detected devices are stored in the two arrays result1 and result2. Finally, there are four different cases which distinguished by the algorithm:

- No responses at all and therefore continue charging (result1 = result2 = [0,0,0]).
- One response of a mobile phone (eg result1 = [1,0,0]; result2 = [0,0,1]).
- One response of an NFC card (eg result1 = result2 = [1,0,0]) and abort charging.
- In case of multiple responses, at least one is supposed to be from an NFC card. Therefore, charging is aborted.

The algorithm requires, that all mobile phones supports at least two NFC technologies. And it requires, that they always answer to the first technology and not to the other ones until the NFC field is reset. [3]

[3]To my knowledge, these requirements are not defined in any standard. It is an observation, which is used by the distinguishing algorithm proposed by the WPC as well.

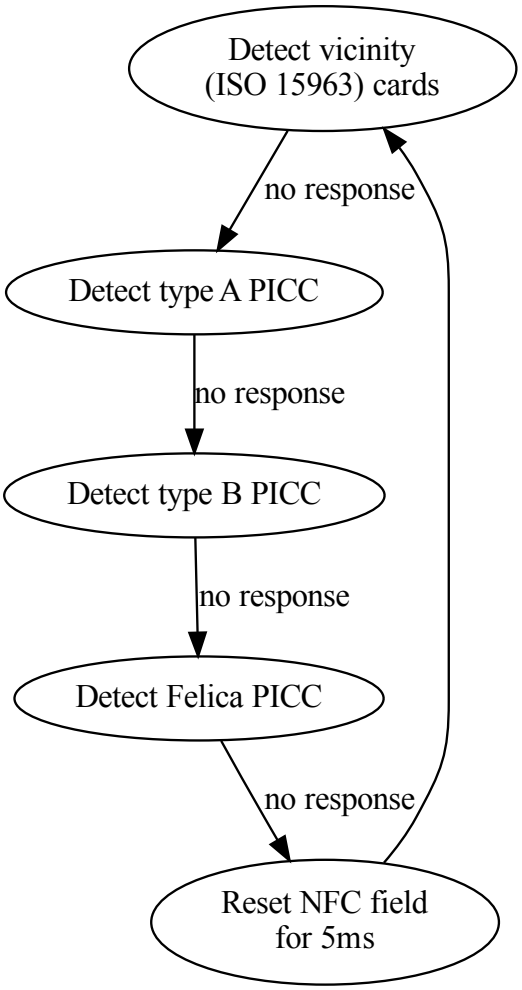

Figure 4.4: Flow chart of a simple detection loop without device distinguishing

The pseudo code in algorithm 1 shows how this strategy of the different polling orders can be utilized. Furthermore, in the real implementation different kinds of early exits are used. Also additional strategies are implemented, when only one technology is found.

4.3.5 Parallel card detection algorithm with card emulating device II

A potentially faster alternative to the approach in the last section is, to activate the phone with card emulation (CE) once and set it into the halt state. A device in this state will not respond to requests anymore, until it receives a wake up command.

Then all protocols can be polled for while keeping the field on. Any response belongs to a card.

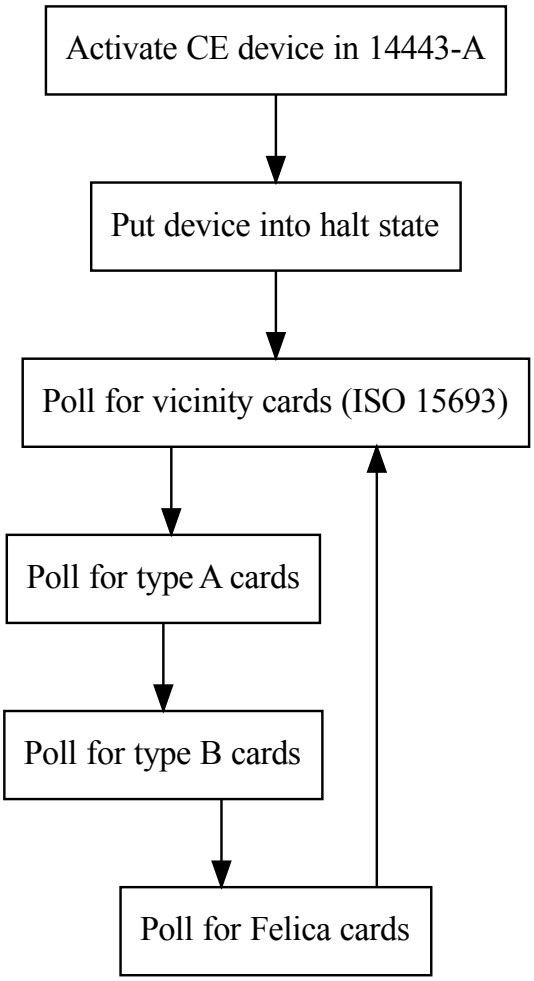

Figure 4.5: Flow chart of a detection loop, which puts CE devices into the halt state

Figure 4.5 shows a flow chart of this NFC card detection strategy when the mobile phone supports card emulation. First, the mobile phone is selected in type A technology and put into the halt state. Afterwards, the same detection loop as in section 4.3.3 but without the field resets is implemented. As soon as an answer to a vicinity (ISO15693), type A, type B or type F request is detected, wireless charging is aborted.

One major advantage of this algorithm compared to the algorithm 1 is, that it does not require to reset the NFC field. That saves 10ms minus the request guard time between any two protocols. Furthermore, because the mobile phone is not supposed to answer anything, no anti collision loop needs to be done.This algorithm is mostly based on behaviour *required* in ISO-14443 and other standards.

4.3.6 RX Threshold adaption

The voltage at the RX pins is distorted by the magnet field of the wireless charger. After the demodulation, the distortions may lead to wrong decisions. This is derived in section 3.3. As a result, the NFC front end might report framing or collision errors.

In the NFC front end used, the base band signal is compared to a threshold level to parse the symbols and to determine low and high phases. The threshold level can be set by writing to the register RxThreshold. The interesting part is the amplitude threshold level, which consist of the first 4 bits (and can take values from 0 to 15).

Too high values make it more likely, that the NFC chip misses a modulated period. In theory, this will cause a negative effect on the operating volume. However, an actual reduction of the distance, where the communication breaks, could not be observed. It seems, that cards will first fail to harvest enough energy before their answer is not understood anymore.

For passive devices, greater values perform better. By sweeping the threshold value from 0 to 15, for each protocol a statistic was created, which contains false positives and false negatives. Then the RX threshold values were adapted to the optimal values, which can be found in the following table:

Protocol	Optimal Threshold
ISO-14443-A	0xA
ISO-14443-B	0xA
Felica 212	0xE
Felica 424	0xE
ISO-15693	0x7

These values are loaded instead of the default ones whenever wireless charging and NFC are operating at the same time.

Modeling the noise

Besides the intended modulated NFC carrier, the signal at the RX pins of the NFC reader also contains components caused by the wireless charging. The threshold level method treats the wireless charging signal as unpredictable noise. However, the charging field is quasi-periodic and very predictable.

By finding an appropriate model, the noise could be described in a probabilistic way. Moreover, such a model could be used to predict and filter out noise components caused by the charging field.

A first idea was to calculate the auto correlation function during wireless charging, when there is no NFC signal. The auto correlation could then be used to predict the noise. However, the process is more complicated and a more advanced model is required.

An adaptive algorithm similar to a Kalman filter could learn the properties of the NFC carrier and the properties (frequency, amplitude and step response) of the noise caused by the wireless charging.

However, no investigations were made on this topic. It cannot be prototyped with a cheap NFC front end, but it would require a stronger hardware like an FPGA board or at least a digital signal processor.

4.4 Evaluation of hardware approaches

4.4.1 NFC reader antenna design

As analyzed in section 3.5.2, the wireless charging coils can be decoupled from the NFC reader coil by routing the NFC antenna in a way to exclude some of the area that is common to both coils. Similarly, common area can be excluded for each of the charging coils in the MP-A9 setup.

The antenna shape, in which all charging coils are completely decoupled in simulation, showed significant coupling when tested on top of the real MP-A9 setup. The difference is related to limitations in the simulation of the ferrite.

Finally, the optimal solution was found manually by first measuring the mutual inductances between every of the three charging coils, the outer NFC loop and wire loops with different diameters, which were concentrically aligned once with each charging coil. Because all considerations are linear, the loops could be combined in order to minimize the coupling of the NFC antenna to each charging coil.

Measuring the mutual inductance was done as described in section 3.5. One of the charging coils was supplied with a sinusoidal current. The frequency of the current was 158kHz, because a self-made matching circuit had a resonance there. Finally, the voltage at the NFC side is measured.

From that data optimal diameters were calculated. The new antenna design uses three compensation loops with two windings each.

The new antenna has small mutual inductances to the charging coils, but they are not as small as expected. Mainly, the remaining coupling can be explained by the metallic shield, which was not used in the design phase. Therefore the coupling situation changed in the actual setup.

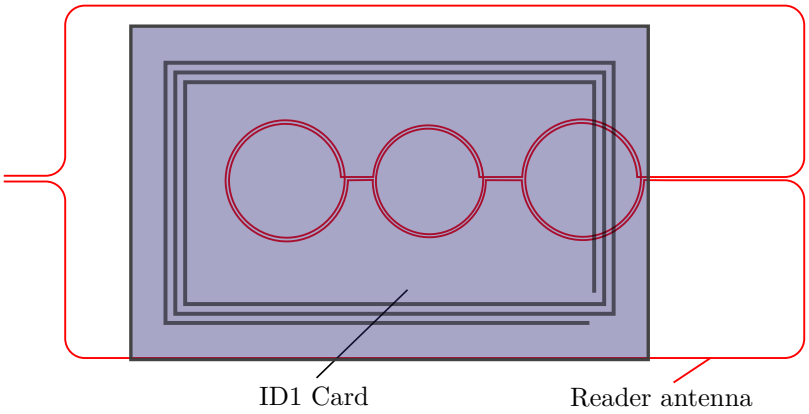

Figure 4.6: Position of a blind spot of the decoupled NFC reader antenna

One fundamental problem still exists with the antenna. There are blind spots on the NFC reader, where ID1 NFC cards do not couple with the reader. If an ID1 card is positioned on the NFC reader for example as shown in figure 4.6, it will be decoupled from the readers antenna. Therefore, no NFC communication is possible anymore in this spot.

Consistently with the analysis in section 3.5, it can be concluded, that full decoupling of a single NFC reader antenna to all three charging coils is not practicable due to the blind spot problem.

4.4.2 Three switched NFC Reader antennas

For one charging coil, decoupling can be achieved, with little problems with blind spots. It was achieved on the WCT1012 15W Single Coil TX design[4]. The reader can contain three NFC antennas. Each one is decoupled on only one charging coil.

The same signals used for switching the charging coils can be used to switch the NFC coils. However, this approach has a few weaknesses. Currently, the charging system will disconnect all coils, when it is inactive. This has to be changed, in order to have NFC available when not charging.

Another weakness is, that when the charging system switches, the NFC system switches immediately. There might be some communication ongoing, which might break.

Every single NFC antenna is small and therefore will not be able to create an operating volume over the whole product.

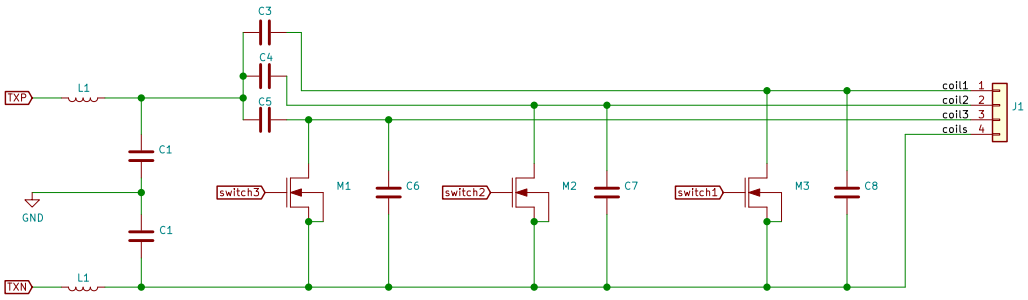

Figure 4.7: Circuit for Matching and switching of three NFC coils

The NFC antennas would be switched by shorting two out of the three antennas with a circuit as shown in figure 4.7.

No antenna design was done for this approach, because it only addresses one failure mode and other approaches look more promising.

4.4.3 Two NFC Reader antennas with separate switching

Designing a reader antenna, which decouples from the three charging coils is easy if blind spots do not play a role. The easiest approach is to use a rectangular antenna and adjust the position until no voltage is induced in the antenna anymore. The antenna built overlaps by approximately 50% with the charging coils.

Figure 4.8 shows a setup with two simple antennas. Both of them are decoupled from all three charging coils. Therefore, both of them show increased immunity against RX failures according to the classification in section 3.2.

The idea of having two antennas is, that each of them may have blind spots, but the blind spots of the one antenna are different from the blind spots of the other antenna.

[4] `www.nxp.com/docs/en/user-guide/WCT1012V31SYSUG.pdf`

Figure 4.8: Two NFC antennas, which both are decoupled from the wireless charging coils

Therefore, if a PICC lies in a blind spot, only the communication with one antenna is affected. For this to work, the antennas needs to be switched periodically during the card detection procedure. For switching between the two antennas, again a network as suggested in figure 4.7 could be used, but was not implemented.

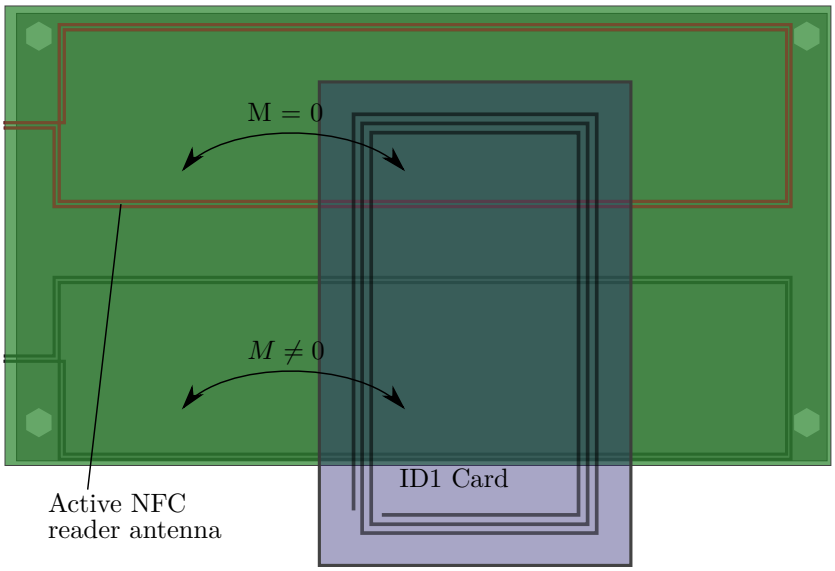

Figure 4.9: Demonstration of blind spots for the upper antenna I

The position of the blind spots depends on the orientation of the NFC card. In figure 4.9 a blind spot for cards with ID1 dimensions can be seen, where the card is orthogonal to the NFC reader. In this setup the upper antenna, which is highlighted in red, provides an NFC field. The position of the blind spot was found with an commercially available field strength indicator card with ID1 dimensions.

When the lower NFC reader antenna is powered, the position of the blind spot is mirrored because of the symmetry. It can be seen, that for this orientation always at least

one of the two NFC reader antennas couples to the NFC card.

Therefore, by switching between the two reader antennas, an ID1 card in this orientation can be detected. For ID1 cards orthogonal to the antenna, there are no central blind spots common to both antennas.

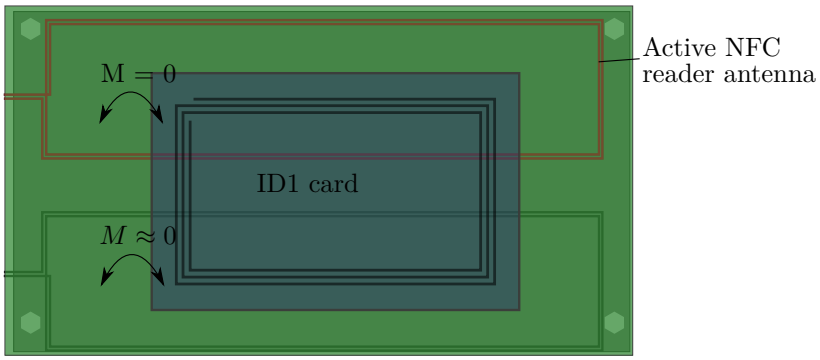

Figure 4.10: Demonstration of blind spots for the upper antenna II

Unfortunately, the blind spots of the upper and the lower reader antenna get close to each other, when the ID1 card is oriented in parallel to the reader. Figure 4.10 shows a blind spot for the upper NFC reader antenna with an ID1 card orientated in parallel to the reader.

Both, upper and lower reader antenna, have a blind spot for centrally aligned cards. However, this result is not surprising, because the antennas were designed to decouple to the charging coils. If the card is placed in a position to cover the charging coils (and the height of the charging coils is similar to the height of an ID1 card), the coupling to both NFC reader antennas is low by design.

The experiments with the two antennas support the statement from section 3.5, that decoupling of the NFC reader antenna and the three charging coils inevitably causes blind spots.

4.4.4 Low pass filter in the Qi circuit

Because of the driver principle used by Qi wireless charging, unwanted spectral components are emitted. The sharp edges of a rectangular pulse as created by the H-bridge create the well-known 1/f envelope in the frequency domain (see section 3.3). This noise can cause failures in the NFC communication. Moreover, it was found, that especially spectral components close to 13.56MHz ± 848kHz are critical for the performance.

In order to reduce this issue, the idea to add a filter to the charging circuit was evaluated. Such a filter could not only help to improve the NFC communication, but it may be used for reducing electromagnetic emissions in general. According to section 3.3.7, a low pass filter should flatten the edges and therefore improve the spectrum.

The frequency components of the pulse shaped charging voltage decay with −20dB per decade. In theory a second-order low pass filter consisting of a coil and a capacitor has a damping value which decays with -40dB/decade. Therefore, by adding an LC low pass filter, the dependency of the spectral components on the frequency should be of third order (-60 dB/decade).

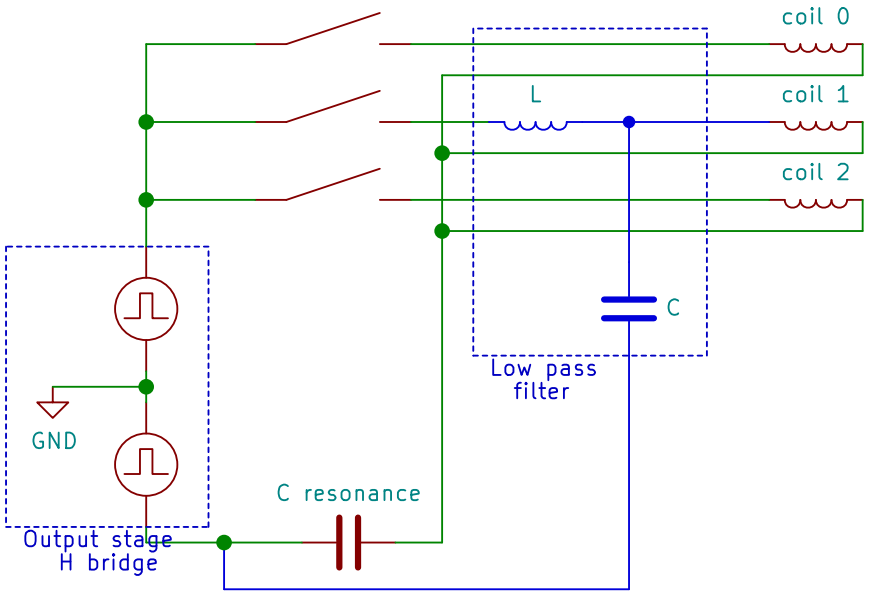

Figure 4.11: First version of a low pass filter in the QI circuit

Figure 4.11 shows, how the first low pass filter was integrated in the Qi circuitry. On the very left the output stage for the Qi signal is schematically drawn as voltage pulse sources. On the lower part of the figure, a capacity is shown, which is used to create a resonance circuit with the active charging coil. On the right of figure 4.11 the three charging coils can be seen. All of them are connected to the capacitor on the bottom. The upper left part of the figure shows the switches used to select one of the charging coils. Finally the coil and the capacitor in the middle of the circuit show the modification of the original schematic. A coil and a capacitor are added to one of the three charging coil in order to further filter higher frequency components.

The first approaches for low pass filters intended to not affect the existing resonance circuit. Therefore, the cutoff frequency was significantly lower than the 13.56MHz of NFC and significantly higher than 128kHz, which is the fundamental frequency of Qi wireless charging. For the first design a value of 1MHz was chosen as target cutoff frequency, because it is close to the geometrical mean of the Qi and the NFC operating frequency. L and C together decide the filter frequency.

Choice of L:
The inductance was chosen much smaller than the inductance of the charging coil in order to not affect the main resonance of the system significantly. Furthermore, higher inductances tend to have higher losses and to have a lower self resonance frequency. However, if L is too small, then the capacitor has to be very big. Then again the losses would increase because of more reactive power oscillating between capacitor and power source. Moreover, big capacitors have a smaller self resonance frequency. For the first design an inductance of 300nH was used.

Then the capacity can be calculated as: $c = \frac{1}{\omega^2 L} = 84.4nF$ A value of 100nF was chosen.

The problem with such a low pass filter is, that it creates overshoots in the frequency domain. This behaviour can be observed when investigating the transmission function of an unloaded Lc low pass: $A(s) = \frac{V_{out}}{V_{in}} = \frac{X_c}{X_c+X_l} \lim_{\omega \to \omega_0} A(j\omega_{res}) = \infty$ The transmission function has a pole at the corner frequency!

The simulation of the circuit (with parasitic resistivity already added) verifies that behaviour (figure 4.12). For the simulation, a rectangular voltage with 50% duty cycle and 125kHz was applied to the circuit. The massive oscillations are caused by the filter. In blue, the input voltage can be seen. Red is the current and violet the voltage at the charging coil.

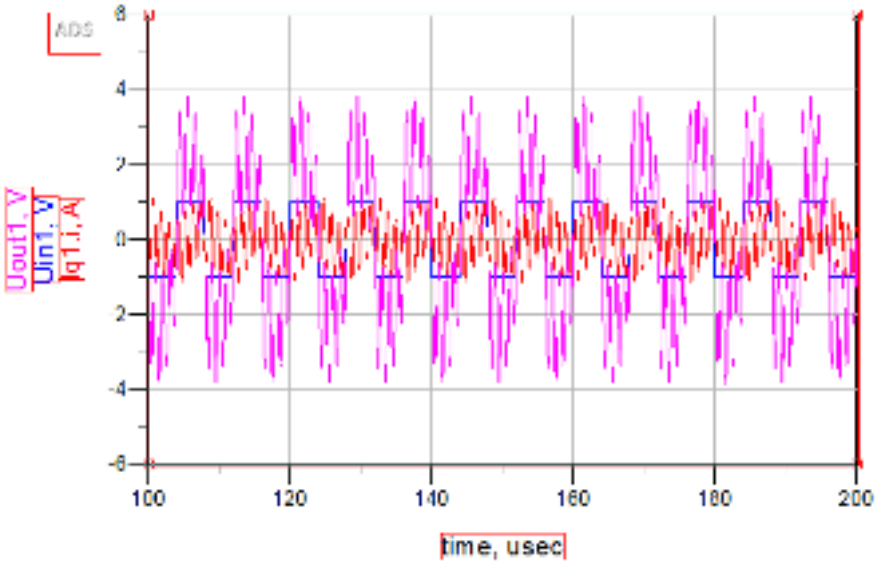

Figure 4.12: Simulation of an under-damped low pass filter

In order to avoid this unwanted behaviour, the quality factor of the filter must be reduced. If the quality factor is 0.5 or less, no ringing will occur. In the bode plot, no voltage overshoot will be seen at the corner frequency.

How to limit the quality factor?

The quality factor is determined by the real part of the pole. However, only ohmic resistivity causes the factor to reduce. As long as all components are purely reactive, the real part of the poles is always zero. The natural sources for resistivity are the output resistance of the H-bridge, the resistivity of the coil and the parasitic resistivity of the capacitor.

The quality factor can be reduced by adding a resistor in series or in parallel to the filter coil or to the filter capacitor as shown in figure 4.13. However, a resistor in series to the wireless charging coil creates high losses for the fundamental charging frequency as well, because the whole current has to pass it. Likewise, a resistor in parallel to the capacitor will cause high losses for the fundamental signal, because it directly sees the whole coil voltage. Therefore, the two configurations on the left were not considered any further.

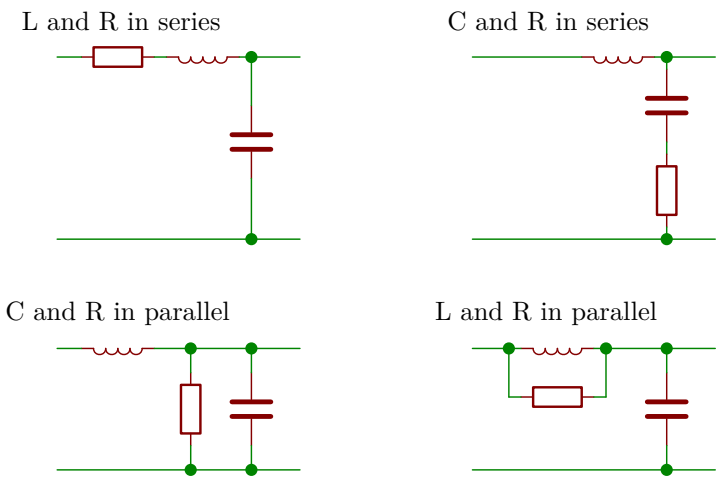

Figure 4.13: Four different configurations to reduce the quality factor of an LC low pass by adding a resistor

The remaining topologies are a resistor in parallel to the coil and a resistor in series to the capacitor (to the right side of figure 4.13. However both variants have the disadvantage of reducing the filter characteristic to a first order low pass for higher frequencies.

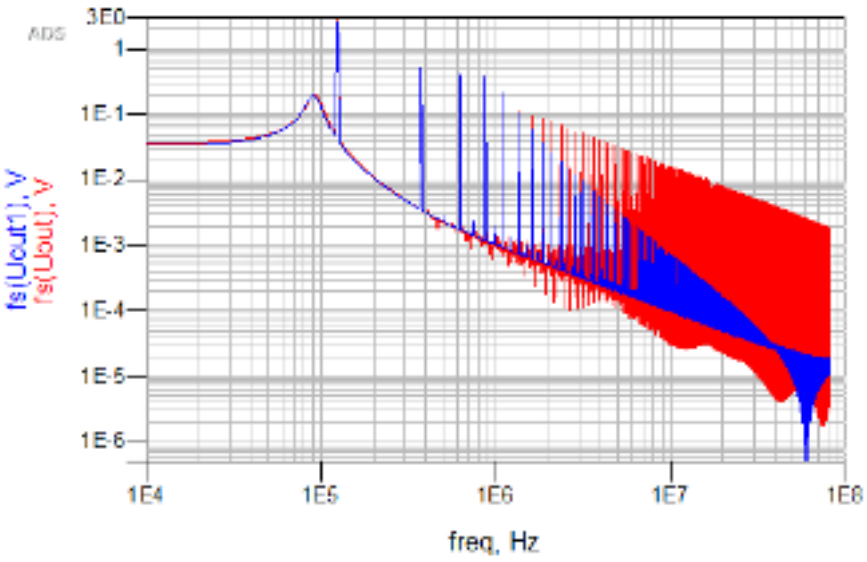

Figure 4.14: Simulation with a low pass filter with reduced quality in the frequency domain

In figure 4.14 the spectre of the original coil voltage can be seen in red. The blue spectre is one with a low pass filter added. A resistor of 0.9Ω is put in series to the capacitor.

A filter was built and put into the setup as shown in figure 4.11.

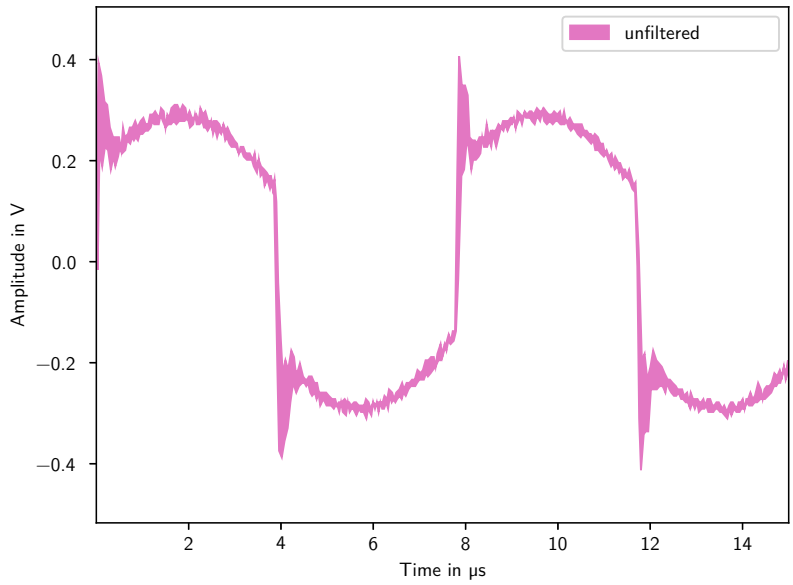

Figure 4.15: Plot of the measured voltage at the charging coil without filter

When the capacitor is not connected, the voltage at the charging coil is almost equal to the unfiltered signal. The waveform can be seen in figure 4.15. The voltage was measured with a pickup coil just above the charging coil. The rectangular shape can be still seen and the steep flanks create voltage overshoots and the 1/f behaviour in the harmonics. The rail voltage was kept low to avoid losses in the filter.

Figure 4.16 shows the waveform of the same voltage when the capacitor is added, but without series resistance. Again, the voltage is measured at a pickup coil. The oscillations can be seen clearly.

An optimal value seems to be 2 Ohms. Figure 4.17 shows the shape with 1.95Ω (two times 3.9 in parallel). It can be observed, that the filter effect is to limit the steepness of the flanks.

At higher frequencies, the expected filter effect could not be seen. One major reason, why it is ineffective, are the parasitic properties. The coil has a parasitic capacity and has a ferrite with frequency dependent behaviour inside. Moreover, the capacitor and the resistors contain parasitic inductances. In order to reduce the parasitic effects, the wire length was reduced and SMD components were used.

Figure 4.18 shows the odd harmonics of the voltage induced on a pickup coil above the active charging coil. The induced voltage is preferred over the conducted measurements, because the measurement has less influence on the signal. The even harmonics are much smaller, because a square shape with 50% duty cycle has only odd harmonics.

In the legend, the resistor values can be seen. The blue curve shows the unfiltered signal (without parallel capacitor). The voltage overshoot of the under-damped filters can be seen clearly. The behaviour with 2Ω can be seen at the green curve. It shows almost no overshoot at the corner frequency. Also, in the NFC region, it's performance is good.

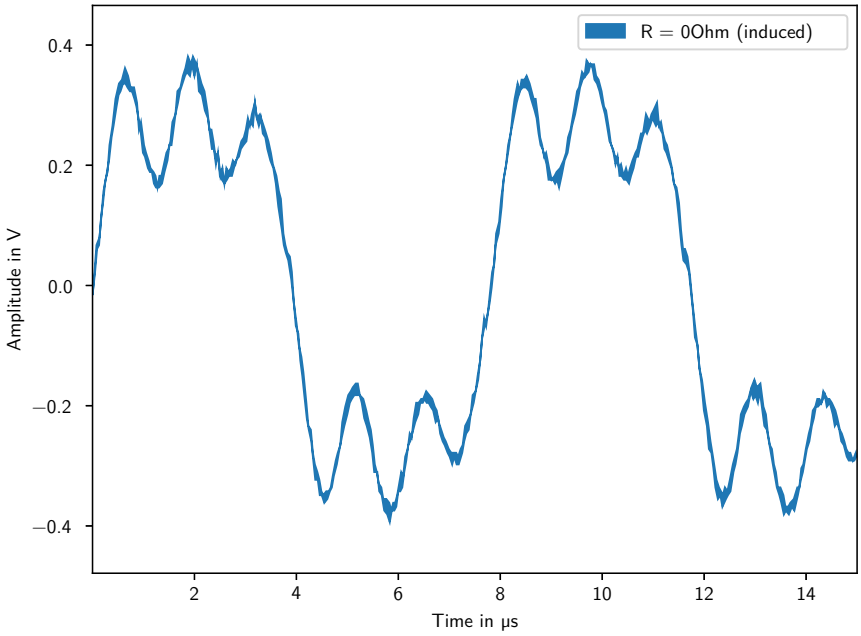

Figure 4.16: Plot of the coil voltage with an Lc low pass (R=0)

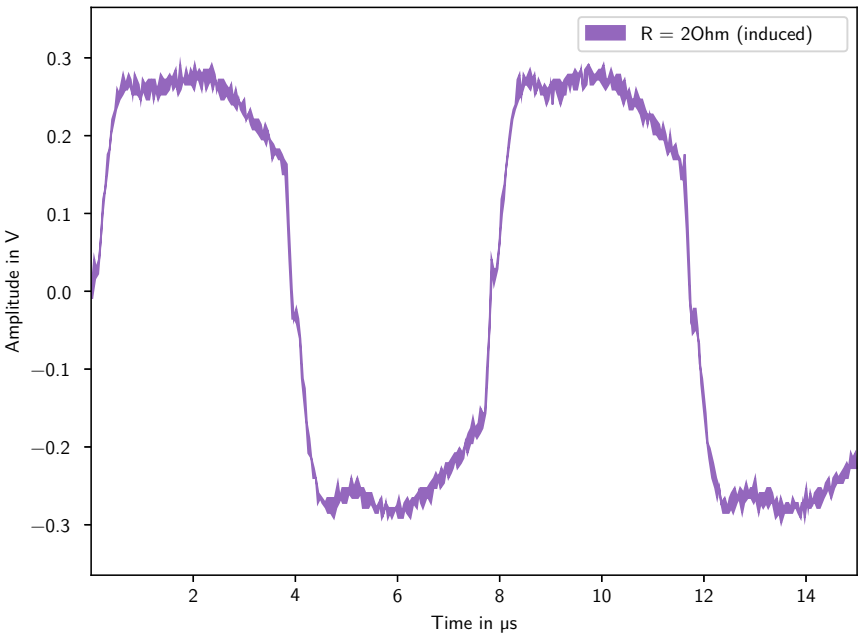

Figure 4.17: Plot of the voltage with an Lc low pass (R=1.95Ohm)

2 Ohms seem to be an optimal value.

Especially with the unfiltered version, a significant overshoot can be seen at around

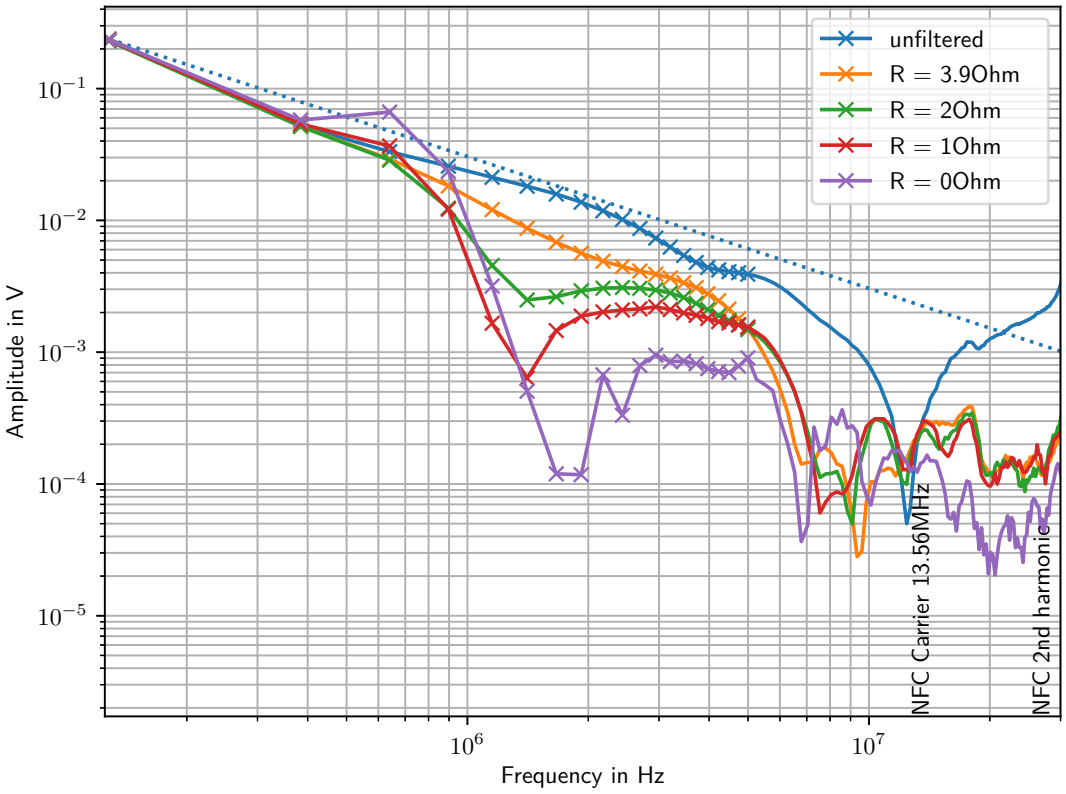

Figure 4.18: Comparison of low pass filters: Spectre of induced voltage at Vrail=3V

30MHz. This overshoot is partly caused by the pick-up coil. But also the charging coil has further resonances, which can be also seen in figure 4.21.

Figure 4.19 shows the effect of a power receiver, which draws 15W.

A problem with the measurements was, that the resistors heat up quickly with higher voltages. Simulation revealed losses of 4.6W at 10V rail voltage on a 2Ω resistor for quality reduction. Interestingly, the losses are only slightly dependent on the resistor value.

This can be explained in the time domain. As long as the oscillations of the voltage decay within a half period, the filter capacitor is loaded in every period from about $-V_{rail}$ to V_{rail} and back again. This loading and unloading limits the steepness of the slope and therefore causes the low pass effect. The pulse can be seen as transient switching (as long as the ringing decays within a half period). By analyzing the signal in the time domain, the energy, dissipated in the resistor during switching, can be calculated approximately.

Looking at the component values, the capacitor will unload mostly over the resistor, the H-Bridge and the filter coil. The only device in that loop, which can dissipate the energy of the capacitor is the resistor. Using these simplifications, the following formula can be derived for the losses in the filter resistor:

$P \approx \frac{2E_{capacitor}}{T} = \frac{2Q\Delta U f_{Wch}}{2} \approx 4c_{flt}U_{rail}^2 f_{Wch}$ For the simulated setup, the approximation gives a value of 5W. The simulated value is 4.6W.

This result is fascinating, because it is independent of the resistor value. However,

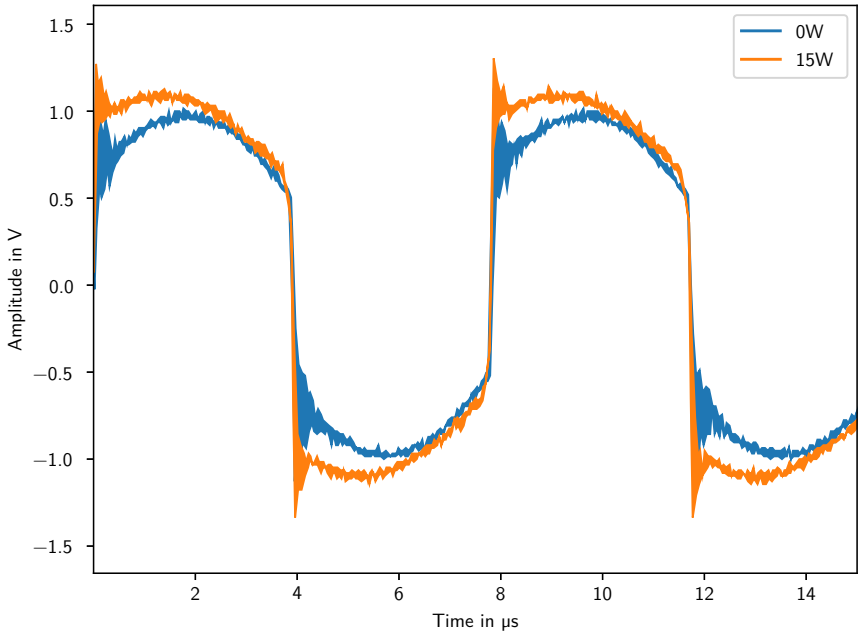

Figure 4.19: Effect of loading: The coil voltage with and without load

if the resistor is very small (short), the assumption, that the energy is burned, is wrong. Furthermore, if the resistor is very big (open), the assumption, that the capacitor is loaded to $\pm V_{rail}$ is not true anymore.

To restrict the losses to 1W even for rail voltages of 20V at 125kHz, the filter capacity must not be bigger than 5nF. To get the pole at 1MHz, then the coil has to have a huge inductance. Hand calculations give $5\mu H$.

The capacity was reduced to 47nF and the resistor replaced by a resistor array. This filter structure could be used with the full wireless charging power without damaging any filter components. However, with that filter no measurable improvements on parallel communication with a mobile phone could be observed.

Classic filter design considerations

For the classical manual passive filter design approach, first the impedance of the input and the impedances of the output are evaluated. In the end, the impedances inside the filter have to be renormalized to those impedances.

Next, by using the filter requirements and the factor between the input and output impedance, the filter topology and the number of reactive components can be decided. In order to assign impedances to the components of the filter, for all major filter types (like Bessel, Butterworth or Chebyshev filters) tables are provided, from which the normalized impedances can be read out. Finally, the values for the inductors and capacitors can be calculated after renormalizing back to the actual impedances.

However, a fundamental problem with this procedure is that the output impedance of the H-bridge is almost zero. Moreover, the impedance of the load on the other hand is an

L c series circuit. For the lookups in the filter tables, only real impedances are allowed. Depending on the filter topology, the real part of the load impedance is either $R_L \to \infty$ or $R_L \to 0$ in the unloaded case and changes with the load.

Finally, the problem manifests in the (re-)normalization step. When dividing by the tiny output resistances of the H-Bridge, the calculated capacitors will be huge and the inductors tiny.

It can be concluded, that using classical filter design strategies does not work for the Qi output stage. The problem of getting real parts at the poles without creating losses seems to have no solution.

4.4.5 Notch filter in the Qi circuit

Instead of creating a low pass filter, which reduces the emissions of the charging system in general, a filter can be designed for only some specific problematic frequencies. According to section 3.3.7 a notch filter will not flatten the edges or create a visible improvement on the time domain signal. However, because the NFC circuit is only susceptible in a narrow frequency band, still the performance should be improved by blocking frequencies close to 13.56MHz.

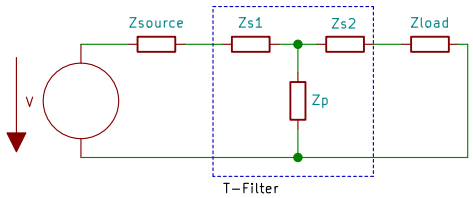

Figure 4.20: Circuit of a general T filter

Figure 4.20 shows a generic T filter design with passive components. The impedance Z_{s1} to the left is added to the impedance of the source. Therefore a part of the source voltage drops over this impedance, so that the output voltage is reduced. Because the output stage of the charging setup has a low impedance[5], this series impedance is effective[6].

The parallel impedance Z_p in the center of figure 4.20 creates a bypass for the current. If either the source has a high impedance (current source) or the load has a high impedance, a parallel impedance is necessary to create a path for the current.

The impedance Z_{s2} to the right is required, if the impedance of the load is small. In this case, the series impedance makes the parallel impedance Z_p more effective. However, in the region of 13.56MHz, the impedance of the charging coil is already big. Not only is the inductive reactance big (about 400Ω), but the parasitic capacitance further increases the impedance (see figure 4.21). When designing a filter for NFC frequencies, Z_{s2} is not required for this reason[7].

[5] At NFC frequencies, the impedance is mainly inductive, $L \approx 100nH$.

[6] If the source impedance was already high (current source behaviour), then the effect of this impedance was small and it could be omitted.

[7] For higher frequencies, an additional coil could be added to compensate the impedance drop due to dominant parasitic capacitances.

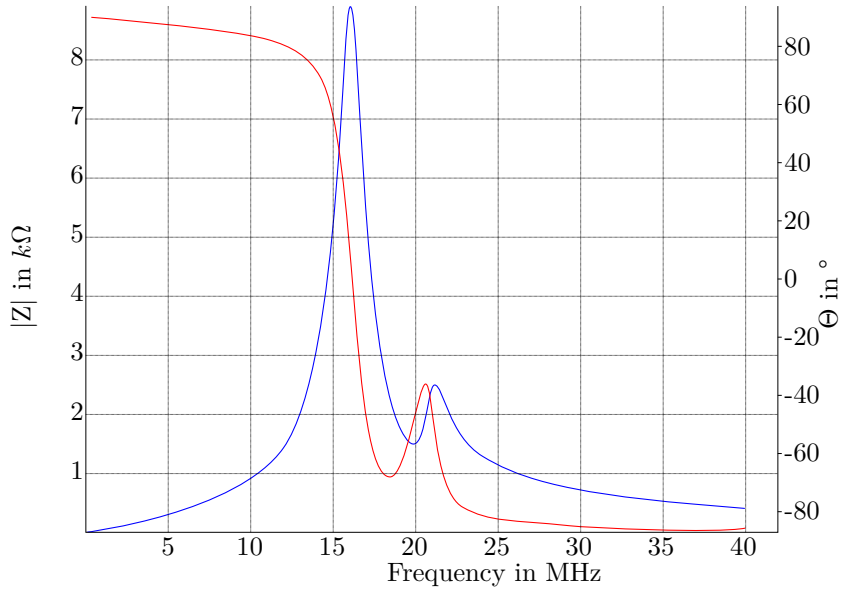

Figure 4.21: Impedance plot of the middle charging coil over Frequency

Figure 4.21 shows the impedance curve of the middle coil of the MP-A9 wireless charging setup, measured with a Vector Network Analyzer (VNA). The blue curve shows the absolute value of the impedance of the coil over the frequency. Furthermore, the red curve shows the phase of the impedance. For frequencies lower than 10MHz, the impedance curve is almost linear and the phase curve at about 90°, as expected of an inductance. However for higher frequencies the impedance increases strongly and the phase drops until at about 16MHz the self resonance frequency is reached. Because of a resonance of the inductance and the parasitic parallel capacity, the impedance is maximal at a phase shift of zero. For higher frequencies the impedance drops again. Moreover the coil is capacitive for higher frequencies.

Because of the spiral geometry of the charging coil, an approximating schematic circuitry with lumped components is more complex, than a single resistor, a single ideal coil and a single ideal capacitor. The second maximum at about 21MHz in the impedance curve in figure 4.21 is probably caused by another (minor) resonance.

Figure 4.22 shows four realized filter designs. They were simulated, built and measured. The serial notch impedance consists of a $1\mu H$ coil with a 150pF capacitor in parallel. The resonance was designed to be at 13.56MHz + 848kHz. The parallel impedance of the first setup consists of a 4.7nF capacitor and 16Ω a resistor (realized as 3x47Ω in parallel). By choosing the target for the resonance to be at 13.56MHz - 848kHz, the necessary inductance is 33nH. This value is so small, that the parasitic inductance plays a role. It was realized with a one turn loop. The 400nF capacitor is used for creating the resonance and it is part of the MP-A9 configuration in the QI standard.

Simulation shows, that the position of the capacitor for the QI resonance is not important. The second implementation keeps the capacitor closer to the H-bridge. The main advantage is, that the parasitic wire inductances could be reduced.

In the third setup, the series impedance was duplicated on the other side of the H-

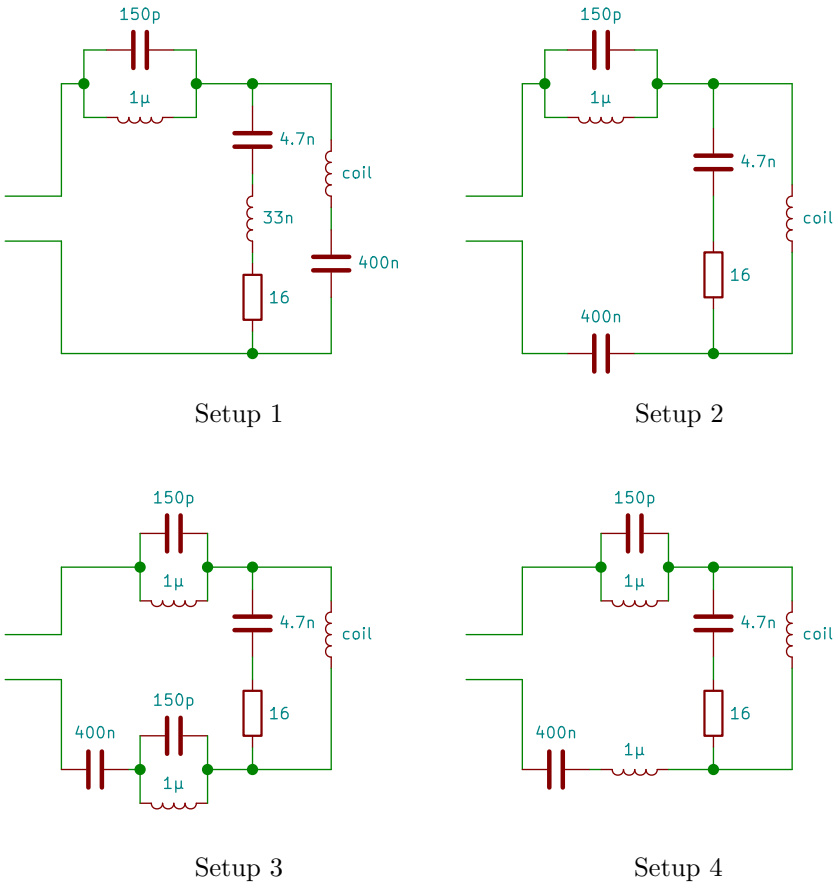

Figure 4.22: Circuits of realized notch filter designs

bridge. For higher frequencies, this setup is more symmetrical.

The fourth setup combines the low pass with the notch filter approach.

Figure 4.23 and 4.24 show a comparison of the different filters. The signals are taken with a pickup coil above the active charging coil. Plotted are the odd harmonics of the recorded signal. All signals are normalized to have a fundamental amplitude of 1. The dotted line shows the theoretical -20db/decade decay of a periodic pulse with 50% duty cycle.

The orange signal shows the unfiltered signal. The low pass filter shows its effect already at frequencies of 1MHz (blue line). The notch filter approaches reduce the induced voltage by 10 to 20dB in the region of the NFC carrier ±848kHz. The goal of filtering exactly 13.56MHz ± 847.5kHz was missed. This is probably because of too low quality factors.

It can be observed, that in ratio to the fundamental, the single ended notch approach (setup 2) has the best damping in the NFC region. It is followed by the setup 4 and 3. The low pass filter has worse performance in this region.

Other critical frequencies are the harmonics of the NFC carrier. At twice the NFC carrier frequency, the low pass and the notch plus low pass setup (4) outperform the others. When comparing setup 3 and 4 (violet and green), it can be seen, that at around 18MHz,

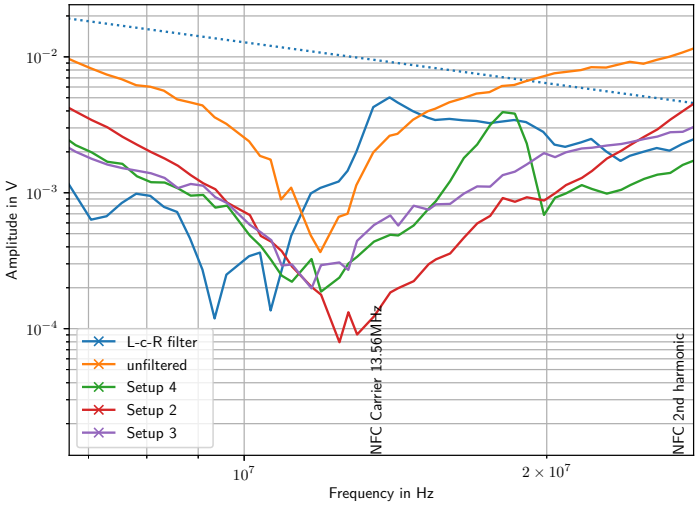

Figure 4.23: Comparison of different filters in the QI circuit close to the NFC frequency

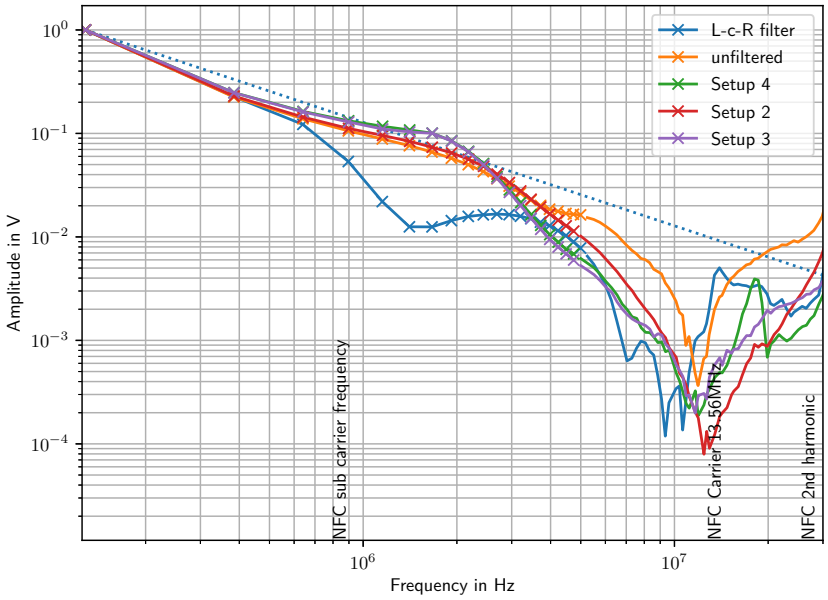

Figure 4.24: Comparison of different filters in the QI circuit

the notch plus low pass variant has an increased amplification. This can be explained by calculating the series impedance of the filter (see figure 4.25).

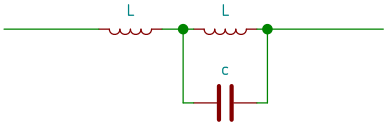

Figure 4.25: The series impedance of the 4th notch filter approach

The impedance of the circuit is:

$$Z = sL + \frac{1}{\frac{1}{sL} + sc}$$

It has a zero at:

$$0 = sL + \frac{1}{\frac{1}{sL} + sc}$$

$$0 = 1 + s^2Lc + 1$$

$$s_{1,2} = \pm j\sqrt{\frac{2}{Lc}} = \pm j115\frac{\text{Mrad}}{\text{s}} \rightarrow 18.4\text{MHz}$$

At this zero, the capacity and the two inductances compensate. Below the notch resonance, the impedance is inductive. Above this zero, the impedance is inductive as well. In between, the impedance is capacitive.

Result: This algorithm returns, as soon as an NFC card is detected. Therefore, when returning the wireless charging shall be aborted.

```
repeat
    scan for vicinity tags;
    if vicinity tag found then
        return card;
    // Poll for A, B, F
    result1 ← [0,0,0];
    scan for type A cards;
    result1[0] ← number of type A cards found ;
    scan for type B cards;
    result1[1] ← number of type B cards found ;
    scan for type F cards;
    result1[2] ← number of type F cards found ;
    reset NFC field;
    // Poll for F, B, A
    result2 ← [0,0,0];
    scan for type F cards;
    result2[2] ← number of type F cards found ;
    scan for type B cards;
    result2[1] ← number of type B cards found ;
    scan for type A cards;
    result2[0] ← number of type A cards found ;
    // Evaluate results:
    switch ∑ result1 do
        case 0 do
            // No card or CE device found, continue
        case 1 do
            if result1 = result2 then
                return card ;                    // Further checks necessary
            else
                // A card emulating device is found. Continue...
        otherwise do
            // More than one device detected.
            return card;
        end
    end
until forever;
```

Algorithm 1: Pseudo code for a card detection loop, which excludes card emulating devices

Chapter 5

Outcomes

In this section, the results of the previous chapters are summarized. The section is separated in three blocks. First the practical work is discussed with a working demonstration setup and the implemented modifications. Then the most interesting results of investigations for the thesis are summarized. Finally, future work is identified.

5.1 Card protection demonstration system

A system for demonstration was built, using two separate boards for NFC and for charging. Firmware for both boards was developed. Charging status and NFC status are transmitted between the two systems. The core logic was implemented on the NFC side.

Following countermeasures are included:

- Card and Device distinguishing (section 4.3.2) to prevent charging
- Simple card detection and Parallel card detection variant II (section 4.3.3 and 4.3.5) for dynamic cases (a card moves into the operating region)
- Sub carrier detection algorithm (not described in this thesis for legal reasons).
- Static RX Threshold adaption (section 4.3.6) to configure the NFC front end to the higher noise floor.

Critical for a good performance is a good matching circuit on the NFC reader. It is strongly effected by the wireless charging system. The matching process must be done with the Qi coils and with all shielding elements in place. The NFC reader matching was optimized for operation with and without a mobile phone on top of the charger.

Following countermeasures are not included in the card protection demonstration:

- Time slot approaches (section 4.2) are not implemented, because there is no support of the power receivers and the PWM freeze is not efficient enough.
- A single NFC reader antenna to decouple (section 4.4.1) creates too many blind spots.
- Switchable NFC coils (section 4.4.2 and 4.4.3) are not implemented. The antenna can be exchanged, but the switching circuit was not implemented.

- Low pass filters in the QI circuit (section 4.4.4) did not show measurable improvement on the overall performance. They create additional losses, because in a system with little resistive components, additional resistors must be added to control the quality factors.
- Notch filters in the QI circuit (section 4.4.5) are not implemented, because they did not improve the communication with phones. The filters damp the QI field in specific frequency ranges, but amplify it in others.

The system reliably protects cards during normal operation. Cards, which move into the field during charging are detected as well. The following technologies are covered: ISO-14443 (A and B), JIS X6319-4 (Felica) and ISO-15693 (vicinity cards).

From the analysis and the tests, it can be observed, that there are situations, where cards cannot be protected. However, those scenarios are not realistic.

5.2 Conclusions

A card protection functionality was successfully implemented. This feature does not only work in a static setup, but also in a dynamic one, where a card is moved into the operating area *during* wireless charging.

Therefore, integrating NFC readers into wireless chargers is an effective measure against the threat of damaging NFC cards while charging a device. Note, that the findings are limited to the power class 0 of the Qi wireless charging standard, which is the most common for charging phones.

Several ideas for improving card protection were evaluated, one of which was also filed as a patent. Because some of the improvements require low level access to hardware, they can be implemented only on devices with direct access to the front end.

During the work on the thesis, different influences of wireless charging on NFC were investigated and analyzed. As a result, formulas were derived to assess the effect of inductive wireless charging on NFC cards. These formulas identify the major sources for the stress on cards, which can lead to permanent damage: the number of turns of the cards NFC antenna, the voltage at the charging coils and the threshold voltage of the limiter on the card. This information can be used in the design of wireless chargers to define a save operating zone. Besides also card manufacturers can make use of these formulas for designing cards with enhanced immunity against low frequency magnet fields as produced by wireless chargers.

Furthermore, the effect of wireless charging on NFC readers was investigated. It was found, that the suppressing of frequencies close to 13.57MHz $\pm$ 848kHz of the wireless charging field helps to improve the communication. Unfortunately, filtering the wireless charging signals is difficult, due to the high currents. Moreover, it was found that because of the multiple coil design of the charger, decoupling of the NFC reader antenna and the wireless charging coils is not possible[1].

Despite the distortions in the NFC reader caused by the wireless charger, the card protection feature was implemented successfully without any additional filter on the wireless

[1]This approach was successfully used with one coil chargers before. On the MP-A9 setup with three charging coils, decoupling causes too many blind spots.

charger.

Currently many mobile phones turn off NFC when being charged wirelessly. Therefore, running NFC services while charging is not possible natively. If certain tasks shall be performed via NFC during charging, currently the only solution is to pause charging for the time of the communication.

The first defined goal to overcome the threat of damaging NFC cards by multi-coil Qi chargers was successfully fulfilled. The second goal was to enable NFC communication during Qi charging. It could not be fulfilled, because of the current behaviour of mobile phones.

5.3 Future work

This section about future work is split in three sub sections. First, further investigations are identified, which could not be performed. Then further improvements on the setup and the hardware are identified. Finally, several ideas for standardization are presented.

5.3.1 Further analysis

The analysis in section 3 of the combined system focuses on interferences between the NFC and the wireless charging system caused by mutual inductances. The capacitive coupling of NFC reader, NFC card and power receiver was not considered, but could be analyzed in future work.

In this analysis also the common mode effects of the wireless charging signals can be analyzed. Eventually common mode chokes and capacitors towards ground are effective. Ideally the signal is purely differential. However, at the signal edges there could be asymmetry caused by the switching of the H bridge. Also the circuitry of the driver is not symmetrical.

Another idea, which could be developed further is the switchable antenna from section 4.4.3. For instance it could be extended by a third antenna, which fills the blind spots common to the other two antennas.

5.3.2 Improvements on the hardware

The effects of wireless charging can be considered for new NFC IC designs. For example the ideas, described in section 4.3.6, can be implemented in hardware. Another topic is the wrong sub carrier detection issue with strongly non-linear loads (section 3.4.3). It could be considered for future designs of demodulators.

For the analyzed setup, the power adaption is achieved by adjustment of the rail voltage only. If the requirement of the fixed frequency was dropped, the frequency could be adjusted to be closer to the resonance point. As a result, the harmonic distortion of the charging signal could be decreased.

5.3.3 Standardization

In my opinion, the ideal solution of card and device distinguishing requires further standardization. One disadvantage of the current approach is, that it relies on non-standardized

assumptions. The information, if a chip is susceptible to wireless charging could be encoded in the NFC protocol. For example by storing a specific NFC application with a fixed AID to all phones. Then, the reader can poll for that application and can conclude, if it is a phone, or not. Alternatively, additional commands could be defined or bits currently reserved for future use could be used for this purpose.

The effects of magnetic fields for Qi charging on NFC cards were analyzed in this thesis, because there are no applicable limits defined. Currently the standard for proximity cards (ISO 14443) only defines maximum ratings of the field strength at the carrier frequency of 13.56MHz[2][3]. Moreover, as the resonance circuit on the card is not effective for low frequencies, it is also not possible to calculate an equivalent maximal field strength for different frequencies, which would be then acceptable for every card.

Therefore it would make sense to have another limit added to the standard. A possible measure for a limit at low frequencies could be on the product of field strength and frequency. A formulation which matches the $7.5\,\mathrm{A\,m^{-1}}$ limit, could be, that for any frequency significantly below the NFC carrier the product of ωH must not exceed $639\,\mathrm{MA\,m^{-1}\,s^{-1}}$, measured with an ID1 card.

[2]Although, it is not stated in the standard that it is only valid at this frequency.

[3]The FeliCa standard (JIS X6319-4) requires a card to withstand static magnetic fields of 640kA/m.

Bibliography

[1] *AN10833, MIFARE Type Identification Procedure*. NXP Semiconductor Devices. July 2016.

[2] CardLogix Corporation. *Types of Smart Card*. URL: www.smartcardbasics.com/smart-card-types.html. accessed:24.03.2019.

[3] M. Chung et al. "A dual-mode antenna for wireless charging and Near Field Communication". In: *2015 IEEE International Symposium on Antennas and Propagation USNC/URSI National Radio Science Meeting*. July 2015, pp. 1288–1289. DOI: 10.1109/APS.2015.7305033.

[4] *Digital Protocol - Technical Specification*. NFC Forum. Apr. 2019.

[5] Michael Gebhart and Michael Stark. "How to guarantee Phase-Synchronicity in Active Load Modulation for NFC and Proximity". In: *4th International Workshop on Near Field Communication (IEEE)*. Jan. 2013.

[6] S. Hong et al. "Dual-directional near field communication tag antenna with effective magnetic field isolation from wireless power transfer system". In: *2017 IEEE Wireless Power Transfer Conference (WPTC)*. May 2017, pp. 1–3. DOI: 10.1109/WPT.2017.7953874.

[7] *Identification cards - Contactless integrated circuit cards - Proximity cards*. ISO / IEC. June 2018.

[8] M. Kang, E. Noh, and K. Kim. "NFC transmitter coil placement to minimise degradation of A4WP wireless power transfer efficiency". In: *Electronics Letters* 53.9 (2017), pp. 616–618. DOI: 10.1049/el.2017.0660.

[9] L. Li, Z. Gao, and Y. Wang. "NFC antenna research and a simple impedance matching method". In: *Proceedings of 2011 International Conference on Electronic Mechanical Engineering and Information Technology*. Vol. 8. Aug. 2011, pp. 3968–3972. DOI: 10.1109/EMEIT.2011.6023890.

[10] Otto Mildenberger. *Entwurf analoger und digitaler Filter*. Vieweg+Teubner Verlag, 1992. ISBN: 978-3-528-06430-3. DOI: 10.1007/978-3-322-90444-7.

[11] *NFC Data Exchange Format - Technical Specification*. NFC Forum. Nov. 2017.

[12] D. Rinner, H. Witschnig, and E. Merlin. "Broadband NFC - A system analysis for the uplink". In: *2008 6th International Symposium on Communication Systems, Networks and Digital Signal Processing*. July 2008, pp. 292–296. DOI: 10.1109/CSNDSP.2008.4610713.

[13] T. Sekiguchi et al. “Study on the effective loading method of the magnetic sheet for NFC / WPT dual-band antenna”. In: *2016 International Symposium on Antennas and Propagation (ISAP)*. Oct. 2016, pp. 946–947.

[14] NXP Semiconductors. *How to distinguish a Tag from a Device*. URL: members.wirelesspowerconsortium.com/members/documents/?download=true&downloadSingle=3256133. accessed: 21.03.2019.

[15] Esko Strommer et al. “NFC-Enabled Wireless Charging”. In: *2012 4th International Workshop on Near Field Communication*. Mar. 2012, pp. 36–41. DOI: 10.1109/NFC.2012.17.

[16] *Technical Report - Identification cards - Contactless integrated circuit cards - Proximity cards - Multiple PICCs in a single PCD field*. ISO / IEC. Dec. 2013.

[17] *The Qi Wireless Power Transfer System Power Class 0 Specification*. Wireless Power Consortium. Feb. 2018.

[18] Miroslaw Wcislik and Tomasz Kwasniewski. “Circuit analysis of magnetic couplings between circular turn and spiral coil”. In: *Computer Applications in Electrical Engineering*. Vol. Vol. 12. 2014, pp. 82–91.

[19] H. Witschnig et al. “Eigenvalue Analysis of Close Coupled 13.56 MHz RFID-Labels”. In: *2006 IEEE MTT-S International Microwave Symposium Digest*. June 2006, pp. 324–327. DOI: 10.1109/MWSYM.2006.249516.